

BIFURCATION IN A REACTION DIFFUSION SYSTEM

Thesis by

Edward J. Bissett

In Partial Fulfillment of the Requirements

For the Degree of

Doctor of Philosophy

California Institute of Technology

Pasadena, California

1978

(Submitted May 23, 1978)

ACKNOWLEDGMENTS

My deepest gratitude goes to my thesis advisor, Professor Donald S. Cohen. He supplied me with encouragement when I needed it, left me on my own when I needed that, and had the wisdom to discriminate between the two.

I would also like to thank the rest of the department, especially the other graduate students, for their support and many interesting discussions. Financial support was from Caltech Fellowships, Teaching Assistantships, and Research Assistantships. Special thanks go to my good friend, Pam Hagan, for an excellent job of typing.

Lastly, I would like to express my sincere appreciation to my wife, Cheri. The emotional support and balance that she supplied were more important than any other factor in seeing this thesis to completion.

ABSTRACT

The bifurcation and nonlinear stability properties of the Meinhardt-Gierer model for biochemical pattern formation are studied. Analyses are carried out in parameter ranges where the linearized system about a trivial solution loses stability through one to three eigenfunctions, yielding both time independent and periodic final states. Solution branches are obtained that exhibit secondary bifurcation and imperfection sensitivity and that appear, disappear, or detach themselves from other branches.

TABLE OF CONTENTS

CHAPTER	PAGE
Acknowledgments	ii
Abstract	iii
Table of Contents	iv
Introduction	v
I PRELIMINARY DISCUSSION AND CALCULATIONS	2
1.1 Explanation of the Model	2
1.2 Bifurcating Solutions and Pattern Formation	5
1.3 The Stability Boundary	6
1.4 Asymptotic Expansions of the Solutions and Their Governing Equations	15
II BIFURCATION THROUGH ONE REAL EIGENVALUE	22
III BIFURCATION THROUGH TWO REAL EIGENVALUES	37
IV BIFURCATION THROUGH ONE REAL EIGENVALUE AND A COMPLEX PAIR OF EIGENVALUES	45
4.1 Differential Equations for the Slow-Time Behavior	45
4.2 Expected Behavior and the Broader Context	51
4.3 Dynamics of a Special Case	53
4.4 Loss of Stability Without Exchange of Stability	61
4.5 Analysis of the Slow-Time Behavior	64
4.6 Phase Portraits for the Various Cases	72
REFERENCES	92

## INTRODUCTION

H. Meinhardt and A. Gierer have put forward a series of reaction-diffusion systems intended to model biochemical pattern formation. In the first chapter, the important general features of these models are briefly discussed and a particular set of equations is chosen for study. These equations permit a unique trivial solution which is independent of both space and time. The stable and unstable regions for this trivial solution are identified in a relevant parameter space, and the stability boundary between these regions is obtained. Asymptotic formulas for bifurcating solutions close to the trivial solution are obtained when the parameters lie close to the stability boundary. These solutions, representing rudimentary patterns, depend on two time scales, called "fast" and "slow", and show the effects of different types of perturbations of the parameters.

In the second chapter, parameter values are explored that lead to final states that correspond to simple bifurcation of a single, purely spatial mode. The effect of an imperfection parameter resulting from a slight nonhomogeneity in one of the parameters is included.

The third chapter concerns parameter values that lead to final states possessing two spatial modes that are independent of the fast time. The analysis leads to a two-dimensional, nonlinear, autonomous system for the slow-time behavior of the amplitudes of these two modes. This system is shown to reduce to the corresponding equation of Chapter 2 in the appropriate limits.

In the fourth chapter, parameter values are taken that lead to final states that are either purely spatial or a combination of this spatial

mode and a mode varying little in space but periodic in time. The slow-time amplitudes of both the purely spatial and the periodic modes are studied as a phase plane system. Special attention is paid to a situation in which a Hopf bifurcation might be expected in this phase plane system, but the exceptional case is shown to always occur in which the Hopf bifurcation need not happen. Particular attention is also paid to the effect of the imperfection parameter. In addition to phenomena similar to that of Chapter 2, its variation can lead to the appearance or disappearance of bifurcation branches, detaching or joining of different branches, and the sweeping of bifurcation points around branches, including through vertical tangents.

BIFURCATION IN A REACTION DIFFUSION SYSTEM

CHAPTER 1

PRELIMINARY DISCUSSION AND CALCULATIONS

1.1 Explanation of the Model

In a series of papers, H. Meinhardt and A. Gierer have proposed a theory of biological pattern formation. In this theory, they attempt to explain how spatial patterns might develop from homogeneous or near homogeneous conditions in simple biological systems. To accomplish this, they propose the existence of two chemical agents, an activator,  $a$ , and an inhibitor,  $h$ , whose behavior is modeled by a reaction-diffusion system:

$$\begin{aligned}\frac{\partial a}{\partial t} &= D_a \frac{\partial^2 a}{\partial x^2} + P(a, h) \\ \frac{\partial h}{\partial t} &= D_h \frac{\partial^2 h}{\partial x^2} + Q(a, h)\end{aligned}\tag{1.1}$$

Here,  $t$  and  $x$  are the independent variables for time and one-dimensional space, respectively, and  $P$  and  $Q$  represent particular nonlinear functions. The spatial variation of the activator, at any point in time, is said to exhibit the pattern. For instance, in a hydra, a good example of a one-dimensional organism, if high activator concentration stimulates the formation of a head or of buds, then the pattern would represent the distribution of buds and the head along the body of the hydra.

There are two main features embodied in these equations. First,  $P$  should contain a nonlinear reaction term,  $P_1$ , such that



$$\frac{\partial P_1}{\partial a} > 0, \quad \frac{\partial P_1}{\partial h} < 0. \quad (1.2)$$

That is, the production of  $a$  should increase as  $a$  increases, and the production of  $a$  should decrease as  $h$  increases. This latter effect is the reason that  $h$  is called the inhibitor. The second main feature is that the ratio of diffusion constants,  $D_a/D_h$ , should be small so that the inhibitor diffuses over a relatively larger region than the activator.

The creation of a pattern-enhancing model from the combination of the above two features can be seen as follows. Suppose a small initial peak of activator concentration occurs, due to some random fluctuations or some slight inhomogeneity in the initial conditions. Then, locally, the production of more activator is stimulated due to the  $\frac{\partial P_1}{\partial a}$  term. Since  $D_a/D_h$  is small, this increased activator remains much closer to the original peak than does whatever inhibitor is also produced ( $Q$  also turns out to contain a term  $Q_1$  such that  $\frac{\partial Q_1}{\partial a} > 0$ ). Therefore, the local peak of activator is enhanced, while the more diffusive inhibitor suppresses the production of  $a$  in neighboring regions. The net effect is to magnify the original activator pattern. Such behavior was observed in numerical studies of such models by Meinhardt and Gierer.

Of course, many possible functional forms for  $P$  and  $Q$  should suffice for pattern formation. Meinhardt and Gierer have proposed several of these and have studied various features of many of them. In the present work, we will focus on a modified form of what they refer to

as a conversion model. In their notation, it is

$$\begin{aligned}\frac{\partial a}{\partial t} &= \rho_0 \rho + \rho c \frac{a^2}{h^2} - \mu a + D_a \frac{\partial^2 a}{\partial x^2} \\ \frac{\partial h}{\partial t} &= \mu a - \nu h + D_h \frac{\partial^2 h}{\partial x^2}\end{aligned}\tag{1.3}$$

All variables and parameters are considered positive except  $x$ , which may be taken between  $-l$  and  $l$ . Note the term  $-\mu a$  in the first equation and  $+\mu a$  in the second equation. These terms are the reason that this is referred to as a conversion model, since they describe the chemical conversion of  $a$  into  $h$  at rate  $\mu$ . Also note that the second equation is linear, although this will be utilized only in simplifying the later computations and will play no fundamental role.

To obtain the final form of (1.3) that we will use in this work, drop the term  $\rho_0 \rho$  as an inessential complication for our purposes, and then, without loss of generality, let  $c = 1$ . Partially non-dimensionalize by

$$\begin{aligned}t &\longrightarrow \mu t \\ x &\longrightarrow \frac{x}{l} \\ \nu &\longrightarrow \frac{\nu}{\mu} \\ \rho &\longrightarrow \frac{\rho}{\mu} \\ D_a &\longrightarrow \sigma D_h \\ D_h &\longrightarrow D \mu l^2\end{aligned}\tag{1.4}$$

Then (1.3) becomes

$$\begin{aligned}\frac{\partial a}{\partial t} &= \rho \frac{a^2}{h^2} - a + \theta D \frac{\partial^2 a}{\partial x^2} \\ \frac{\partial h}{\partial t} &= a - \nu h + D \frac{\partial^2 h}{\partial x^2} \\ x &\in [-1, 1], \quad t \in [0, \infty) .\end{aligned}\tag{1.5}$$

This is the form we will take as the starting point for the subsequent analysis.

## 1.2 Bifurcating Solutions and Pattern Formation

First note that, if all parameters are constant, equations (1.5) permit the following simple solution.

$$\begin{pmatrix} a \\ h \end{pmatrix} = \rho \begin{pmatrix} \nu^2 \\ \nu \end{pmatrix}\tag{1.6}$$

For certain values of the parameters, this solution will be stable. As the parameters are changed, this solution may lose stability, and neighboring solutions might be expected. In the following chapters, these neighboring solutions will be studied. It is important to recognize that these results will be interpretable on two levels.

On a more physical level, the solution represented by equation (1.6) is a steady, inhomogeneous state, exhibiting no pattern. In studying pattern formation, we are interested in how states with some

recognizable spatial pattern can be formed from such patternless states. To see the genesis of such patterns, we are naturally led to consider parameter values where we expect new, more complex states than those of (1.6) to appear. As stated above, this can be expected to occur where the solution (1.6) loses its stability.

On a more mathematical level, the subsequent analysis will be a relatively complete study of the bifurcating solutions of the specific, dynamic system, (1.5). The solution represented in equation (1.6) is the trivial solution upon which the bifurcation analysis builds; the parameter values where this trivial solution loses stability are the bifurcation points; and the new, more complex states that will be found in the neighborhoods of the bifurcation points are the bifurcating solutions, or patterns.

In the remainder, the mathematical viewpoint will be stressed. However, it should not be forgotten that all new solutions found can be interpreted as the beginnings of a pattern and that equations (1.5) are models for a physical system, in addition to being a convenient example of a reaction-diffusion system.

### 1.3 The Stability Boundary

In this section, the linearized stability of the state (1.6) will be studied. To this end, let

$$\begin{pmatrix} a \\ h \end{pmatrix} = \rho \begin{pmatrix} v^z \\ v \end{pmatrix} + \begin{pmatrix} A \\ H \end{pmatrix} , \quad (1.7)$$

substitute this into (1.5) and retain only first order terms. The result is the following linear system.

$$\frac{\partial}{\partial t} \begin{pmatrix} A \\ H \end{pmatrix} = L \begin{pmatrix} A \\ H \end{pmatrix} \quad , \quad (1.8)$$

where

$$L = \begin{pmatrix} 1 + \theta D \frac{\partial^2}{\partial x^2} & -2v \\ 1 & -v + D \frac{\partial^2}{\partial x^2} \end{pmatrix} .$$

To proceed from this point, we need boundary conditions to accompany (1.5). The following will suffice.

$$\begin{aligned} \begin{pmatrix} q \\ h \end{pmatrix} - \gamma_1 \frac{\partial}{\partial x} \begin{pmatrix} q \\ h \end{pmatrix} &= \rho \begin{pmatrix} v^2 \\ v \end{pmatrix} , \quad \text{at } x = -1 \\ \begin{pmatrix} q \\ h \end{pmatrix} + \gamma_2 \frac{\partial}{\partial x} \begin{pmatrix} q \\ h \end{pmatrix} &= \rho \begin{pmatrix} v^2 \\ v \end{pmatrix} , \quad \text{at } x = 1 \end{aligned} \quad (1.9)$$

$$\text{with } \gamma_1, \gamma_2 > 0 , \quad \gamma_1 \neq \gamma_2$$

These conditions have been chosen primarily for convenience. That is, the trivial solution satisfies them, and higher order corrections to the trivial solution will satisfy the homogeneous form of (1.9). The idea here is that these conditions introduce no extra complications at the boundaries that might obscure the analysis that we want to carry out, and that a prescribed combination of function and outwardly directed derivative is reasonably general already. The requirement of mixed, rather than Dirichlet or Neumann, conditions and the requirement that

$\gamma_1 \neq \gamma_2$  are chosen to destroy spatial symmetries that would force certain integrals to be zero in the subsequent analysis. In physical terms, the conditions (1.9) can be considered as representing boundaries that allow only partial diffusion through them.

In any case, (1.9) imply the appropriate boundary conditions to accompany (1.8).

$$\begin{aligned} \begin{pmatrix} A \\ H \end{pmatrix} - \gamma_1 \frac{\partial}{\partial x} \begin{pmatrix} A \\ H \end{pmatrix} &= 0 \quad \text{at } x = -1 \\ \begin{pmatrix} A \\ H \end{pmatrix} + \gamma_2 \frac{\partial}{\partial x} \begin{pmatrix} A \\ H \end{pmatrix} &= 0 \quad \text{at } x = 1 \end{aligned} \tag{1.10}$$

The solution of (1.8) subject to (1.10) can be written

$$\begin{pmatrix} A \\ H \end{pmatrix} = \sum_{n=1}^{\infty} \begin{pmatrix} p_n \\ q_n \end{pmatrix} e^{\sigma_n t} y_n(x), \tag{1.11}$$

where  $y_n(x)$  is one of the eigenfunctions of the regular Sturm Liouville problem

$$\begin{aligned} -\frac{d^2}{dx^2} y_n &= k_n^2 y_n \\ y_n - \gamma_1 \frac{dy_n}{dx} &= 0 \quad \text{at } x = -1 \\ y_n + \gamma_2 \frac{dy_n}{dx} &= 0 \quad \text{at } x = 1 \end{aligned} \tag{1.12}$$

and  $\begin{pmatrix} p_n \\ q_n \end{pmatrix}$  satisfies

$$\begin{pmatrix} 1 - \theta Dk_n^2 - \sigma_n & -2\nu \\ 1 & -\nu - Dk_n^2 - \sigma_n \end{pmatrix} \begin{pmatrix} p_n \\ q_n \end{pmatrix} = 0 \quad (1.13)$$

For  $\begin{pmatrix} p_n \\ q_n \end{pmatrix} \neq 0$ , the determinant of the multiplying matrix in (1.13)

must be zero, which gives an equation for  $\sigma_n$ , the eigenvalue of L. Since this equation is quadratic in  $\sigma_n$ , for each n there are two values of  $\sigma_n$ . Call them  $\sigma_n^{\pm}$ .

$$\sigma_n^{\pm} = \frac{1}{2} \left[ 1 - \nu - (1 + \theta) Dk_n^2 \pm \sqrt{[1 + \nu + (1 - \theta) Dk_n^2]^2 - 8\nu} \right], \quad (1.14)$$

where this square root is positive for positive argument.

Then, from (1.13), we easily obtain

$$\begin{pmatrix} p_n^{\pm} \\ q_n^{\pm} \end{pmatrix} = C_n^{\pm} \begin{pmatrix} 1 + \nu + (1 - \theta) Dk_n^2 \pm \sqrt{[1 + \nu + (1 - \theta) Dk_n^2]^2 - 8\nu} \\ 2 \end{pmatrix} \quad (1.15)$$

where  $C_n^{\pm}$  are constants. Therefore (1.11) can be written

$$\begin{pmatrix} A \\ H \end{pmatrix} = \sum_{n=1}^{\infty} \begin{pmatrix} p_n^- \\ q_n^- \end{pmatrix} e^{\sigma_n^- t} y_n(x) + \begin{pmatrix} p_n^+ \\ q_n^+ \end{pmatrix} e^{\sigma_n^+ t} y_n(x) \quad (1.16)$$

Recalling the definition of  $A$  and  $H$  from (1.7) it is now clear that the trivial solution can be considered locally asymptotically stable if and only if all the  $\sigma_n^+$  have negative real parts. From the expression for  $\sigma_n^+$ , (1.14), we see that once we know  $k_n$ , and considering  $D$  as given, there should be a region in the  $v - \sigma$  plane where each  $\sigma_n^+$  has negative real part. The intersection of all such regions for all  $n$  will give the region in which all  $\sigma_n^+$ 's have negative real parts, and therefore give the parameter values where the trivial solution is stable. The edge of such a region is called a stability boundary, and according to the plan set out in Section 1.2, it is near such a stability boundary that new solutions can be expected to be found.

However, before proceeding to actually obtaining the stability boundary, the preceding calculations should be completed by explicitly displaying the  $y_n$  and  $k_n$ . Any of the following three equivalent forms may be taken as the solution of (1.12), depending upon what is convenient at the moment.

$$\begin{aligned}
 y_n &= N_n \left[ \frac{\gamma_2 - \gamma_1}{2} k_n \sin k_n x + \frac{\gamma_1 \gamma_2 k_n^2 \cos^2 k_n - \sin^2 k_n}{\cos 2k_n} \cos k_n x \right] \\
 &= N_n (\sin k_n + \gamma_2 k_n \cos k_n) [\sin k_n (x+1) + \gamma_1 k_n \cos k_n (x+1)] \quad (1.17) \\
 &= N_n (\sin k_n + \gamma_1 k_n \cos k_n) [\sin k_n (1-x) + \gamma_2 k_n \cos k_n (1-x)] ,
 \end{aligned}$$

where  $N_n$  is the positive normalization constant,



$$N_n = \left[ \frac{(\gamma_2 - \gamma_1)^2}{4} k_n^2 \left(1 - \frac{\sin 2k_n}{2k_n}\right) + \frac{(\gamma_1 \gamma_2 k_n^2 \cos^2 k_n - \sin^2 k_n)^2}{\cos^2 k_n} \left(1 + \frac{\sin 2k_n}{2k_n}\right) \right]^{-\frac{1}{2}} \quad (1.18)$$

so that

$$\int_{-1}^1 y_m(x) y_n(x) dx = \delta_{mn} \quad . \quad (1.19)$$

$k_n$  is a solution of the transcendental equation

$$\tan 2k_n = \frac{(\gamma_1 + \gamma_2) k_n}{\gamma_1 \gamma_2 k_n^2 - 1} \quad , \quad (1.20)$$

or equivalently,

$$\sqrt{\gamma_1 \gamma_2} k_n = \frac{\gamma_1 + \gamma_2}{2\sqrt{\gamma_1 \gamma_2}} \cot 2k_n \pm \sqrt{1 + \left(\frac{\gamma_1 + \gamma_2}{2\sqrt{\gamma_1 \gamma_2}} \cot 2k_n\right)^2} \quad (1.21)$$

Without loss of generality, let  $k_n > 0$ . Then clearly only the plus sign is relevant in (1.21). Figure 1-1 shows the graphical solution of (1.21) by plotting the left hand side and the right hand side with the plus sign as functions of  $k_n$ . The actually possible values of  $k_n$  are the intersections of these two curves.

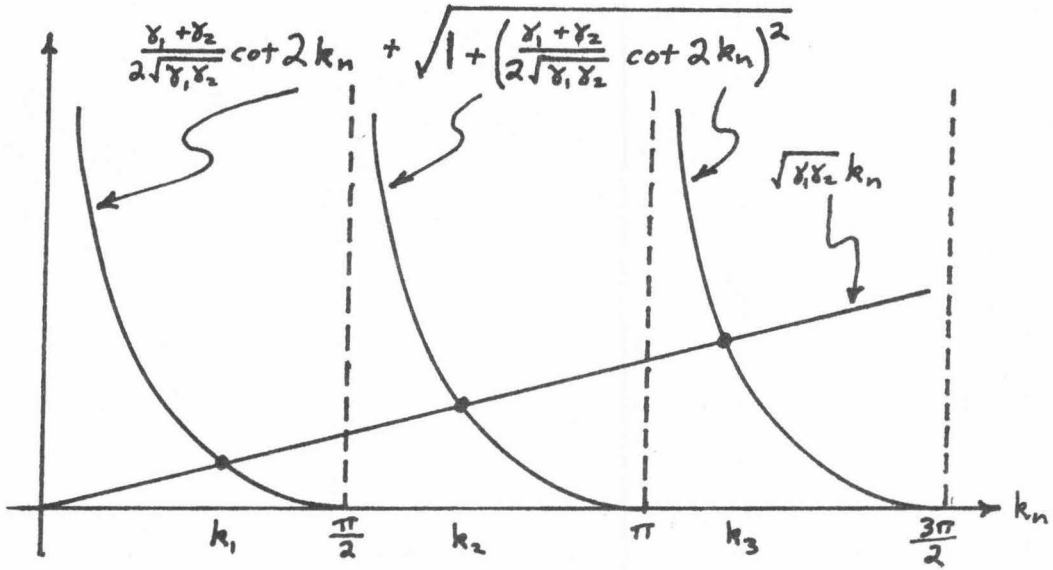


FIGURE 1-1

Now the stability boundary can be derived. As proposed, for each  $n$ , a stable area in the  $\nu - \theta$  plane will be found for that particular mode. The  $\nu - \theta$  area that is stable to all perturbations can then be found by intersecting the areas for the individual modes.

Focusing on a particular value of  $n$ ,  $\sigma_n^{\pm}$  are the two solutions of

$$\sigma_n^2 + \sigma_n (\theta D k_n^2 + \nu + D k_n^2 - 1) + (\theta D^2 k_n^4 + \theta \nu D k_n^2 + \nu - D k_n^2) = 0. \quad (1.22)$$

If one of  $\sigma_n^{\pm}$  is real and equal to zero, the parameters  $\nu$  and

$\sigma$  must lie on the hyperbola,  $R_n(\nu, \sigma)$ , given by the following.

$$R_n: \quad \sigma D^2 k_n^4 + \sigma \nu D k_n^2 + \nu - D k_n^2 = 0 \quad (1.23)$$

This curve may take part in the stability boundary, since  $\sigma \frac{\pm}{n} = 0$  implies neutral stability for one of the eigenvalues.

Similarly, if  $\sigma \frac{\pm}{n}$  are complex conjugate pairs, but have zero real part, the parameters  $\nu$  and  $\sigma$  must lie on the line,  $S_n(\nu, \sigma)$ , given by the following.

$$S_n: \quad \sigma D k_n^2 + \nu + D k_n^2 - 1 = 0 \quad (1.24)$$

Part of this curve may also take part in the stability boundary, as above.

The above observations plus a few other simple considerations allow the determination of the stable region for each particular mode. The two possibilities, depending upon whether or not  $D k_n^2$  is greater or less than  $\frac{1}{2}$  are contained in Figure 1-2 and 1-3.

Combining the relevant curves for all values of  $n$  gives the full stability boundary in Figure 1-4, assuming  $D$  is sufficiently small that  $S_1$  takes part in the stability boundary.

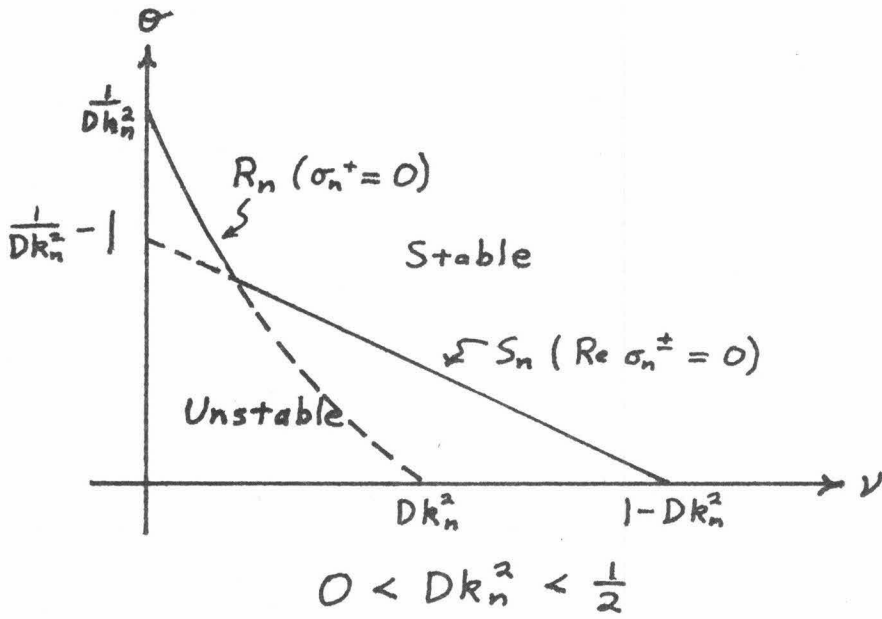


FIGURE 1-2

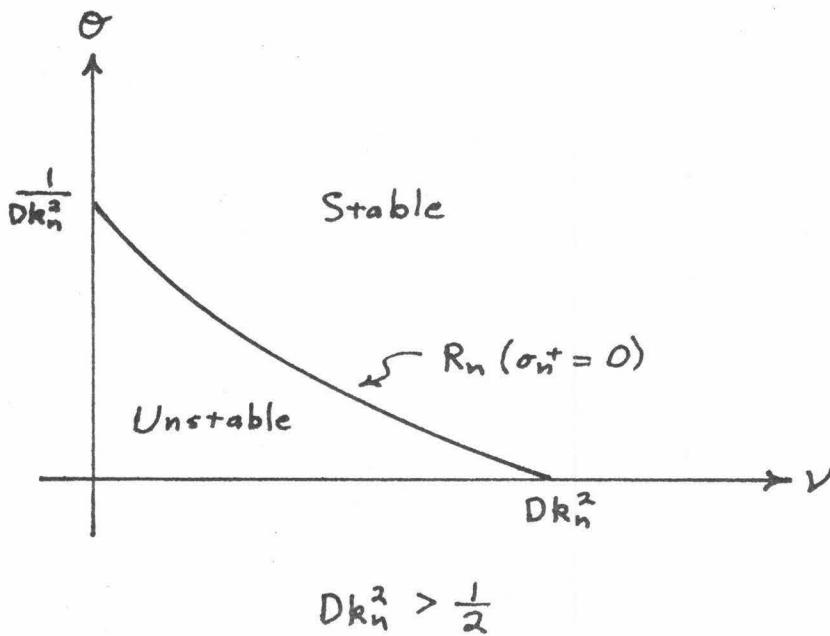


FIGURE 1-3

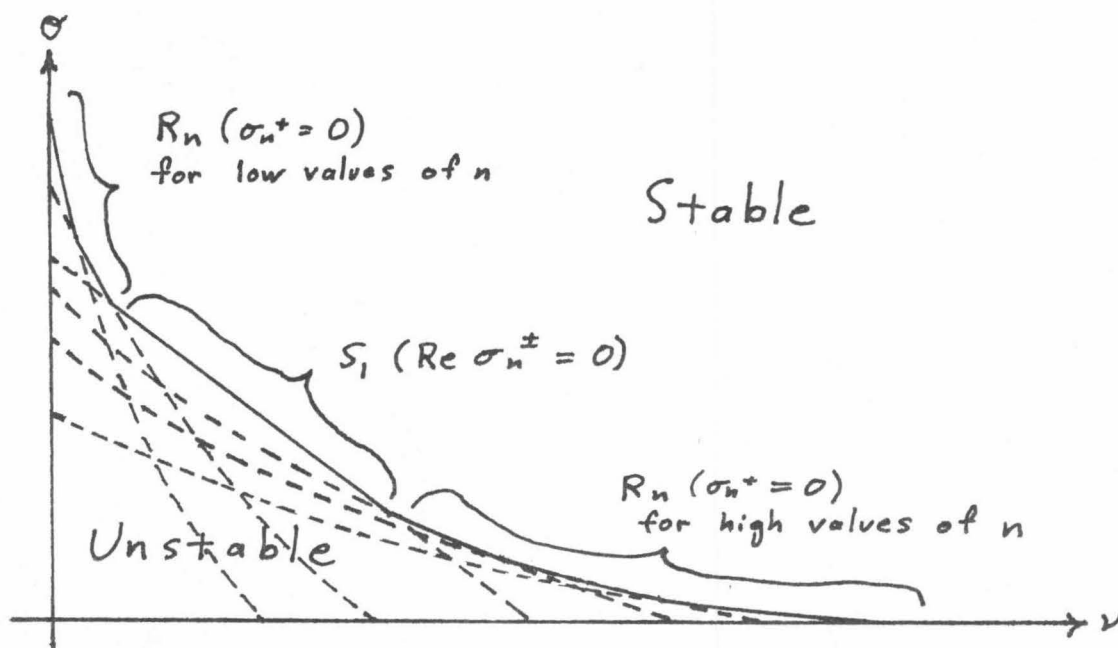


FIGURE 1-4

1.4 Asymptotic Expansions of the Solutions and Their Governing Equations

In this section, the asymptotic form of the solutions to (1.5) are proposed that are expected to be valid near the stability boundary. In the following chapters, the precise forms of the solutions are obtained and their features are discussed, relative to the different portions of the stability boundary to which they pertain.

To mathematically express being close to the stability boundary, we introduce a small parameter,  $\epsilon$ , such that

$$0 < \epsilon \ll 1 \quad . \quad (1.25)$$

$\nu$  and  $\theta$  are assumed to depend smoothly on this parameter, and when  $\epsilon = 0$ ,  $\nu$  and  $\theta$  must lie on the stability boundary. That is, let

$$v = v_0 + \varepsilon v_1 + O(\varepsilon^2) \quad (1.26)$$

$$\theta = \theta_0 + \varepsilon \theta_1(x) + O(\varepsilon^2) , \quad (1.27)$$

where  $v_0$  and  $\theta_0$  are chosen to be precisely on the stability boundary. Note that  $\theta$  is allowed a slight spatial inhomogeneity, in order to see what role this might play in the solution.

The parameter  $\rho$ , although playing no role in the stability, does play a substantially different role in the equations than do  $v$  or  $\theta$ . It also represents the source of activator concentration in the biochemical model, and therefore any small spatial inhomogeneity it contained was thought to be important by Meinhardt and Gierer. For these reasons,  $\rho$  is also allowed to be only approximately constant.

$$\rho = \rho_0 + \frac{1}{2} \varepsilon^2 \rho_2(x) + O(\varepsilon^3) \quad (1.28)$$

The fact that  $\rho$  has no  $O(\varepsilon)$  term is a by-product of the form of the solution we desire.

Now that  $\rho$  depends on  $x$ , the trivial solution (1.6) no longer precisely satisfies the equations (1.5). The most convenient way to correct this is to change the definition of the trivial solution to

$$\begin{pmatrix} a \\ h \end{pmatrix} = \rho_0 \begin{pmatrix} v^2 \\ v \end{pmatrix} . \quad (1.29)$$

Then, for the trivial solution to satisfy the boundary conditions, (1.9) should be changed to the following.

$$\begin{pmatrix} q \\ h \end{pmatrix} - \gamma_1 \frac{\partial}{\partial x} \begin{pmatrix} q \\ h \end{pmatrix} = \rho_0 \begin{pmatrix} v^2 \\ v \end{pmatrix} \quad \text{at } x = -1 \quad (1.30)$$

$$\begin{pmatrix} q \\ h \end{pmatrix} + \gamma_2 \frac{\partial}{\partial x} \begin{pmatrix} q \\ h \end{pmatrix} = \rho_0 \begin{pmatrix} v^2 \\ v \end{pmatrix} \quad \text{at } x = 1$$

Since the linearized problem about the trivial solution, (1.8) and (1.10), is independent of  $\rho$ , the above two changes have no effect on the stability boundary. Therefore, the above two changes can be considered permanent, and (1.29) and (1.30) are the new trivial solution and boundary conditions, respectively.

The asymptotic form of the solution may now be written.

$$a = \rho_0 v^2 + \epsilon A_1(x, t, \tau) + \frac{1}{2} \epsilon^2 A_2(x, t, \tau) + O(\epsilon^3) \quad (1.31)$$

$$h = \rho_0 v + \epsilon H_1(x, t, \tau) + \frac{1}{2} \epsilon^2 H_2(x, t, \tau) + O(\epsilon^3)$$

$$\tau = \epsilon t \quad (1.32)$$

Note that we take the solution to be close to the trivial solution and that two time scales are employed: the normal time,  $t$ , and a "slow time",  $\tau$ . The multiple time scales are a manifestation of the fact that, although the linear theory of Section 1.3 predicts exponential growth in time of solutions near the trivial solution in the unstable region, a properly formulated nonlinear theory can focus more carefully on the solution's local behavior and therefore obtain nicely bounded solutions in time, if the proper time scales are simultaneously studied. To the order in which we will be working to obtain the solution, the time scales of  $t$  and  $\epsilon t$  are sufficient.

Substituting (1.31) into (1.5) and (1.30), the following hierarchy of equations is obtained, by collecting terms with the same order of  $\epsilon$ . Of course, the  $O(1)$  terms vanish due to the assumed form of the solution.

$$\epsilon^1: \quad \frac{\partial}{\partial t} \begin{pmatrix} A_1 \\ H_1 \end{pmatrix} = L_0 \begin{pmatrix} A_1 \\ H_1 \end{pmatrix}, \quad (1.33)$$

where  $L_0 = \begin{pmatrix} 1 + \theta_0 D \frac{\partial^2}{\partial x^2} & -2\nu_0 \\ 1 & -\nu_0 + D \frac{\partial^2}{\partial x^2} \end{pmatrix}$

$$\begin{pmatrix} A_1 \\ H_1 \end{pmatrix} - \gamma_1 \frac{\partial}{\partial x} \begin{pmatrix} A_1 \\ H_1 \end{pmatrix} = 0 \quad \text{at } x = -1 \quad (1.34)$$

$$\begin{pmatrix} A_1 \\ H_1 \end{pmatrix} + \gamma_2 \frac{\partial}{\partial x} \begin{pmatrix} A_1 \\ H_1 \end{pmatrix} = 0 \quad \text{at } x = 1$$

$$\epsilon^2: \quad \frac{\partial}{\partial t} \begin{pmatrix} A_2 \\ H_2 \end{pmatrix} - L_0 \begin{pmatrix} A_2 \\ H_2 \end{pmatrix} = -2 \frac{\partial}{\partial x} \begin{pmatrix} A_1 \\ H_1 \end{pmatrix} + 2 \begin{pmatrix} \theta_1(x) D \frac{\partial^2}{\partial x^2} & -2\nu_1 \\ 0 & -\nu_1 \end{pmatrix} \begin{pmatrix} A_1 \\ H_1 \end{pmatrix} \quad (1.35)$$

$$+ \frac{2}{\rho_0 \nu_0^2} \begin{pmatrix} (A_1 - \nu_0 H_1)(A_1 - 3\nu_0 H_1) \\ 0 \end{pmatrix} + \begin{pmatrix} \nu_0^2 \rho_2(x) \\ 0 \end{pmatrix}$$

$$\begin{pmatrix} A_2 \\ H_2 \end{pmatrix} - \gamma_1 \frac{\partial}{\partial x} \begin{pmatrix} A_2 \\ H_2 \end{pmatrix} = 0 \quad \text{at } x = -1 \quad (1.36)$$

$$\begin{pmatrix} A_2 \\ H_2 \end{pmatrix} + \gamma_2 \frac{\partial}{\partial x} \begin{pmatrix} A_2 \\ H_2 \end{pmatrix} = 0 \quad \text{at } x = 1$$



Note that the operator  $L_0$ , is just the operator  $L$  of (1.8) in Section 1.3, with  $\theta$  replaced by  $\theta_0$  and  $v$  replaced by  $v_0$ . It is therefore a simple matter to carry over results concerning the solution of (1.8) and (1.10) to results concerning the solution of (1.33) and (1.34). In particular,

$$\begin{pmatrix} A_1 \\ H_1 \end{pmatrix} = \sum_{n=1}^{\infty} C_n^+(\tau) U_n^+(x) e^{\sigma_n^+ t} + C_n^-(\tau) U_n^-(x) e^{\sigma_n^- t}, \quad (1.37)$$

where

$$U_n^{\pm}(x) = \left( \frac{1 + v_0 + (1 - \theta_0) D k_n^2 \pm \sqrt{[1 + v_0 + (1 - \theta_0) D k_n^2]^2 - 8 v_0}}{2} \right) y_n(x)$$

and

$$\sigma_n^{\pm} = \frac{1}{2} \left[ 1 - v_0 - (1 + \theta_0) D k_n^2 \pm \sqrt{[1 + v_0 + (1 - \theta_0) D k_n^2]^2 - 8 v_0} \right].$$

Note that in Section 1.3, when there were two independent variables,  $x$  and  $t$ , the  $C_n^{\pm}$  were constants, independent of  $x$  and  $t$ . However, now that there are three independent variables,  $x$ ,  $t$  and  $\tau$ , the  $C_n^{\pm}$  are still independent of  $x$  and  $t$ , but must also, in general, depend on  $\tau$ .

Before proceeding further, a few words should be said about initial conditions for the problem. The primary interest, in the subsequent analysis, will be to find solutions that are stable relative to a certain set of initial conditions, without being particularly explicit about exactly what that set is. Often, an unstable solution may be made to appear stable by artificially restricting the set of initial conditions allowed. Similarly, most stable solutions will not be approached from conditions chosen sufficiently far from those solutions. Therefore, it is probably better left up to the dynamics of each specific case to see under what particular set of initial conditions a particular solution

is stable. However, certain general remarks will assist in this determination.

First, any initial conditions considered must be close to the trivial solution in the sense described above. That is, if

$$\begin{pmatrix} a \\ h \end{pmatrix}_{t=0} = g(x, \epsilon) \quad , \quad (1.38)$$

then

$$g(x, 0) = \rho_0 \begin{pmatrix} v^2 \\ v \end{pmatrix} \quad . \quad (1.39)$$

Also,  $g$  must be sufficiently smooth in  $\epsilon$  near  $\epsilon = 0$  so that it has an adequate number of derivatives at  $\epsilon = 0$  for the order in  $\epsilon$  to which the solution is desired. In particular, the initial conditions for (1.33)-(1.34) are

$$\begin{pmatrix} A_1 \\ H_1 \end{pmatrix}_{t=0} = \frac{\partial g}{\partial \epsilon}(x, 0) \quad . \quad (1.40)$$

For (1.35)-(1.36), they are

$$\begin{pmatrix} A_2 \\ H_2 \end{pmatrix}_{t=0} = \frac{\partial^2 g}{\partial \epsilon^2}(x, 0) \quad . \quad (1.41)$$

These simply come from expanding  $g$  in a Taylor series in  $\epsilon$  about  $\epsilon = 0$ , keeping track of the order, and comparing with (1.31).

If we were to solve (1.33)-(1.34), subject to the initial conditions (1.40), but without including the effect of the "slow time",  $\tau$ ,

the constants  $C_n^+$  in the solution (1.37) would be determined by the standard techniques of linear theory. However, since it is critical that  $C_n^+(\tau)$  depend on  $\tau$ , the same techniques of linear theory applied at  $t = 0$  also imply  $\tau = 0$ , so the initial conditions (1.40) will imply initial conditions for each  $C_n^+(\tau)$ .

In the following chapters, various analyses will be performed near various points of the stability boundary in the sense described above. The main pattern or basic structure of the solution will be seen in the first order correction to the trivial solution (1.37).

Being near the stability boundary will mean that almost all eigenvalues,  $\sigma_n^+$ , in (1.37) will have negative real parts and so decay exponentially quickly on the fast time scale. The corresponding modes will then have no time to develop on the  $\tau = \epsilon t$  time scale. Therefore, the corresponding  $C_n^+(\tau)$  may be taken to be constant, equal to their initial value. These modes can be considered transients and are not of primary interest.

There will, however, be one or more  $\sigma_n^+$  which have zero real parts. For these, the behavior on the slow time scale is all important. Obtaining this behavior in the various cases is the primary goal of the remaining chapters.

CHAPTER 2

BIFURCATION THROUGH ONE REAL EIGENVALUE

This chapter deals with the behavior of solutions near one of the hyperbolic sections of the stability boundary (see Figure 1-4). That is,  $v_0$  and  $\sigma_0$  are chosen to lie on a portion of one of the curves,  $R_n$ , that form part of the stability boundary for a particular value of  $n$ , say  $n = b$ . Therefore,  $v_0$  and  $\sigma_0$  satisfy the equation,

$$\sigma_0 D^2 k_b^4 + \sigma_0 v_0 D k_b^2 + v_0 - D k_b^2 = 0 \quad (2.1)$$

By construction of the stability boundary,  $\sigma_b^+ = 0$ , and all other eigenvalues have negative real parts. Therefore, in this case, (1.37) can be written

$$\begin{pmatrix} A_1 \\ H_1 \end{pmatrix} = 2 C_b^+(\tau) \begin{pmatrix} v_0 + D k_b^2 \\ 1 \end{pmatrix} y_b(x) + \text{transient terms} \quad (2.2)$$

So if a new pattern or stable bifurcating solution is to be found near this portion of the stability boundary, it will be proportional to  $U_b^+(x)$ . As mentioned earlier, the only physically important quantity yet to be determined is  $C_b^+(\tau)$ . This is done by considering the next higher order terms in  $\epsilon$ .

(1.35) becomes the following.

$$\begin{aligned}
 \frac{\partial}{\partial t} \begin{pmatrix} A_2 \\ H_2 \end{pmatrix} - L_0 \begin{pmatrix} A_2 \\ H_2 \end{pmatrix} &= -4 \frac{d}{d\tau} C_b^+(\tau) \begin{pmatrix} \nu_0 + Dk_b^2 \\ 1 \end{pmatrix} y_b(x) \\
 &- 4 C_b^+(\tau) \begin{pmatrix} Dk_b^2 (\nu_0 + Dk_b^2) \theta_1(x) + 2\nu_1 \\ \nu_1 \end{pmatrix} y_b(x) \\
 &+ \frac{8 Dk_b^2}{\rho_0 \nu_0^2} [C_b^+(\tau)]^2 \begin{pmatrix} Dk_b^2 - 2\nu_0 \\ 0 \end{pmatrix} y_b^2(x) \\
 &+ \begin{pmatrix} \nu_0^2 \rho_2(x) \\ 0 \end{pmatrix} + \text{transient terms}
 \end{aligned} \tag{2.3}$$

In order to have a consistently ordered asymptotic expansion, uniformly valid for long times, it is necessary that  $A_2$  and  $H_2$  remain bounded in time, so that their associated terms in (1.31) never become as large as the lower order terms in (1.31) that are associated with  $A_1$  and  $H_1$ . However, since the homogeneous form of (2.3) has the nontrivial solutions found in Section 4, and since some of them do not decay in time, there is the strong possibility that the inhomogeneous equation (2.3) will have solutions unbounded in time. Therefore, certain conditions are required on the right hand side of (2.3) to insure that  $A_2$  and  $H_2$  are bounded in time. Usually, such requirements are obtained by constructing the adjoint to the homogeneous form of (2.3), applying the Fredholm Alternative Theorem, and so forth. In this simple case, it is easier and just as instructive to note the following easily verified lemma, which will also be useful in subsequent chapters.

Lemma 1. A particular solution of

$$\frac{\partial}{\partial t} \begin{pmatrix} A \\ H \end{pmatrix} - L_0 \begin{pmatrix} A \\ H \end{pmatrix} = \begin{pmatrix} v \\ w \end{pmatrix} y_n(x) e^{\sigma t} \tag{2.4}$$

is given as follows:

a) If  $\sigma \neq \sigma_n^{\pm}$ , then

$$\begin{pmatrix} A \\ H \end{pmatrix} = \frac{1}{\sigma_n^+ - \sigma_n^-} \cdot$$

$$\left( \begin{array}{c} \frac{v-w(\sigma_n^- + \nu_0 + Dk_n^2)}{\sigma_n - \sigma_n^+} (\sigma_n^+ + \nu_0 + Dk_n^2) - \frac{v-w(\sigma_n^+ + \nu_0 + Dk_n^2)}{\sigma_n - \sigma_n^-} (\sigma_n^- + \nu_0 + Dk_n^2) \\ \frac{v-w(\sigma_n^- + \nu_0 + Dk_n^2)}{\sigma_n - \sigma_n^+} - \frac{v-w(\sigma_n^+ + \nu_0 + Dk_n^2)}{\sigma_n - \sigma_n^-} \end{array} \right) \cdot \quad (2.5)$$

$$\cdot y_n(x) e^{\sigma t}$$

b) If  $\sigma = \sigma_n^-$ , then

$$\begin{pmatrix} A \\ H \end{pmatrix} = \frac{1}{\sigma_n^+ - \sigma_n^-} \cdot$$

$$\left( \begin{array}{c} \frac{v-w(\sigma_n^- + \nu_0 + Dk_n^2)}{\sigma_n^- - \sigma_n^+} (\sigma_n^+ + \nu_0 + Dk_n^2) - t[v-w(\sigma_n^+ + \nu_0 + Dk_n^2)](\sigma_n^- + \nu_0 + Dk_n^2) \\ \frac{v-w(\sigma_n^- + \nu_0 + Dk_n^2)}{\sigma_n^- - \sigma_n^+} - t[v-w(\sigma_n^+ + \nu_0 + Dk_n^2)] \end{array} \right) \cdot \quad (2.6)$$

$$\cdot y_n(x) e^{\sigma_n^- t}$$

c) If  $\sigma = \sigma_n^+$ , then

$$\begin{pmatrix} A \\ H \end{pmatrix} = \frac{1}{\sigma_n^+ - \sigma_n^-} \cdot$$

$$\left( \begin{array}{c} t[v-w(\sigma_n^- + \nu_0 + Dk_n^2)](\sigma_n^+ + \nu_0 + Dk_n^2) - \frac{v-w(\sigma_n^+ + \nu_0 + Dk_n^2)}{\sigma_n^+ - \sigma_n^-} (\sigma_n^- + \nu_0 + Dk_n^2) \\ t[v-w(\sigma_n^- + \nu_0 + Dk_n^2)] - \frac{v-w(\sigma_n^+ + \nu_0 + Dk_n^2)}{\sigma_n^+ - \sigma_n^-} \end{array} \right) y_n(x) e^{\sigma_n^+ t}$$

(2.7)

Observe that the exponential behavior in  $t$  dominates for large  $t$ , unless  $\text{Re}(\sigma) = 0$ . In that case, the solution is bounded if  $\sigma \neq \sigma_n^+$ , but the solution grows linearly with  $t$  if  $\sigma = \sigma_n^+$ . These terms that grow linearly with time are called secular terms.

Returning to (2.3), the condition that  $A_2$  and  $H_2$  be bounded in time is now easily observed. The homogeneous part of the solution presents no problem, since it is the sum of terms that either decay exponentially in time or, at worst, are constant. As for the particular solution, the right hand side of (2.3) can be resolved into the spatial components  $\{y_n(x)\}$ , since this set is complete. Then each term is of a form suitable for application of Lemma 1. All the transient terms in the right hand side of (2.3) lead to transient terms for  $A_2$  and  $H_2$ . Of the remaining forcing terms, only those with spatial component  $y_b(x)$  (corresponding to  $\sigma_b^+ = 0$ ) will produce secular terms for  $A_2$  and  $H_2$ . The other terms will produce terms for  $A_2$  and  $H_2$  that are constant in  $t$ . Therefore, if the secularity-producing terms in the right hand side of (2.3) are written as

$$\begin{pmatrix} v \\ w \end{pmatrix} y_b(x) e^{\sigma_b^+ t} = \begin{pmatrix} v \\ w \end{pmatrix} y_b(x) \quad , \quad (2.8)$$

for comparison with Lemma 1, then the condition for  $A_2$  and  $H_2$  to be bounded in time is simply

$$v - w(\sigma_b^- + \nu_0 + Dk_b^2) = 0 \quad , \quad (2.9)$$

from (2.7). From (1.22),

$$\sigma_b^+ + \sigma_b^- = 1 - \sigma_0 D k_b^2 - \nu_0 - D k_b^2 .$$

So

$$\sigma_b^- = 1 - \sigma_0 D k_b^2 - \nu_0 - D k_b^2 , \quad (2.10)$$

since

$$\sigma_b^+ = 0 .$$

$$\sigma_b^- + \nu_0 + D k_b^2 = 1 - \sigma_0 D k_b^2 = \frac{2\nu_0}{\nu_0 + D k_b^2}$$

from (2.1). Therefore the condition that  $A_2$  and  $H_2$  be bounded in time is

$$(\nu_0 + D k_b^2) v - 2\nu_0 w = 0 . \quad (2.11)$$

Substituting the actual expressions for  $v$  and  $w$ , (2.11) becomes

$$\begin{aligned} & -4 [(\nu_0 + D k_b^2)^2 - 2\nu_0] \frac{d}{d\tau} C_b^+(\tau) \\ & - 4 D k_b^2 [2\nu_1 + (\nu_0 + D k_b^2)^2] \int_{-1}^1 \sigma_1(x) y_b^2(x) dx C_b^+(\tau) \\ & + \frac{8 D k_b^2}{\rho_0 \nu_0^2} (D k_b^2 - 2\nu_0) (\nu_0 + D k_b^2) \int_{-1}^1 y_b^3(x) dx [C_b^+(\tau)]^2 \\ & + \nu_0^2 (\nu_0 + D k_b^2) \int_{-1}^1 \rho_2(x) y_b(x) dx = 0 . \end{aligned} \quad (2.12)$$

Rewriting this equation, it becomes

$$\frac{d}{d\tau} C_b^+ = \beta [C_b^+]^2 + \alpha C_b^+ + \eta , \quad (2.13)$$

where

$$\beta = \frac{2 D k_b^2}{\rho_0 \nu_0^2} \frac{(\nu_0 + D k_b^2)(D k_b^2 - 2\nu_0)}{[(\nu_0 + D k_b^2)^2 - 2\nu_0]} \int_{-1}^1 y_b^3(x) dx \quad (2.14)$$



$$\eta = \frac{\nu_0^2 (\nu_0 + Dk_b^2)}{4[(\nu_0 + Dk_b^2)^2 - 2\nu_0]} \int_{-1}^1 \rho_2(x) y_b(x) dx \quad (2.15)$$

$$\alpha = - \frac{Dk_b^2}{[(\nu_0 + Dk_b^2)^2 - 2\nu_0]} \left[ 2\nu_1 + (\nu_0 + Dk_b^2)^2 \int_{-1}^1 \theta_1(x) y_b^2(x) dx \right] \quad (2.16)$$

Equation (2.13) gives the dynamic behavior of the last important unknown term,  $C_b^+(\tau)$ , of the bifurcating solution, (2.2). Since its qualitative features depend on the signs of  $\alpha$ ,  $\beta$  and  $\eta$ , the signs of the various factors involved that are not already obvious will first be analyzed.

First consider the sign of  $(\nu_0 + Dk_b^2)^2 - 2\nu_0$ , which has simple zeros at

$$\nu_0 = 1 - Dk_b^2 \pm \sqrt{1 - 2Dk_b^2} \quad (2.17)$$

They exist, of course, only if  $Dk_b^2 < \frac{1}{2}$ . The values for  $\nu_0$  given by (2.17) are also the values of  $\nu_0$  at the intersection of  $R_b$  and  $S_b$ , if these intersections occur. After noting that  $(\nu_0 + Dk_b^2)^2 - 2\nu_0 > 0$  at  $\nu_0 = 0$ , a comparison of the above observations with Figures 1-2 and 1-3 should make it clear that

$$R_b \text{ is part of the stability boundary} \rightarrow (\nu_0 + Dk_b^2)^2 - 2\nu_0 > 0 \quad (2.18a)$$

$$S_b \text{ is part of the stability boundary} \rightarrow (\nu_0 + Dk_b^2)^2 - 2\nu_0 < 0 \quad (2.18b)$$

Therefore, in the present case,  $(\nu_0 + Dk_b^2)^2 - 2\nu_0 > 0$ .

As for the sign of  $\int_{-1}^1 y_b^3(x) dx$ , after very tedious and

unrevealing calculations using trigonometric identities, (1.20), and (1.21), one can eventually obtain the following expression.

$$\int_{-1}^1 y_b^3(x) dx = N_b^3 \left[ \frac{2}{3k_b} \frac{(\gamma_1 \gamma_2 k_b^2 \cos^2 k_b - \sin^2 k_b)}{\cos^2 2k_b} (2 + \cos^2 k_b) + \frac{k_b}{2} (\gamma_2 - \gamma_1)^2 \sin^2 k_b \right] \frac{\cos^2 k_b}{(\gamma_1 + \gamma_2) k_n \cos k_n} \cdot \left\{ (1 + \gamma_1 \gamma_2 k_b^2) + \frac{B}{2} \pm \sqrt{(1 + \gamma_1 \gamma_2 k_b^2)^2 + B} \right\}, \quad (2.19)$$

where

$$B = (\gamma_1 - \gamma_2)^2 k_b^2 > 0. \quad (2.20)$$

An easy way to see that the term in brackets, { }, is positive is from Figure 2-1.

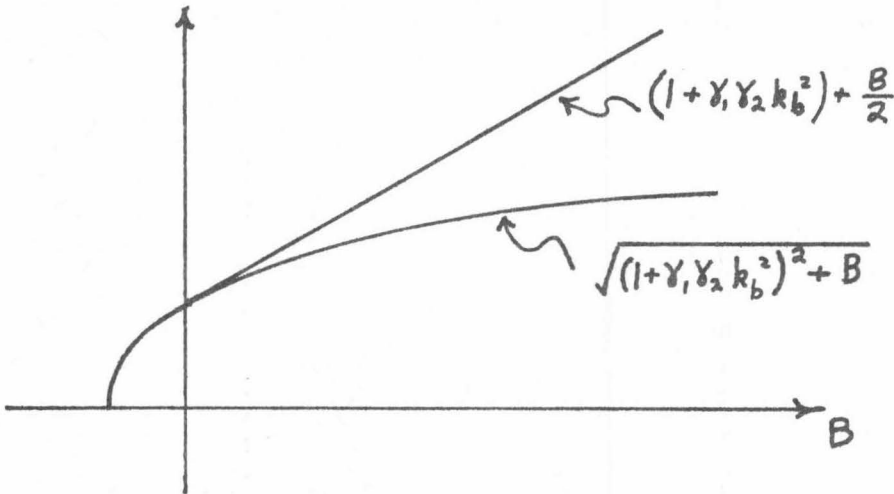


FIGURE 2-1

Therefore, all terms in the expression for  $\int_{-1}^1 y_b^3(x) dx$  are positive except  $\frac{1}{\cos k_n}$ . So

$$\int_{-1}^1 y_b^3(x) dx \begin{cases} > 0 & \text{if } b=0 \text{ or } 1, \text{ mod } 4 \\ < 0 & \text{if } b=2 \text{ or } 3, \text{ mod } 4 \end{cases} \quad (2.21)$$

The remaining factor that must be analyzed,  $Dk_b^2 - 2v_0$ , requires a more careful look at the family of hyperbolas,

$$R_n: \quad \sigma_0 D^2 k_n^4 + \sigma_0 v_0 Dk_n^2 + v_0 - Dk_n^2 = 0 \quad , \quad (2.22)$$

parts of which were found in Section 1.3 to make up the stability boundary. If  $Dk_n^2$  is temporarily considered as a continuous variable, the family of all such  $R_n$ 's are easily seen to fill the area in the  $v_0 - \sigma_0$  plane under their envelope,

$$\sigma_0 v_0 = 3 - 2\sqrt{2} \quad , \quad (2.23)$$

with each point in this  $v_0 - \sigma_0$  region having two curves of the family passing through it. To find which two curves of the family pass through a particular point, simply solve equation (2.22) for  $Dk_n^2$ .

$$Dk_n^2 = \frac{1}{2\sigma_0} \left\{ 1 - \sigma_0 v_0 \pm \sqrt{[\sigma_0 v_0 - (3 + 2\sqrt{2})][\sigma_0 v_0 - (3 - 2\sqrt{2})]} \right\} \quad (2.24)$$

See Figure 2-2.  $R_n^+$  and  $R_n^-$  were obtained from the two solutions of (2.24).

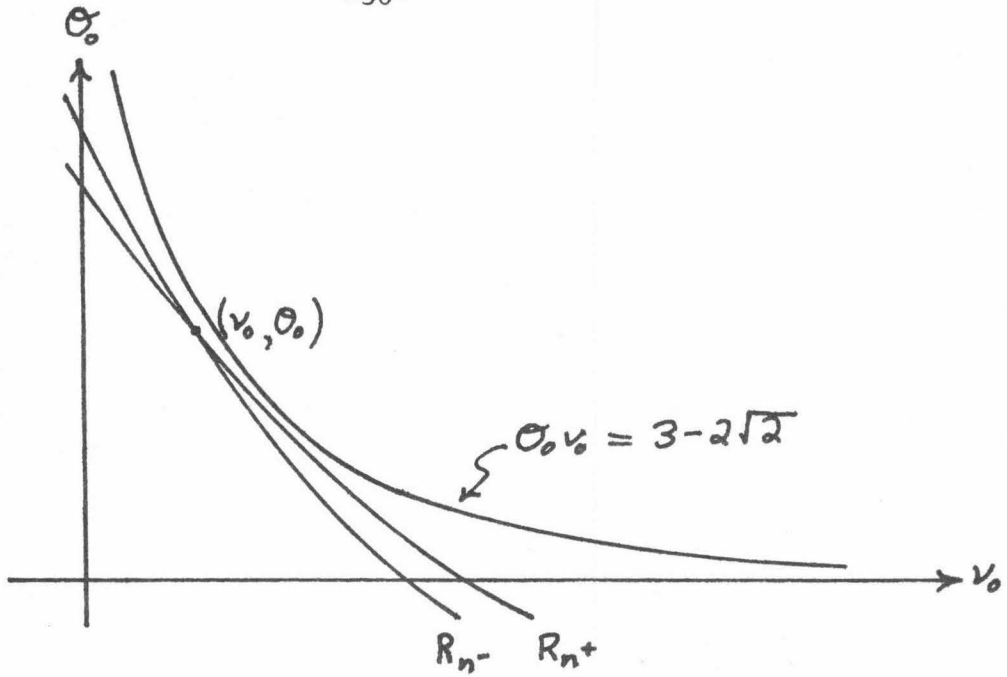


FIGURE 2-2

Now return to  $Dk_n$  discrete and look at a magnified and exaggerated portion of the stability boundary, Figure 2-3.

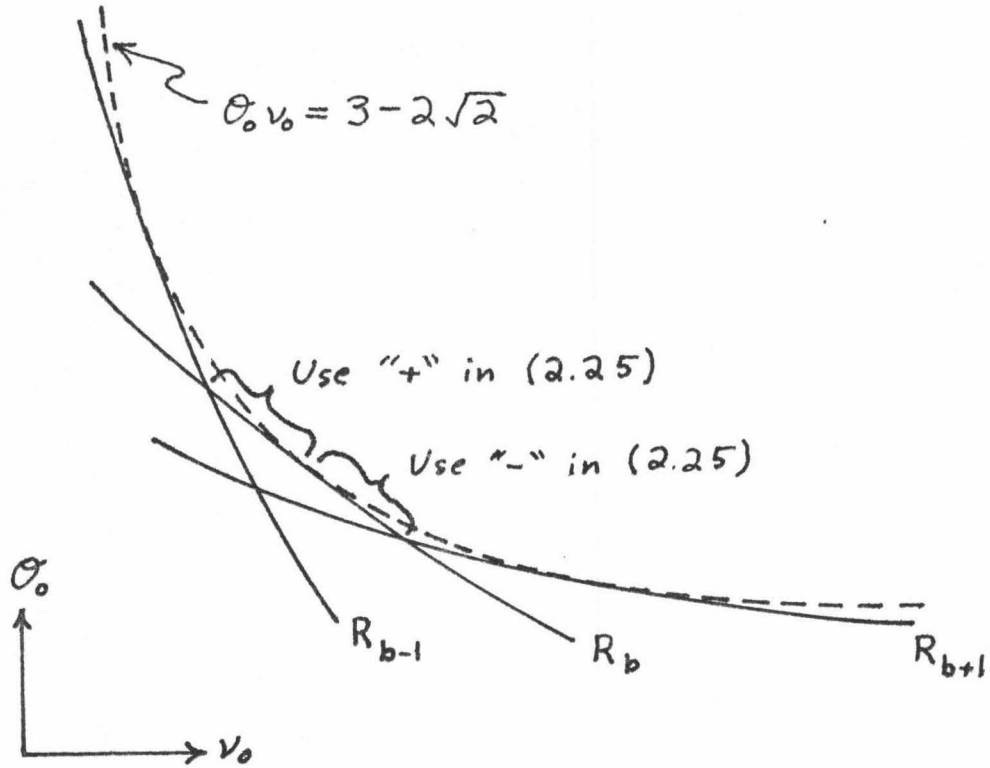


FIGURE 2-3

The idea now is to pick some values of  $\nu_0$  and  $\sigma_0$  that lie on the stability boundary portion of  $R_b$ . Equation (2.24) then gives two choices for the value of  $Dk_b^2$  at this point. Whether to use "+" or "-" in (2.24) can be seen by comparing the geometry of Figures 2-2 and 2-3 and seeing how, if  $Dk_n$  were taken to be continuous, the second member of the family of hyperbolas would have to intersect the first member (the stability boundary itself) at this point.

Knowing which sign to use in (2.24), we can then proceed as follows.

$$Dk_b^2 - 2v_0 = \frac{1}{2\sigma_0} \left\{ 1 - 5\sigma_0 v_0 \pm \sqrt{[\sigma_0 v_0 - (3+2\sqrt{2})][\sigma_0 v_0 - (3-2\sqrt{2})]} \right\} \quad (2.25)$$

Along the portion of  $R_b$  where "+" is relevant,  $Dk_b^2 - 2v_0$  is always positive. However, where "-" is relevant, there is a change in sign where

$$\sigma_0 v_0 = \frac{1}{6} < 3 - 2\sqrt{2} \quad . \quad (2.26)$$

That is, for this lower portion of  $R_b$ ,

$$Dk_b^2 - 2v_0 > 0 \iff \sigma_0 v_0 > \frac{1}{6} \quad . \quad (2.27)$$

However, since  $R_b$  stops being part of the stability boundary when it intersects  $R_{b+1}$ ,  $\sigma_0 v_0$  may remain larger than  $\frac{1}{6}$  for all of the stability boundary portion of  $R_b$ . In fact, further analysis shows that this is indeed the case for all but the first few values of  $b$ .

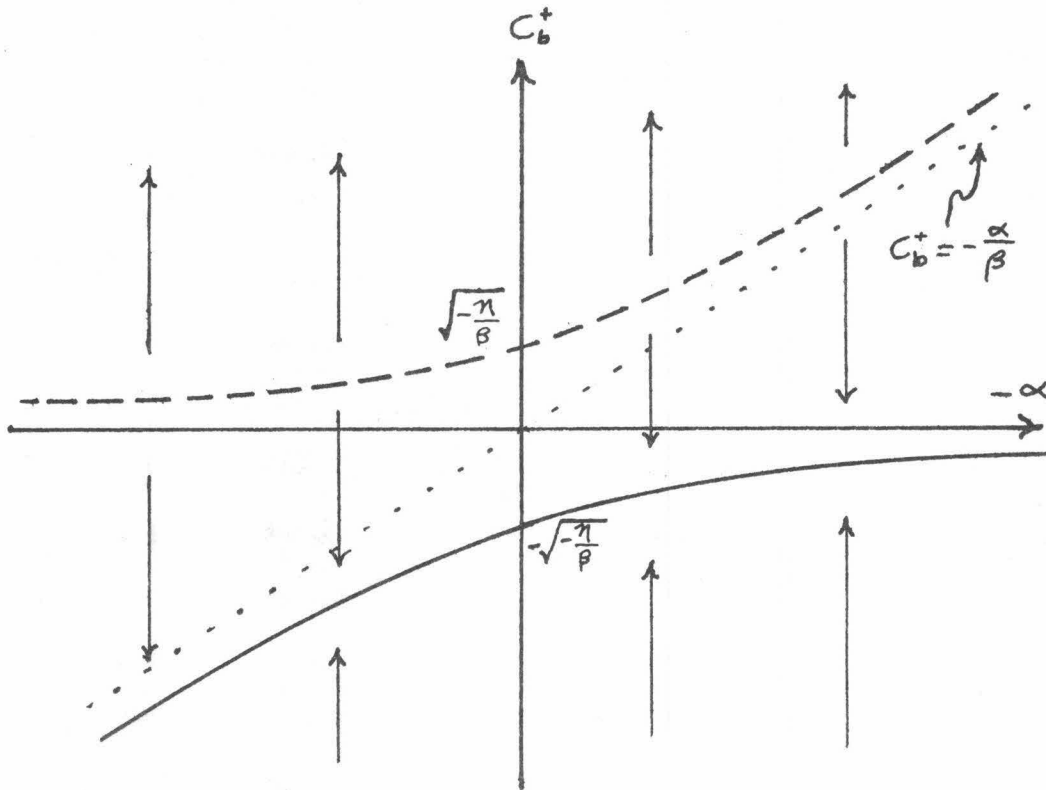
In summary then,  $Dk_b^2 - 2v_0 > 0$  all along the hyperbolic sections of the stability boundary, except that for the first few values of  $b$  there is a small segment of  $R_b$  adjacent to  $R_{b+1}$  for which  $Dk_b^2 - 2v_0 < 0$ .

With these results in hand, (2.13) may now be analyzed with a good understanding of the signs of the various factors involved.

Recalling that  $v = v_0 + \epsilon v_1 + O(\epsilon^2)$ , it is clear that  $v_1$  large and positive corresponds to the stable region of the trivial solution and that  $v_1$  large and negative corresponds to the unstable region,

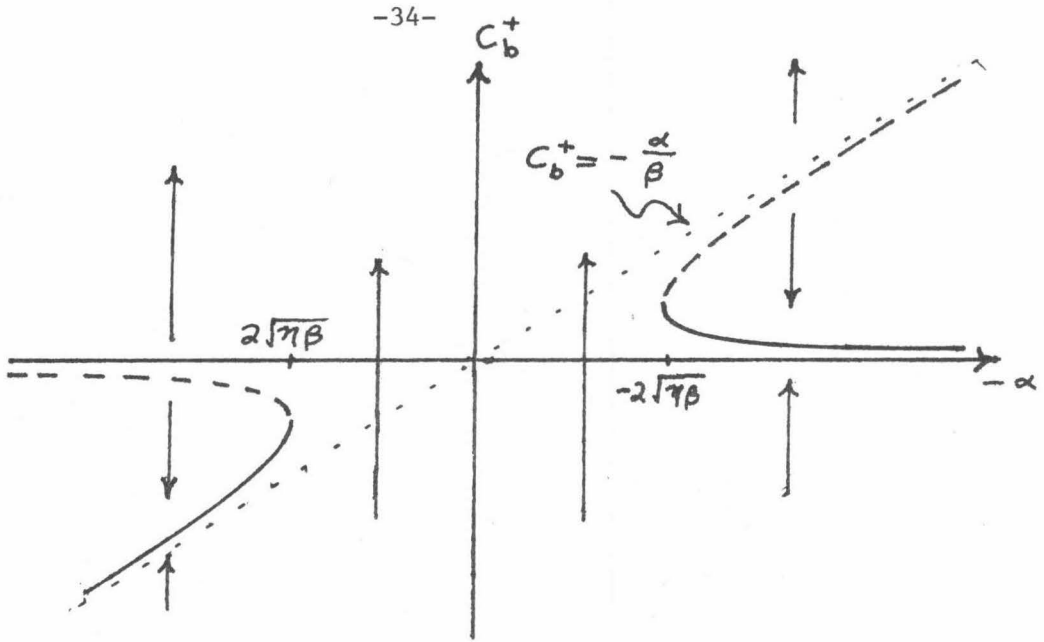
where new, stable solutions are expected. To answer our questions about how new solutions appear as the unstable region is entered, the most enlightening procedure is to look at the behavior of (2.13) as  $v_1$  changes from large and positive to large and negative, which from (2.16) is the same as changing  $(-\alpha)$  from large and positive to large and negative.

The four possible qualitative behaviors are contained in Figures 2-4 through 2-7. Solid lines indicate stable steady states, and dashed lines indicate unstable steady states. The arrows are meant to indicate the dynamic behavior of (2.13) for each value of  $\alpha$ .

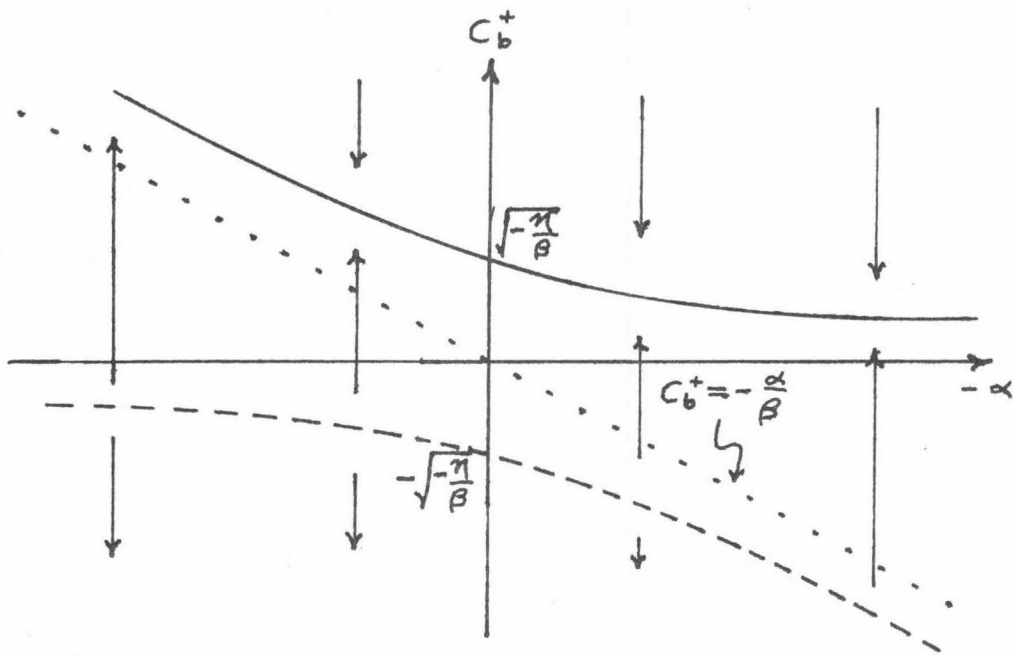


$$\beta > 0, \eta < 0$$

FIGURE 2-4



$\beta > 0, \eta > 0$   
FIGURE 2-5



$\beta < 0, \eta > 0$   
FIGURE 2-6



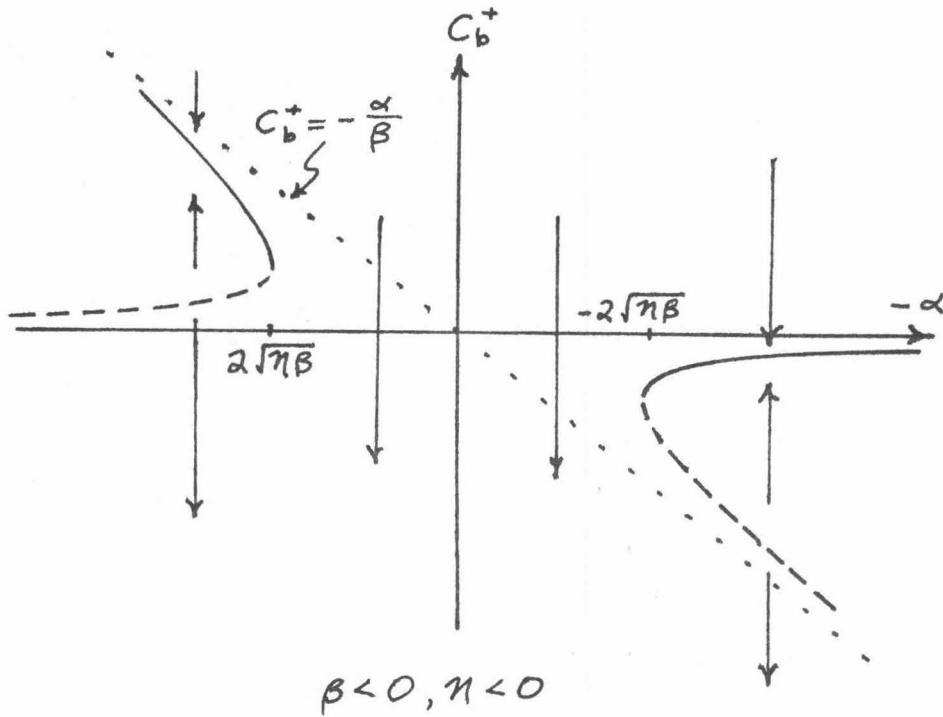


FIGURE 2-7

In these diagrams,  $-\alpha$  plays the role of the bifurcation parameter, since it is just proportional to  $v_1$  but shifted due to the integral of  $\theta_1(x)$  in (2.16).  $\eta$  plays the role of an imperfection parameter, in which  $\eta = 0$  separates the cases where there is a smooth transition from stable trivial solution to stable nontrivial solution as the stability boundary is crossed (Figures 2-4 and 2-6) and the cases where, as the stability boundary is crossed, there is an intermediate region where no steady states exist (Figures 2-5 and 2-7).

For those initial conditions that lead to trajectories that do not approach some steady state, the above analysis says little, since the solution at each order must stay bounded for the asymptotic expansion to give a consistent ordering of terms. However, for those initial conditions that do lead to solutions that approach steady states of

(2.13), the entire story is now clear. As  $\tau \rightarrow \infty$ ,  $C_b^+(\tau)$  approaches one of the two steady states,

$$C_b^+(\infty) = -\frac{\alpha}{2\beta} \pm \sqrt{\left(\frac{\alpha}{2\beta}\right)^2 - \frac{\eta}{\beta}} \quad , \quad (2.28)$$

where the appropriate sign is clear from Figures 2-4 through 2-7. Since the transient terms in (2.2) disappear as  $t \rightarrow \infty$ , the bifurcating solutions just inside the portion of the stability boundary described by the curve  $R_b$  approach the steady state

$$\begin{pmatrix} q \\ h \end{pmatrix} = \rho_0 \begin{pmatrix} v^2 \\ v \end{pmatrix} + 2\epsilon \left( -\frac{\alpha}{2\beta} \pm \sqrt{\left(\frac{\alpha}{2\beta}\right)^2 - \frac{\eta}{\beta}} \right) \begin{pmatrix} v_0 + Dk_b^2 \\ 1 \end{pmatrix} y_b(x) \quad (2.29)$$

to lowest order. A linear analysis would suggest this spatial dependence, but the nonlinear analysis was required to obtain the amplitude.

CHAPTER 3

BIFURCATION THROUGH TWO REAL EIGENVALUES

This chapter deals with the behavior of solutions near the intersection of two hyperbolic sections of the stability boundary (see Figure 1-4). Let the two hyperbolas be called  $R_b$  and  $R_{b+1}$ , for some appropriate integer  $b$ . Then  $v_0$  and  $\sigma_0$  satisfy the two equations:

$$\begin{aligned} \sigma_0 D^2 k_b^4 + \sigma_0 v_0 D k_b^2 + v_0 - D k_b^2 &= 0 \\ \sigma_0 D^2 k_{b+1}^4 + \sigma_0 v_0 D k_{b+1}^2 + v_0 - D k_{b+1}^2 &= 0 \end{aligned} \quad (3.1)$$

In a similar fashion as in Chapter 2, all modes of (1.37) except for  $n = b$  and  $n = b + 1$  have  $\sigma_n^{\pm}$  with negative real parts. Therefore

$$\begin{pmatrix} A_1 \\ H_1 \end{pmatrix} = 2C_b^+(\tau) \begin{pmatrix} v_0 + D k_b^2 \\ 1 \end{pmatrix} y_b(x) + 2C_{b+1}^+(\tau) \begin{pmatrix} v_0 + D k_{b+1}^2 \\ 1 \end{pmatrix} y_{b+1}(x) \quad (3.2)$$

+ transient terms .

(1.35) then becomes

$$\frac{\partial}{\partial t} \begin{pmatrix} A_2 \\ H_2 \end{pmatrix} - L_0 \begin{pmatrix} A_2 \\ H_2 \end{pmatrix} = \quad (3.3)$$

$$-4 \frac{dC_b^+}{d\tau} (\tau) \begin{pmatrix} \nu_0 + Dk_b^2 \\ 1 \end{pmatrix} y_b(x) - 4 \frac{dC_{b+1}^+}{d\tau} (\tau) \begin{pmatrix} \nu_0 + Dk_{b+1}^2 \\ 1 \end{pmatrix} y_{b+1}(x)$$

$$-4 C_b^+(\tau) \begin{pmatrix} Dk_b^2 (\nu_0 + Dk_b^2) \theta_1(x) + 2\nu_1 \\ \nu_1 \end{pmatrix} y_b(x)$$

$$-4 C_{b+1}^+(\tau) \begin{pmatrix} Dk_{b+1}^2 (\nu_0 + Dk_{b+1}^2) \theta_1(x) + 2\nu_1 \\ \nu_1 \end{pmatrix} y_{b+1}(x)$$

$$+ \frac{8D}{\rho_0 \nu_0^2} [C_b^+(\tau)]^2 \begin{pmatrix} k_b^2 (Dk_b^2 - 2\nu_0) \\ 0 \end{pmatrix} y_b^2(x)$$

$$+ \frac{8D}{\rho_0 \nu_0^2} 2 C_b^+(\tau) C_{b+1}^+(\tau) \begin{pmatrix} Dk_b^2 k_{b+1}^2 - \nu_0 (k_b^2 + k_{b+1}^2) \\ 0 \end{pmatrix} y_b(x) y_{b+1}(x)$$

$$+ \frac{8D}{\rho_0 \nu_0^2} [C_{b+1}^+(\tau)]^2 \begin{pmatrix} k_{b+1}^2 (Dk_{b+1}^2 - 2\nu_0) \\ 0 \end{pmatrix} y_{b+1}^2(x)$$

$$+ \begin{pmatrix} \nu_0^2 \rho_2(x) \\ 0 \end{pmatrix} + \text{transient terms} \quad .$$

As in Chapter 2, conditions must be imposed on the right hand side of (3.3) in order to guarantee that  $A_2$  and  $H_2$  remain bounded for all time. Again, the transient terms in (3.3) are harmless, since they produce transient terms for  $A_2$  and  $H_2$ . After the remaining terms are resolved into the spatial components  $\{y_n(x)\}$ , the non-transient terms of the right hand side of (3.3) may be written

$$\begin{pmatrix} v_b \\ w_b \end{pmatrix} y_b(x) e^{\sigma_b^+ t} + \begin{pmatrix} v_{b+1} \\ w_{b+1} \end{pmatrix} y_{b+1}(x) e^{\sigma_{b+1}^+ t} + \left( \begin{array}{c} \text{other} \\ \text{components} \end{array} \right). \quad (3.4)$$

By Lemma 1 of Chapter 2, since  $\sigma_b^+ = 0$  and  $\sigma_{b+1}^+ = 0$  are the only eigenvalues of  $L_0$  that have zero real part, only the components in (3.4) containing  $y_b(x)$  and  $y_{b+1}(x)$  produce secular terms.  $A_2$  and  $H_2$  will be bounded for all  $t$  if

$$\begin{aligned} v_b - w_b (\sigma_b^- + \nu_0 + Dk_b^2) &= 0 \\ v_{b+1} - w_{b+1} (\sigma_{b+1}^- + \nu_0 + Dk_{b+1}^2) &= 0 \end{aligned} \quad (3.5)$$

As in going from (2.8) to (2.11), this is

$$\begin{aligned} (\nu_0 + Dk_b^2) v_b - 2\nu_0 w_b &= 0 \\ (\nu_0 + Dk_{b+1}^2) v_{b+1} - 2\nu_0 w_{b+1} &= 0 \end{aligned} \quad (3.6)$$

After substituting the actual values for  $v_b, w_b, v_{b+1}, w_{b+1}$  from (3.3), (3.6) can be manipulated to the following.

$$\frac{d}{d\tau} C_b^+ = \beta [C_b^+]^2 + \alpha C_b^+ + \eta + \zeta C_{b+1}^+ + \varphi C_b^+ C_{b+1}^+ + \psi [C_{b+1}^+]^2 \quad (3.7a)$$

$$\frac{d}{d\tau} C_{b+1}^+ = \beta' [C_{b+1}^+]^2 + \alpha' C_{b+1}^+ + \eta' + \zeta' C_b^+ + \varphi' C_b^+ C_{b+1}^+ + \psi' [C_b^+]^2 \quad (3.7b)$$

$\beta, \alpha, \eta$  are the same as those defined in Chapter 2, equations (2.14) through (2.16).

$$S = -Dk_{b+1}^2 \frac{(\nu_0 + Dk_b^2)(\nu_0 + Dk_{b+1}^2)}{(\nu_0 + Dk_b^2)^2 - 2\nu_0} \int_{-1}^1 \theta_1(x) y_b(x) y_{b+1}(x) dx \quad (3.8)$$

$$\varphi = \frac{4D(\nu_0 + Dk_b^2) [Dk_b^2 k_{b+1}^2 - \nu_0(k_b^2 + k_{b+1}^2)]}{\rho_0 \nu_0^2 (\nu_0 + Dk_b^2)^2 - 2\nu_0} \int_{-1}^1 y_b^2(x) y_{b+1}(x) dx \quad (3.9)$$

$$\psi = \frac{2Dk_{b+1}^2 (\nu_0 + Dk_b^2) (Dk_{b+1}^2 - 2\nu_0)}{\rho_0 \nu_0^2 (\nu_0 + Dk_b^2)^2 - 2\nu_0} \int_{-1}^1 y_b(x) y_{b+1}^2(x) dx \quad (3.10)$$

The primed quantities are obtained from the unprimed by interchanging  $b$  and  $b + 1$  in the above definitions.

A complete analysis of (3.7) similar to that of (2.13) in Chapter 2 will not be attempted. The added complexities are formidable. Moreover, the range of phenomena that can be expected in equations as general as (3.7) is tremendous, since all possible terms through the quadratic appear. Note especially the presence of the linear cross-terms,  $\zeta$  and  $\zeta'$ , which would not appear if  $\theta_1(x)$  were constant.

Short of finding explicit formulas for all solutions of (3.7), the most desirable way to proceed is to obtain the  $C_b^+ - C_{b+1}^+$  phase plane diagrams for (3.7): one diagram for each value of  $\alpha$ . As the stability boundary is crossed,  $\nu_1$  decreases, which changes  $\alpha$  and therefore alters the phase portrait. This process shows how the dynamic behavior of (3.7) changes as the stability boundary is crossed. However, due to the number and complexity of the parameters in (3.7), even this procedure is all but beyond systematic analysis. Such a procedure will be employed in the following chapter to a set of equations that are of a more restricted form than (3.7).

Before finishing this chapter, the important point of how it relates to the previous chapter will be taken up, again from the geometrical

standpoint of the stability boundary, in order to help solidify ideas.

First recall the expansions for  $v$  and  $\theta$ , (1.26) and (1.27).

$$v = v_0 + \epsilon v_1 + O(\epsilon^2) \quad (1.26)$$

$$\theta = \theta_0 + \epsilon \theta_1(x) + O(\epsilon^2) \quad (1.27)$$

In Chapter 2,  $v_0$  and  $\theta_0$  were chosen to locate a position on the curve  $R_b$ , and  $v_1$  and  $\theta_1(x)$  were considered as perturbations of  $v$  and  $\theta$  from these critical values.  $v_1$  was then used to measure horizontal distance into or out of the unstable region (Figure 1-4), while  $\theta_1(x)$  was considered fixed, since it cannot describe an unambiguous direction in the  $v$ - $\theta$  plane. The results of Chapter 2 for  $v_0$  and  $\theta_0$  lying along  $R_b$  should not be considered valid within  $O(\epsilon)$  of the intersections of  $R_b$  with  $R_{b+1}$  or  $R_{b-1}$ , since in these small regions  $\sigma_{b+1}^+$  or  $\sigma_{b-1}^+$  is so small that its corresponding mode in (1.37) cannot be considered "transient" in (2.2). In this case, it is more appropriate to explicitly keep track of both modes (assume without loss of generality that they correspond to  $b$  and  $b+1$ ). That is, when  $v$  and  $\theta$  are within  $O(\epsilon)$  of the intersection of  $R_b$  and  $R_{b+1}$  on the stability boundary, both  $\sigma_b^+$  and  $\sigma_{b+1}^+$  are so small that the evolution in time of their modes is sufficiently slow that it is only correct to look at them on the slow,  $\tau = \epsilon t$ , time scale. Both these modes should therefore be considered non-transient, and a solution like (3.2) is correct.

To implement this, consider the perturbations of  $v$  and  $\theta$  from  $v_0$  and  $\theta_0$  to have the following form.

$$v_1 = v_{10} + v_{11} \quad (3.11)$$

$$\theta_1 = \theta_{10} + \theta_{11}(x) \quad (3.12)$$

Here, let  $\epsilon v_{10}$  and  $\epsilon \theta_{10}$  be used to locate position along the stability boundary, measured from  $(v_0, \theta_0)$ , the point at which  $L_0$  has two linearly independent eigenvectors with eigenvalue zero. From the definition of  $R_n$ , (1.23),

$$\frac{d\theta}{dv}(v_0, \theta_0) = \frac{-2}{(v_0 + Dk_n^2)^2}$$

Since  $R_b$  and  $R_{b+1}$  can be locally approximated by their tangents, it is clear that

$$\theta_{10} = \frac{-2}{(v_0 + Dk_b^2)^2} v_{10} \quad \text{along } R_b \quad (3.13)$$

and

$$\theta_{10} = \frac{-2}{(v_0 + Dk_{b+1}^2)^2} v_{10} \quad \text{along } R_{b+1}. \quad (3.14)$$

$v_{10}$  can therefore be used to parameterize distance along the stability boundary within  $O(\epsilon)$  of the point  $(v_0, \theta_0)$ .  $v_{11}$  and  $\theta_{11}(x)$  are then left to play the analogous role that  $v_1$  and  $\theta_1(x)$  played in Chapter 2 of giving perturbations from a specific point on the stability boundary.

With these definitions and ideas in hand, it is now easy to show how solutions of (3.7) link up with solutions along  $R_b$  and  $R_{b+1}$  to give solutions all along the hyperbolic sections of the stability boundary,



including their intersections. For the connection of (3.7) with (2.13) for  $R_b$ , substitute (3.11), (3.12) and (3.13) into the coefficients of (3.7). All formulas remain the same except,

$$\alpha = -\frac{Dk_b^2}{[(v_0 + Dk_b^2)^2 - 2v_0]} \left\{ 2v_{10} + 2v_{11} + (v_0 + Dk_b^2)^2 \left[ -\frac{2}{(v_0 + Dk_b^2)^2} v_{10} + \int_{-1}^1 \sigma_{11}(x) y_b^2(x) dx \right] \right\}$$

or

$$\alpha = -\frac{Dk_b^2}{[(v_0 + Dk_b^2)^2 - 2v_0]} \left[ 2v_{11} + (v_0 + Dk_b^2)^2 \int_{-1}^1 \sigma_{11}(x) y_b^2(x) dx \right] \quad (3.15)$$

$$\alpha' = -\frac{Dk_{b+1}^2}{[(v_0 + Dk_{b+1}^2)^2 - 2v_0]} \left\{ 2v_{10} \left[ 1 - \left( \frac{v_0 + Dk_{b+1}^2}{v_0 + Dk_b^2} \right)^2 \right] + 2v_{11} + (v_0 + Dk_{b+1}^2)^2 \int_{-1}^1 \sigma_{11}(x) y_{b+1}^2(x) dx \right\} \quad (3.16)$$

$$S = -Dk_{b+1}^2 \frac{(v_0 + Dk_b^2)(v_0 + Dk_{b+1}^2)}{(v_0 + Dk_b^2)^2 - 2v_0} \int_{-1}^1 \sigma_{11}(x) y_b(x) y_{b+1}(x) dx \quad (3.17)$$

$$S' = -Dk_b^2 \frac{(v_0 + Dk_b^2)(v_0 + Dk_{b+1}^2)}{(v_0 + Dk_{b+1}^2)^2 - 2v_0} \int_{-1}^1 \sigma_{11}(x) y_b(x) y_{b+1}(x) dx \quad (3.18)$$

As the basic stability boundary point from which the perturbations,  $v_{11}$  and  $\sigma_{11}(x)$ , are measured moves from  $(v_0, \sigma_0)$  to the interior of  $R_b$ , this corresponds to  $v_{10}$  becoming very large and negative. From (3.16), this corresponds to  $\alpha'$  also becoming large and negative, so that the term with  $\alpha'$  dominates the right hand side of (3.7b).

$$\frac{d}{d\tau} C_{b+1}^+ = \alpha' C_{b+1}^+ \quad (3.19)$$

Therefore,  $C_{b+1}^+$  very quickly approaches zero. Substituting  $C_{b+1}^+ = 0$

into (3.7a), it becomes (2.13), with  $v_{11}$  playing the role of  $v_1$  and  $\theta_{11}(x)$  playing the role of  $\theta_1(x)$  as previously discussed.

A similar argument holds when the basic stability boundary point from which the perturbations,  $v_{11}$  and  $\theta_{11}(x)$  are measured moves from  $(v_0, \theta_0)$  to the interior of  $R_{b+1}$ . Now (3.11), (3.12) and (3.14) are substituted into the coefficients of (3.7). All coefficients are unaffected except  $\alpha, \alpha', \zeta, \zeta'$ .  $\zeta$  and  $\zeta'$  are still given by (3.17) and (3.18).  $\alpha$  and  $\alpha'$  become the following.

$$\alpha = -\frac{Dk_b^2}{[(v_0 + Dk_b^2)^2 - 2v_0]} \left\{ 2v_{10} \left[ 1 - \left( \frac{v_0 + Dk_b^2}{v_0 + Dk_{b+1}^2} \right)^2 \right] + 2v_{11} + (v_0 + Dk_b^2)^2 \int_{-1}^1 \theta_{11}(x) y_b^2(x) dx \right\} \quad (3.20)$$

$$\alpha' = -\frac{Dk_{b+1}^2}{[(v_0 + Dk_{b+1}^2)^2 - 2v_0]} \left[ 2v_{11} + (v_0 + Dk_{b+1}^2)^2 \int_{-1}^1 \theta_{11}(x) y_{b+1}^2(x) dx \right] \quad (3.21)$$

Moving along  $R_{b+1}$  corresponds to  $v_{10}$  becoming large and positive.

Similarly to the previous case, this makes  $\alpha$  large and negative, which, by (3.7a) makes  $C_b^+$  approach zero exponentially quickly. (3.7b) with  $C_b^+ = 0$  becomes analogous to (2.13) with  $b$  replaced by  $b+1$ ,  $v_1$  replaced by  $v_{11}$ , and  $\theta_1(x)$  replaced by  $\theta_{11}(x)$ .

CHAPTER 4

BIFURCATION THROUGH ONE REAL EIGENVALUE AND A  
COMPLEX PAIR OF EIGENVALUES

In this chapter, the behavior of solutions near either of the two points where  $S_1$  intersects one of the  $R_n$  on the stability boundary (see Figure 1-4) will be demonstrated. This case has the dual advantages of being less well understood and therefore interesting and of leading to more tractable differential equations for the "slow-time" amplitude than occurred in Chapter 3.

4.1 Differential Equations for the Slow-Time Behavior

Let the hyperbolic section intersected by  $S_1$  on the stability boundary be referred to as  $R_b$ . Then  $v_0$  and  $\sigma_0$  satisfy the following two equations.

$$\sigma_0 Dk_i^2 + v_0 + Dk_i^2 - 1 = 0 \quad (4.1)$$

$$\sigma_0 D^2 k_b^4 + \sigma_0 v_0 Dk_b^2 + v_0 - Dk_b^2 = 0 \quad (4.2)$$

This implies that  $\sigma_b^+ = 0$  and that  $\text{Re}(\sigma_1^+) = 0$ . By construction of the stability boundary, all other eigenvalues of  $L_0$  have negative real parts. Therefore, after a little computation, (1.37) becomes the following.

$$\begin{pmatrix} A_1 \\ H_1 \end{pmatrix} = 2C_1(\tau) \left( \nu_0 + Dk_1^2 + i \sqrt{2\nu_0 - (\nu_0 + Dk_1^2)^2} \right) y_1(x) e^{\sigma_1^+ t} + C.C. \quad (4.3)$$

$$+ 2C_b^+(\tau) \left( \nu_0 + Dk_b^2 \right) y_b(x) + \text{transient terms}$$

Here "+ C.C." means "then add the complex conjugate of the previous quantities".  $C_1(\tau)$  is now a complex-valued quantity whose real and imaginary parts take the place of  $C_1^{\pm}(\tau)$ . The additional fact that  $A_1$  and  $H_1$  must be real was also used in writing (4.3) in the above form. Finally note from (2.18b) that

$$2\nu_0 - (\nu_0 + Dk_1^2)^2 > 0, \quad (4.4)$$

so that the argument of the square root in (4.3) is positive. The square root is taken positive for positive argument.

Using (4.3), (1.35) becomes

$$\frac{\partial}{\partial t} \begin{pmatrix} A_2 \\ H_2 \end{pmatrix} - L_0 \begin{pmatrix} A_2 \\ H_2 \end{pmatrix} = \quad (4.5)$$

$$\left[ e^{2\sigma_1^+ t} \frac{8}{\rho_0 \nu_0^2} C_1^2(\tau) \left( \nu_0^2 - 2\nu_0 + 2D^2 k_1^4 + 2i(Dk_1^2 - \nu_0) \sqrt{2\nu_0 - (\nu_0 + Dk_1^2)^2} \right) y_1^2(x) \right. \\ \left. + C.C. \right]$$

$$+ \left\{ e^{\sigma_1^+ t} \left[ -4 \frac{dC_1(\tau)}{d\tau} \left( \nu_0 + Dk_1^2 + i \sqrt{2\nu_0 - (\nu_0 + Dk_1^2)^2} \right) y_1(x) \right. \right.$$

$$-4C_1(\tau) \left( \sigma_1(x) Dk_1^2 (v_0 + Dk_1^2 + i \sqrt{2v_0 - (v_0 + Dk_1^2)^2}) + 2v_1 \right) y_1(x)$$

$$+ \frac{16}{\rho_0 v_0^2} C_1(\tau) C_b^+(\tau)$$

$$\left( Dk_1^2 k_b^2 - v_0 D(k_1^2 + k_b^2) + i(Dk_b^2 - v_0) \sqrt{2v_0 - (v_0 + Dk_1^2)^2} \right) y_1(x) y_b(x)$$

+ C.C. } }

$$-4 \frac{dC_b^+}{d\tau}(\tau) \left( v_0 + Dk_b^2 \right) y_b(x)$$

$$-4C_b^+(\tau) \left( \sigma_1(x) Dk_b^2 (v_0 + Dk_b^2) + 2v_1 \right) y_b(x)$$

$$+ \frac{16}{\rho_0 v_0} C_1(\tau) C_1^*(\tau) \left( -v_0 + 2 - 4Dk_1^2 \right) y_1^2(x)$$

$$+ \frac{8Dk_b^2}{\rho_0 v_0^2} [C_b^+(\tau)]^2 \left( Dk_b^2 - 2v_0 \right) y_b^2(x)$$

$$+ \left( v_0^2 \rho_2(x) \right) + \text{transient terms} ,$$

where  $C_1^*(\tau)$  is the complex conjugate of  $C_1(\tau)$ .

Again, since  $A_2$  and  $H_2$  must be bounded in time, conditions must be imposed on the right hand side of (4.5) to insure that no secular terms are produced in the solution for  $A_2$  and  $H_2$ . As before, after resolving the right hand side of (4.5) into the spatial component  $\{y_n(x)\}$ , Lemma 1 of Chapter 2 (equations (2.4) through (2.7)) easily gives these

conditions. Transient terms in the right hand side of (4.5) produce transient terms for  $A_2$  and  $H_2$ , so there is no secularity from these terms by (2.5). The forcing terms in (4.5) that are proportional to  $e^{\pm 2i\sigma_1^+ t}$  produce terms for  $A_2$  and  $H_2$  that are proportional to  $e^{\pm 2i\sigma_1^+ t}$ , so there is no secularity from these terms by (2.5). Of the forcing terms proportional to  $e^{\pm \sigma_1^+ t}$ , the  $y_1(x)$  component will produce secular terms by (2.6) and (2.7), and all other components will not produce secular terms by (2.5). Of the terms independent of  $t$ , the  $y_b(x)$  component will produce secular terms by (2.7) since  $\sigma_b^+ = 0$ , and all other components will not produce secular terms by (2.5). Therefore, the secularity-producing terms in the right hand side of (4.5) may be written

$$\begin{pmatrix} v_1 \\ w_1 \end{pmatrix} y_1(x) e^{\sigma_1^+ t} + C.C. + \begin{pmatrix} v_b \\ w_b \end{pmatrix} y_b(x) \quad (4.6)$$

Lemma 1 then gives the precise conditions that  $A_2$  and  $H_2$  be bounded in time.

$$v_1 - w_1 (\sigma_1^- + \nu_0 + Dk_1^2) = 0 \quad (4.7)$$

$$\text{Complex conjugate of (4.7).} \quad (4.8)$$

$$v_b - w_b (\sigma_b^- + \nu_0 + Dk_b^2) = 0 \quad (4.9)$$

(4.8) is superfluous. After substituting the actual values for  $v_1$  and  $w_1$ , (4.7) can be manipulated to the following.

$$\frac{dC_1}{d\tau} 2\sqrt{2\nu_0 - (\nu_0 + Dk_1^2)^2} = \quad (4.10)$$

$$C_1 \left\{ Dk_1^2 \left[ -\sqrt{2\nu_0 - (\nu_0 + Dk_1^2)^2} + i(\nu_0 + Dk_1^2) \right] \int_{-1}^1 \theta_1(x) y_1^2(x) dx \right. \\ \left. - \left[ \sqrt{2\nu_0 - (\nu_0 + Dk_1^2)^2} + i(\nu_0 + Dk_1^2 - 2) \right] \nu_1 \right\} \\ + C_1 C_b^+ \frac{4}{\rho_0 \nu_0^2} \left\{ (Dk_b^2 - \nu_0) \sqrt{2\nu_0 - (\nu_0 + Dk_1^2)^2} \right. \\ \left. + i \left[ \nu_0 D(k_1^2 + k_b^2) - D^2 k_1^2 k_b^2 \right] \right\} \int_{-1}^1 y_1^2(x) y_b(x) dx$$

Now express the complex quantity  $C_1$  in polar coordinates.

$$C_1 = \sqrt{F} e^{-i\phi}, \quad (4.11)$$

where  $F$  and  $\phi$  are real. Using the easily derived formulas,

$$\frac{dF}{d\tau} = 2 \text{ Real Part } \left( C_1^* \frac{dC_1}{d\tau} \right) \quad (4.12)$$

$$F \frac{d\phi}{d\tau} = \text{Imaginary Part } \left( C_1^* \frac{dC_1}{d\tau} \right), \quad (4.13)$$

(4.10) implies the following two equations.

$$\begin{aligned} \frac{dF}{d\tau} = & -F \left( \nu_1 + Dk_1^2 \int_{-1}^1 \theta_1(x) y_1^2(x) dx \right) \\ & + FC_b^+ \frac{4}{\rho_0 \nu_0^2} (Dk_b^2 - \nu_0) \int_{-1}^1 y_1^2(x) y_b(x) dx \end{aligned} \quad (4.14)$$

$$\begin{aligned} \frac{d\phi}{d\tau} = & \frac{1}{2\sqrt{2\nu_0 - (\nu_0 + Dk_1^2)^2}} \left[ (2 - \nu_0 - Dk_1^2) \nu_1 \right. \\ & \left. + Dk_1^2 (\nu_0 + Dk_1^2) \int_{-1}^1 \theta_1(x) y_1^2(x) dx \right] \\ & + C_b^+ \frac{2D}{\rho_0 \nu_0^2 \sqrt{2\nu_0 - (\nu_0 + Dk_1^2)^2}} \left[ \nu_0 (k_1^2 + k_b^2) - Dk_1^2 k_b^2 \right] \int_{-1}^1 y_1^2(x) y_b(x) dx \end{aligned} \quad (4.15)$$

With the following definitions,

$$\omega = \frac{1}{2\sqrt{2\nu_0 - (\nu_0 + Dk_1^2)^2}} \left[ (2 - \nu_0 - Dk_1^2) \nu_1 + Dk_1^2 (\nu_0 + Dk_1^2) \int_{-1}^1 \theta_1(x) y_1^2(x) dx \right] \quad (4.16)$$

$$\xi = \frac{2D}{\rho_0 \nu_0^2 \sqrt{2\nu_0 - (\nu_0 + Dk_1^2)^2}} \left[ \nu_0 (k_1^2 + k_b^2) - Dk_1^2 k_b^2 \right] \int_{-1}^1 y_1^2(x) y_b(x) dx \quad (4.17)$$

$$\hat{\alpha} = - \left( \nu_1 + Dk_1^2 \int_{-1}^1 \theta_1(x) y_1^2(x) dx \right) \quad (4.18)$$

$$\hat{\phi} = \frac{4}{\rho_0 \nu_0^2} (Dk_b^2 - \nu_0) \int_{-1}^1 y_1^2(x) y_b(x) dx \quad , \quad (4.19)$$

(4.14) and (4.15) become the following.

$$\frac{d\phi}{d\tau} = \omega + \xi C_b^+ \quad (4.20)$$

$$\frac{dF}{d\tau} = \hat{\alpha} F + \hat{\phi} F C_b^+ \quad (4.21)$$



Similarly to the procedure used in Chapter 2 and 3, after substituting the actual values for  $v_b$  and  $w_b$ , (4.9) can be manipulated to the following.

$$\frac{dC_b^+}{d\tau} = \beta [C_b^+]^2 + \alpha C_b^+ + \eta + \chi F \quad (4.22)$$

where

$$\chi = -\frac{4}{\rho_0 v_0} \left[ \frac{(v_0 + Dk_b^2)(v_0 + 4Dk_b^2 - 2)}{(v_0 + Dk_b^2)^2 - 2v_0} \right] \int_{-1}^1 y_1^2(x) y_b(x) dx \quad (4.23)$$

and  $\beta$ ,  $\alpha$ ,  $\eta$  are defined in Chapter 2, equations (2.14) through (2.16). For convenience, equations (4.21) and (4.22) will be referred to as the system, T.

$$\begin{aligned} T: \quad \frac{dC_b^+}{d\tau} &= \beta [C_b^+]^2 + \alpha C_b^+ + \eta + \chi F \\ \frac{dF}{d\tau} &= \hat{\alpha} F + \hat{\varphi} F C_b^+ \end{aligned} \quad (4.24)$$

The reason for expressing  $C_1(\tau)$  in polar coordinates can now be seen in that (4.21) and (4.22) uncouple from (4.20). Even though there are three quantities to determine, T can be used to completely solve for two of them, then (4.20) yields the third. T can be used to describe  $C_b^+ - F$  phase plane systems, where F must be nonnegative since it represents a positive amplitude.

#### 4.2 Expected Behavior and the Broader Context

Looking ahead a little, three general behaviors will result from the analysis of T. First, there will be trajectories that will approach

infinity as  $\tau$  increases. For these trajectories, the above analysis says little since the unbounded growth of  $A_1$  and  $H_1$ , that these trajectories imply, questions the validity and consistency of the entire asymptotic expansion. Second, there will be trajectories that approach steady states of  $T$  that occur at  $F = 0$ . In this case, it is unnecessary to study (4.20) at these steady states, since  $F = 0$  implies  $C_1 = 0$ . Third, there will be trajectories that approach steady states with  $F \neq 0$ . These steady states yield a definite value for  $C_b^+$ , which may then be substituted in (4.20) to find that  $\frac{d\phi}{d\tau} = \text{constant}$ . It is then clear that at those steady states,  $C_1(\tau)$  undergoes simple harmonic motion in the complex plane.

Experience and some simple observations reveal that the form of equations (4.20) through (4.22), in the case of loss of stability through one real eigenvalue and one complex pair of eigenvalues, is not unique to this problem. Many similar reaction-diffusion systems and even many other dynamic systems would yield the same set of equations when the techniques of this paper were applied to them, although the expressions for the parameters in (4.20) through (4.22) would be somewhat different, of course. Without going into this in detail, for present purposes it is enough to note that the set of equations (4.20) through (4.22) are important in their own right, with minimal reference to the precise values of the parameters.

In fact, the only information needed from the parameters also turns out to be a general feature of these problems. The coefficients of the linear terms,  $\alpha$  and  $\hat{\alpha}$ , are both proportional to the quantities that measure perturbations from the stability boundary,  $v_1$  and  $\theta_1(x)$ . So

treating  $\sigma_1(x)$  as fixed and letting  $v_1$  measure distance into or out of the unstable region,  $\alpha$  and  $\hat{\alpha}$  are first order polynomials in the bifurcation parameter,  $v_1$ . Moreover, it must be that for  $v_1$  sufficiently large in magnitude and in the stable region, T exhibits a stable steady state that can be identified with the stable trivial solution of the full problem. For this particular problem, this condition will be seen to require that

$$\begin{aligned} \alpha &< 0 \\ \hat{\alpha} &< 0 \end{aligned} \tag{4.25}$$

for  $v_1$  very large and positive.

#### 4.3 Dynamics of a Special Case

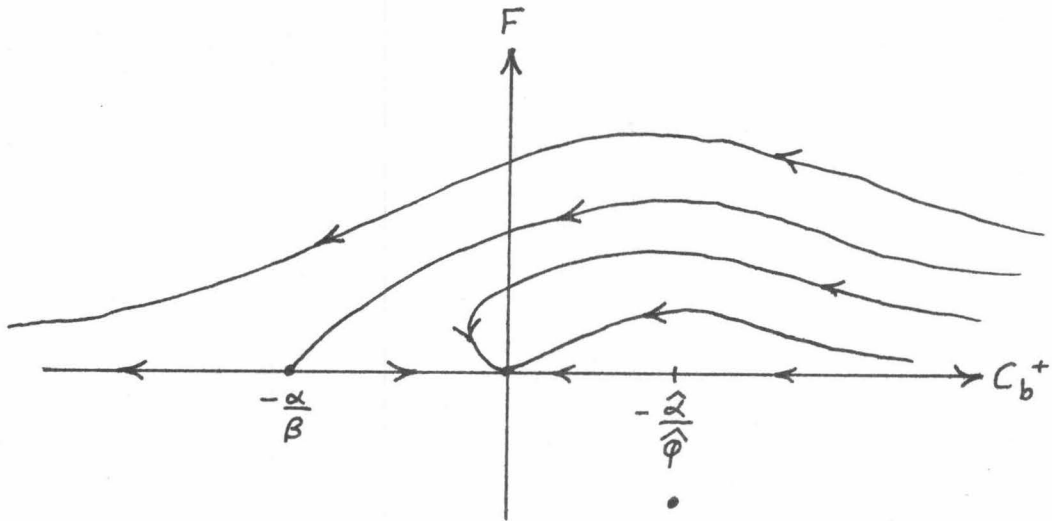
The task now is to analyze the phase plane system T. Begin by taking the special case of  $\beta < 0$ ,  $\kappa < 0$ ,  $\hat{\varphi} > 0$ ,  $\eta = 0$ . This will serve as an introduction and will illustrate the more detailed sort of dynamic analysis that underlies the more steady-state-oriented analyses that will follow.

With  $\eta = 0$ , T has the following three steady states.

$$\begin{aligned} F &= 0 & , & & C_b^+ &= 0 & (4.26a) \\ F &= 0 & , & & C_b^+ &= -\frac{\kappa \hat{\varphi} \alpha}{\hat{\varphi} \kappa} & (4.26b) \\ F &= \frac{\beta}{\alpha} \frac{\hat{\alpha}}{\hat{\varphi}} \left( \frac{\alpha}{\beta} - \frac{\hat{\alpha}}{\hat{\varphi}} \right) & , & & C_b^+ &= -\frac{\kappa \hat{\varphi} \alpha}{\hat{\varphi} \kappa} & (4.26c) \end{aligned}$$

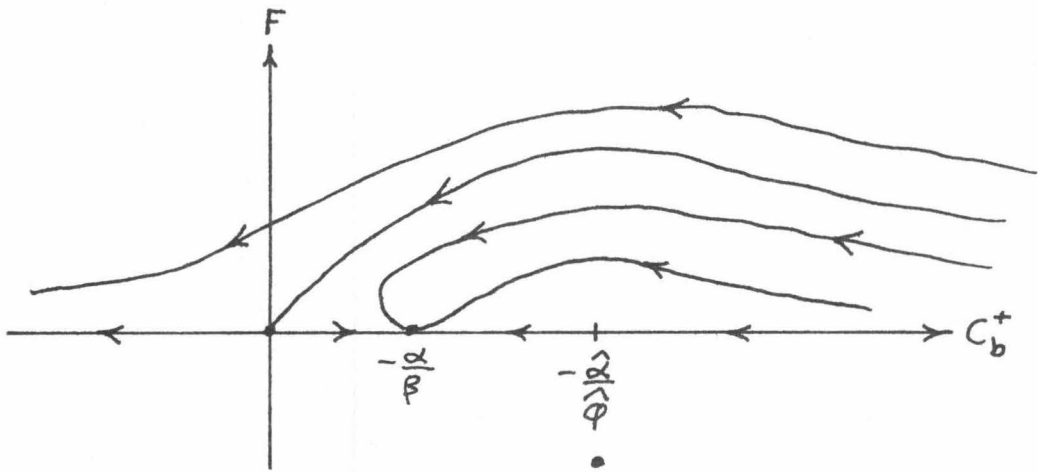
Working directly with these quantities, or applying results from later in the chapter, it is a simple matter to linearize about each of the steady states, make a few global observations, and hence arrive at the

following eight possible phase portraits for T. Recall that only  $F \geq 0$  is relevant.



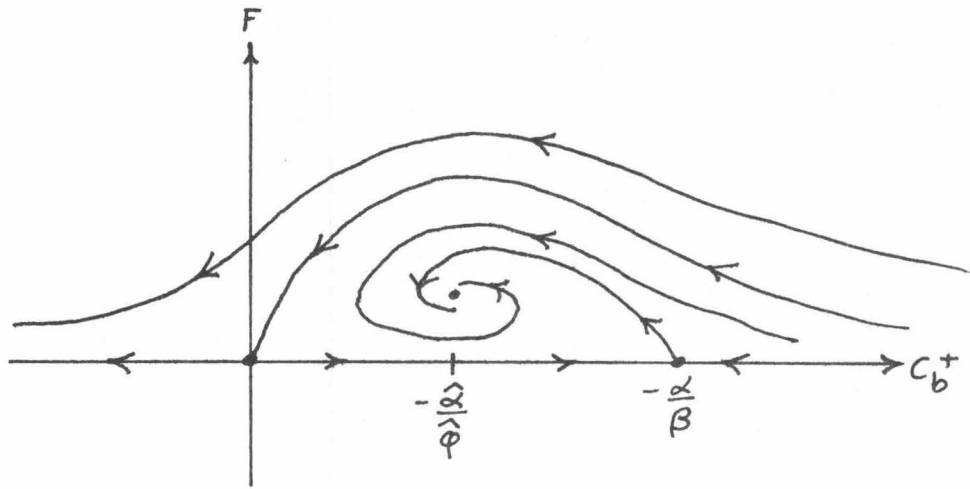
$$\text{Case I: } \frac{\alpha}{\phi} < 0 < \frac{\alpha}{\beta}$$

FIGURE 4-1



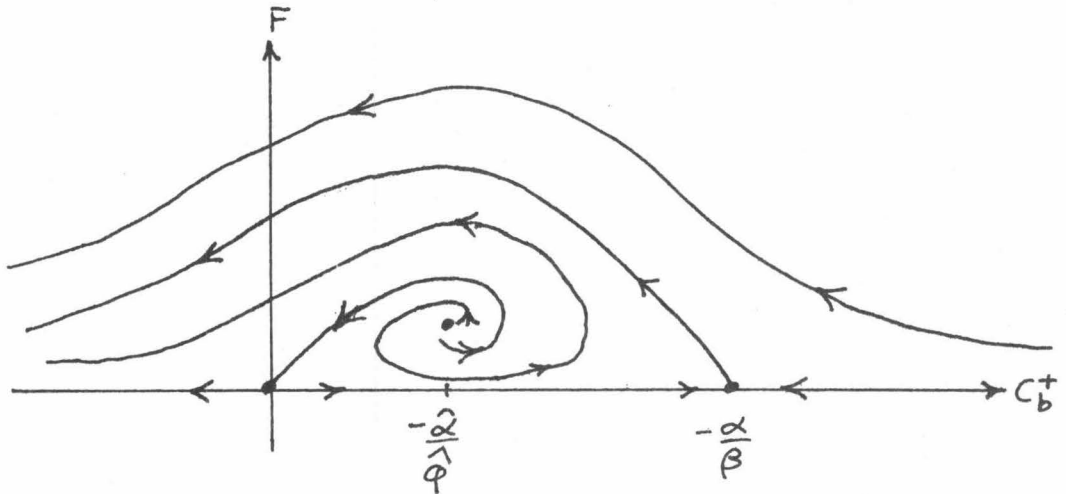
$$\text{Case II: } \frac{\alpha}{\phi} < \frac{\alpha}{\beta} < 0$$

FIGURE 4-2



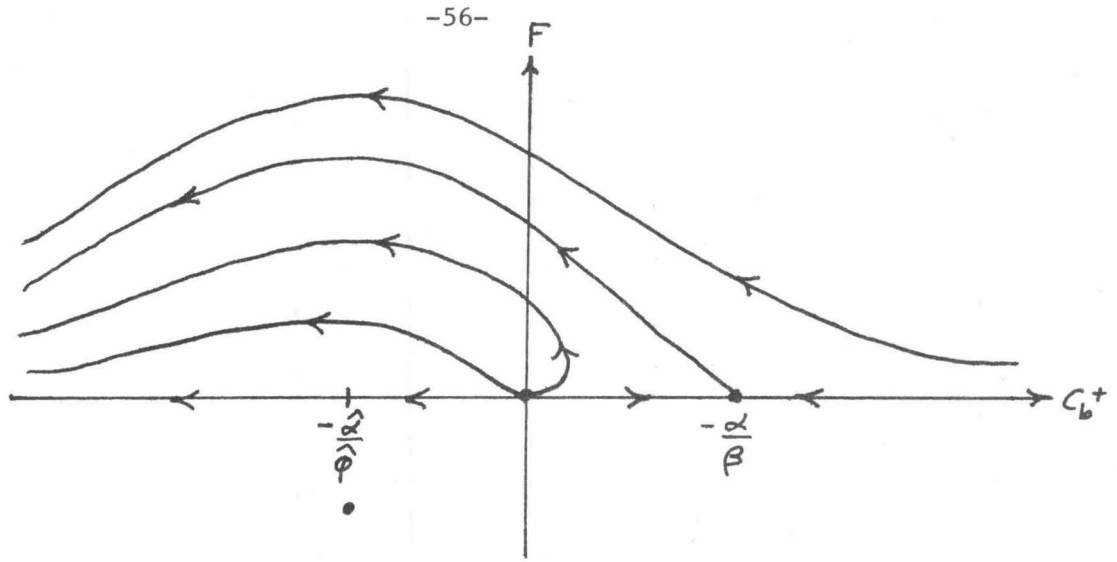
Case III :  $2\left(\frac{\alpha}{\phi}\right) < \frac{\alpha}{\beta} < \frac{\alpha}{\phi} < 0$

FIGURE 4-3



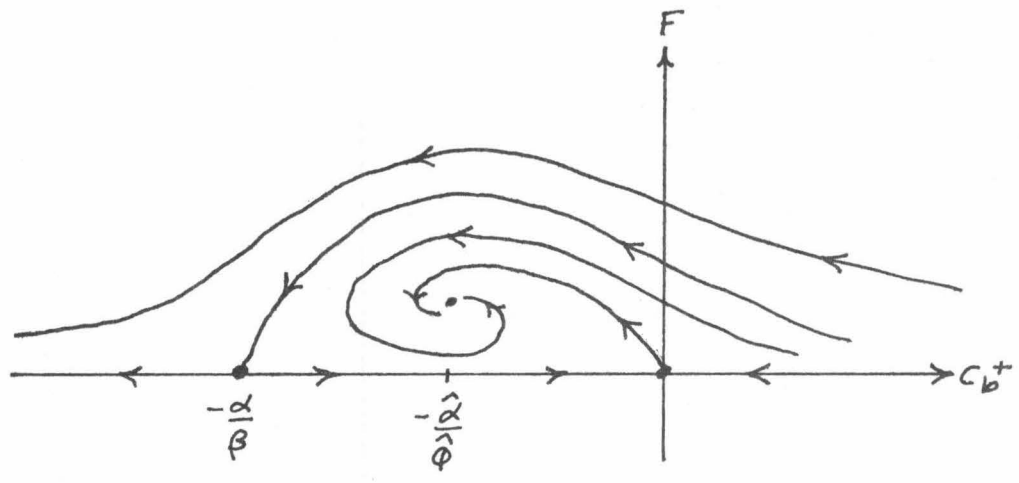
Case IV :  $\frac{\alpha}{\beta} < 2\left(\frac{\alpha}{\phi}\right) < \frac{\alpha}{\phi} < 0$

FIGURE 4-4



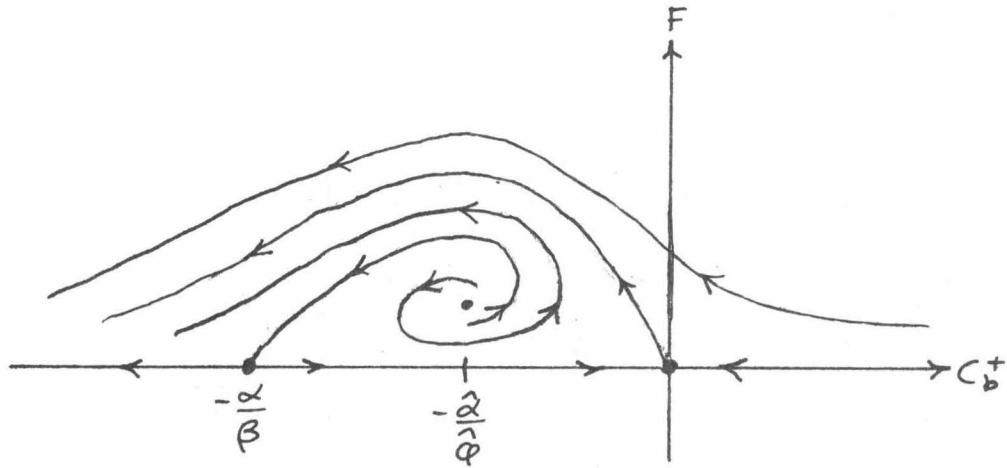
Case V:  $\frac{\alpha}{\beta} < 0 < \frac{\alpha}{\phi}$

FIGURE 4-5



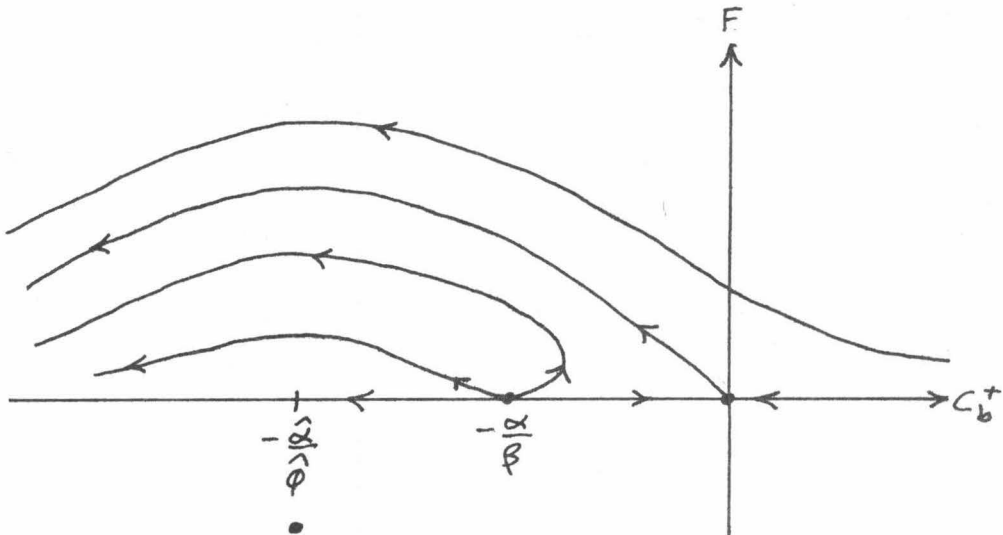
Case VI:  $0 < \frac{\alpha}{\phi} < 2\left(\frac{\alpha}{\phi}\right) < \frac{\alpha}{\beta}$

FIGURE 4-6



Case VII :  $0 < \frac{\alpha/\alpha}{\phi} < \frac{\alpha}{\beta} < 2 \left( \frac{\alpha}{\phi} \right)$

FIGURE 4-7



Case VIII :  $0 < \frac{\alpha}{\beta} < \frac{\alpha/\alpha}{\phi}$

FIGURE 4-8

As the unstable region in the  $v - \theta$  plane is approached,  $v_1$  changes from large and positive to large and negative. As this happens,  $\alpha$  and  $\hat{\alpha}$  must change from large and positive (see (4.25)) to large and negative, since  $\alpha$  and  $\hat{\alpha}$  are first order polynomials in  $v_1$ . Two cases can occur, depending upon which of  $\alpha$  or  $\hat{\alpha}$  has the largest zero as a function of  $v_1$ .

First suppose it is  $\alpha$ . Then  $\alpha$  and  $\hat{\alpha}$  depend on  $v_1$  as in Figure 4-9. This construction allows the  $v_1$  - axis to be partitioned into regions in which different members of Cases I through VIII of Figures 4-1 through Figures 4-8 apply. Then a bifurcation diagram of the steady states of T can be constructed, using the phase plane portraits to show stability or instability. This is done in Figure 4-10. Solid lines indicate stability; dashed lines indicate instability. Straight lines indicate  $F = 0$  since these states are linear in  $v_1$ ; curved lines indicate  $F \neq 0$  since these states are quadratic in  $v_1$ .



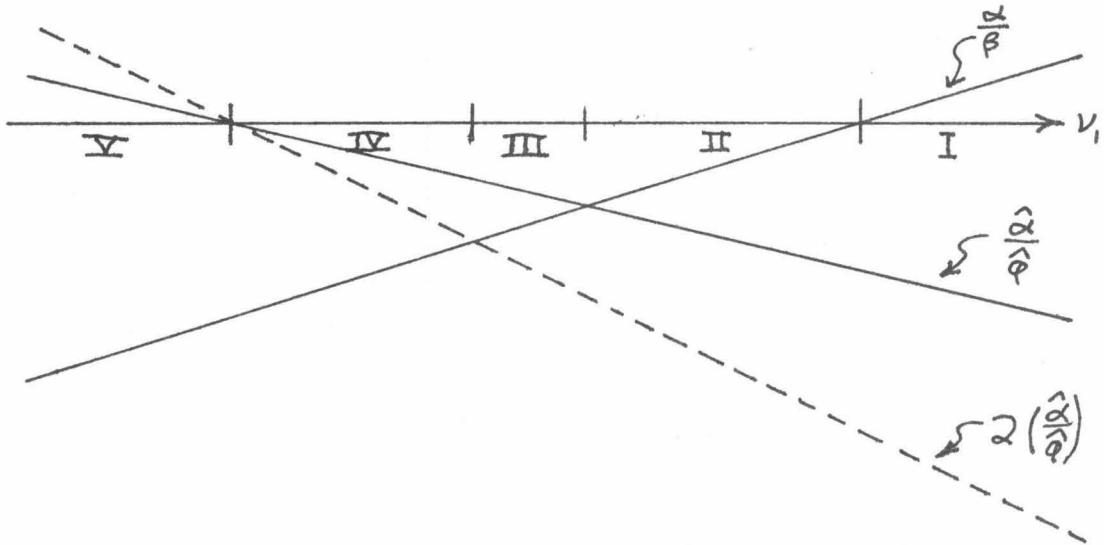


FIGURE 4-9

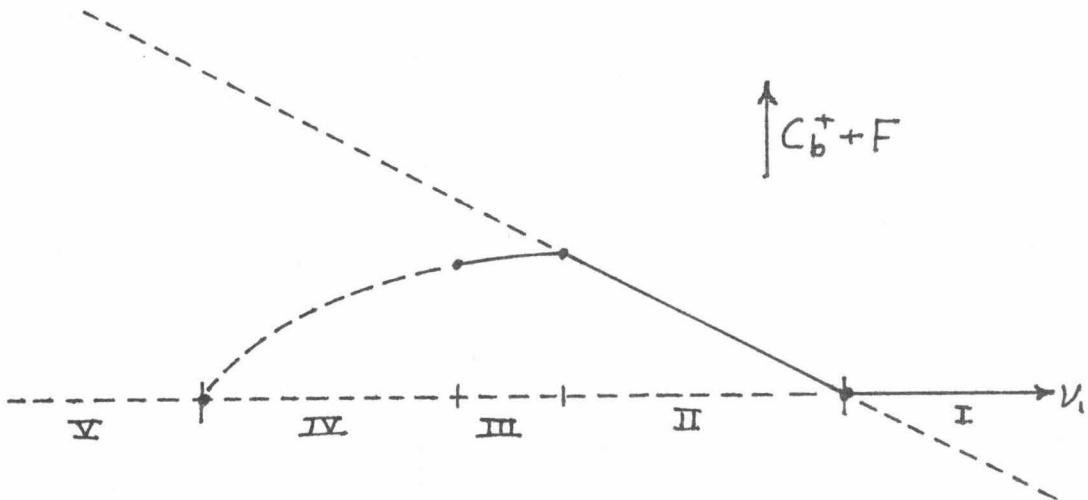


FIGURE 4-10

Now suppose the zero of  $\hat{\alpha}$  is larger than the zero of  $\alpha$ . Then the dependence of  $\alpha$  and  $\hat{\alpha}$  upon  $v_1$  is as in Figure 4-11 and the corresponding bifurcation diagram is Figure 4-12.

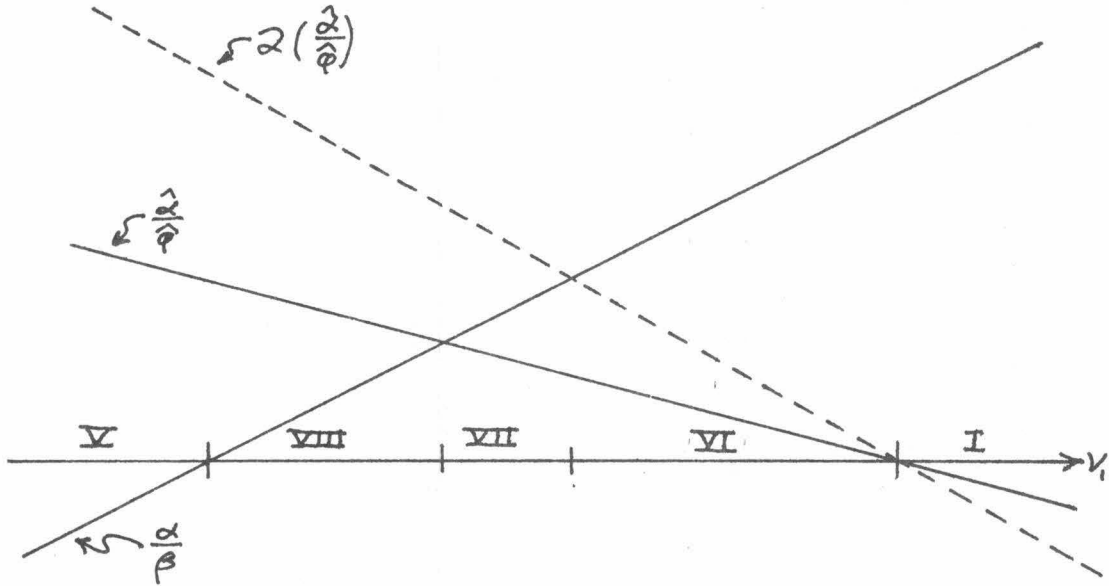


FIGURE 4-11

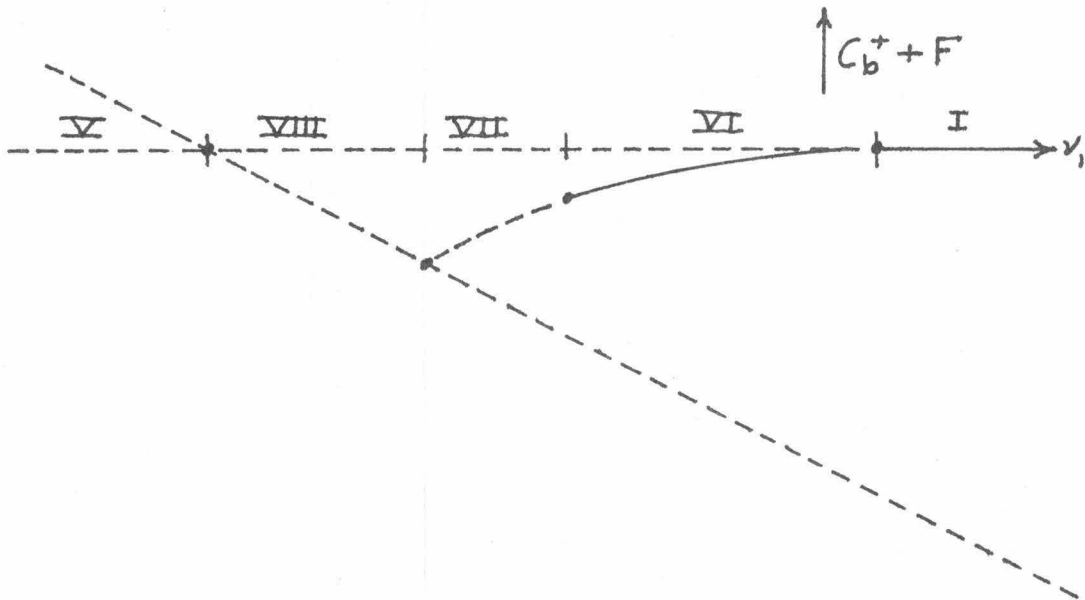


FIGURE 4-12

Note that these bifurcation diagrams exhibit exchange of stability, secondary bifurcation, bridging of two states with a third, and most interestingly, a state that loses its stability without exchanging it with another state.

#### 4.4 Loss of Stability Without Exchange of Stability

This last mentioned feature deserves closer attention. The analyses leading to the phase portraits, Figures 4-1 through 4-8, were based primarily upon finding direction fields consistent with the known local behavior near the steady states, and it was never found to be necessary to introduce more sophisticated final states, such as limit cycles. That is not to say that, for example, limit cycles could not exist in cases possessing the required circulation such as Cases III, IV, VI, and VII. However, it does say that in each individual case, no limit cycles were necessarily introduced.

On the other hand, after seeing the strange behavior between Cases III and IV in Figure 4-10 and between Cases VI and VII in Figure 4-12, and noting that in making this transition, the singular point at  $(C_b^+, F) = (-\frac{\hat{\alpha}}{\hat{\Phi}}, \frac{\beta}{\kappa} \frac{\hat{\alpha}}{\hat{\Phi}} (\frac{\alpha}{\beta} - \frac{\hat{\alpha}}{\hat{\Phi}}))$  changes from an inward winding spiral to an outward winding spiral, it seems prudent to reconsider the nonexistence of limit cycles since this is the classic case in which a Hopf bifurcation will occur. If, precisely at the bifurcation parameter value where the singular point changes from an inward winding spiral to an outward winding spiral, the field is winding inward, then there must be a supercritical bifurcation of a stable limit cycle. If, precisely where the singular point changes from inward winding to outward winding, the field is winding outward, there must be a subcritical bifurcation of an

unstable limit cycle. However, although the argument in favor of bifurcating limit cycles would seem strong at this point, this need not occur, because at the critical bifurcation point, the field winds neither in nor out: the system is conservative. The entire branch of periodic solutions required by the Hopf bifurcation theorem exists only at the critical bifurcation point. When  $\frac{\alpha}{\beta} = 2\left(\frac{\alpha}{\hat{\phi}}\right)$ , the system T possesses the integral

$$M = \begin{cases} \frac{\hat{\phi}}{2} F^{-\frac{2\beta}{\hat{\phi}}} \left[ (C_b^+)^2 + \frac{\alpha}{\beta} C_b^+ - \frac{2\alpha}{\hat{\phi} - 2\beta} F + \frac{\eta}{\beta} \right], & \hat{\phi} \neq 2\beta \\ \frac{1}{F} \left[ \beta (C_b^+)^2 + \alpha C_b^+ + \eta \right] - k \log F, & \hat{\phi} = 2\beta \end{cases} \quad (4.27)$$

This is true even if  $\eta \neq 0$ , and the other parameters have either sign. Therefore this result is not restricted to the present example, and it will play an important role in the rest of this chapter.

This means that the transition between Case III and Case IV looks like the phase portrait in Figure 4-13 and the transition between Case VI and Case VII looks like Figure 4-14.

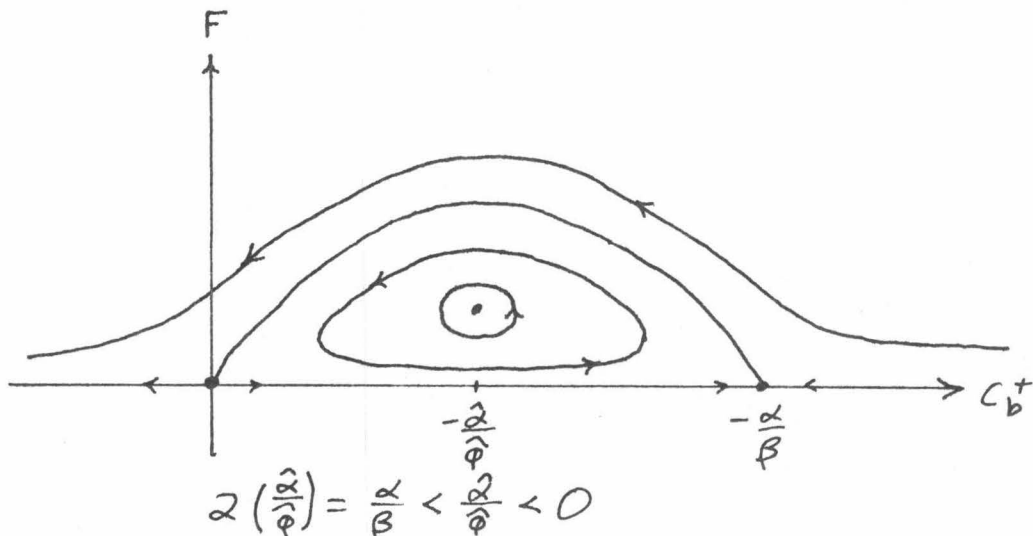


FIGURE 4-13

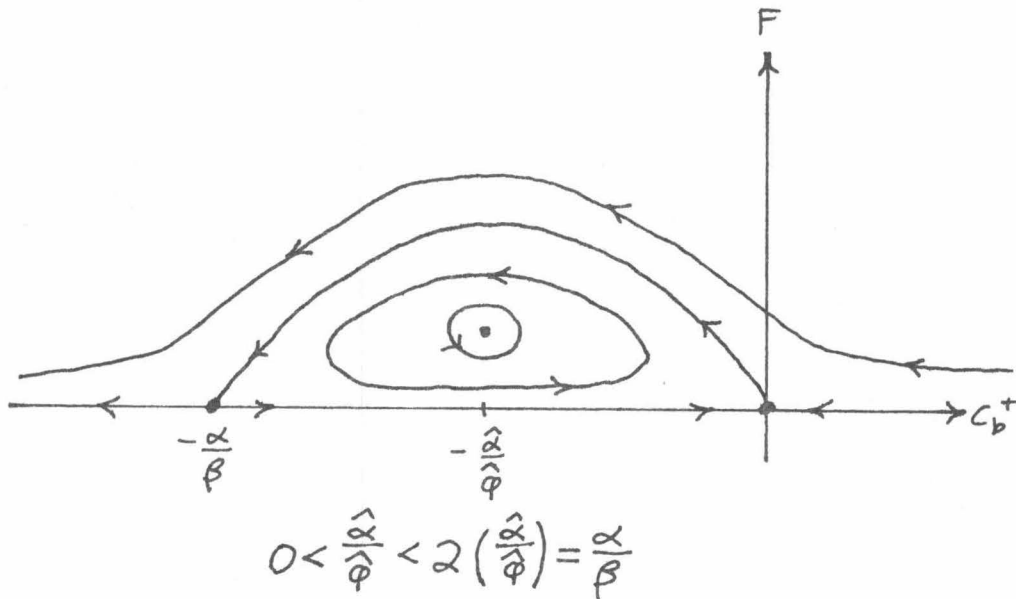


FIGURE 4-14

Therefore, the loss of stability which occurs at  $\frac{\alpha}{\beta} = 2 \left( \frac{\alpha}{\phi} \right)$  for the steady state with  $F \neq 0$  is a global loss of stability. The trajectories which approach this state as  $\tau \rightarrow \infty$  for  $v_1$  greater than the critical value approach the state more and more slowly as  $v_1$  decreases, until at the value of  $v_1$  where  $\frac{\alpha}{\beta} = 2 \left( \frac{\alpha}{\phi} \right)$ , they neither approach nor recede from the state. As  $v_1$  continues to decrease past this critical value, these trajectories begin to wind out, and the steady state becomes globally unstable.

This completes the desired analysis of the preliminary example, and we can now proceed to a case by case analysis of the phase portraits of T. However, the result that T is conservative at  $\frac{\alpha}{2\beta} = \left( \frac{\alpha}{\phi} \right)$  holds in general and can be used as above to show that there need be no bifurcating periodic solution from the  $F \neq 0$  steady state at this point.

#### 4.5 Analysis of the Slow-Time Behavior

The approach now will be to first subdivide the various cases according to the signs of the given parameters,  $\beta$ ,  $\hat{\phi}$ ,  $\kappa$ . Each of these cases will be divided according to the possible dependencies of  $\alpha$  and  $\hat{\alpha}$  upon  $v_1$ . Then for each of these cases, a bifurcation diagram of the steady states of T can be constructed for various values of  $\eta$ . In all cases, it can be verified that the steady states and their stability yield a more or less complete dynamic picture of the bifurcation by studying the individual phase planes as in the preliminary example.

The system, T, has at most three singular points. The first two are called  $SS^{\pm}$ .

$$SS^+: \quad F=0, \quad C_b^+ = -\frac{\alpha}{2\beta} + \sqrt{\left(\frac{\alpha}{2\beta}\right)^2 - \frac{\eta}{\beta}} \quad (4.28)$$

$$SS^-: \quad F=0, \quad C_b^- = -\frac{\alpha}{2\beta} - \sqrt{\left(\frac{\alpha}{2\beta}\right)^2 - \frac{\eta}{\beta}} \quad (4.29)$$

All square roots in this chapter are taken positive for positive argument.

Obviously

$$SS^{\pm} \text{ real} \iff \frac{\eta}{\beta} \leq \left(\frac{\alpha}{2\beta}\right)^2 \quad (4.30)$$

Also, if they are real, then

$$SS^+ \geq SS^- \quad (4.31)$$

$SS^{\pm}$  are intended to be mnemonic names to indicate "steady state", in

the sense of the full problem. That is, they imply  $F = 0$ , which implies  $C_1^+ = 0$ . Therefore, for all trajectories which approach  $SS^+$ , the full problem has the following limiting solution as  $t, \tau \rightarrow \infty$ .

$$\begin{pmatrix} a \\ h \end{pmatrix} = \rho_0 \begin{pmatrix} v^2 \\ v \end{pmatrix} + 2\varepsilon \left[ -\frac{\alpha}{2\beta} \pm \sqrt{\left(\frac{\alpha}{2\beta}\right)^2 - \frac{\eta}{\beta}} \right] \begin{pmatrix} v_0 + Dk_b^2 \\ 1 \end{pmatrix} y_b(x) \quad (4.32)$$

$$+ O(\varepsilon^2)$$

This is obtained from (4.3) and (1.31), where " $\pm$ " is the same as for the steady state of  $T$ ,  $SS^+$ . The third singular point will be referred to as MS.

$$MS: \quad F = \frac{B}{X} \left[ -\frac{\eta}{\beta} + \frac{\hat{\alpha}}{\hat{\phi}} \left( \frac{\alpha}{\beta} - \frac{\hat{\alpha}}{\hat{\phi}} \right) \right], \quad C_b^+ = -\frac{\hat{\alpha}}{\hat{\phi}} \quad (4.33)$$

As mentioned before,  $F$  must be positive, so

$$MS \text{ physical} \iff \frac{B}{X} \left[ -\frac{\eta}{\beta} + \frac{\hat{\alpha}}{\hat{\phi}} \left( \frac{\alpha}{\beta} - \frac{\hat{\alpha}}{\hat{\phi}} \right) \right] \geq 0. \quad (4.34)$$

MS is the mnemonic symbol for "mixed state", since both a steady portion and a portion periodic in  $t$  appear in (4.3). Using (1.31), (4.3), (4.11), (4.20), and (4.33), the corresponding limiting solution for the full problem as  $t, \tau \rightarrow \infty$  is the following.

$$\begin{aligned}
 \begin{pmatrix} a \\ h \end{pmatrix} &= \rho_0 \begin{pmatrix} v^2 \\ v \end{pmatrix} - 2\varepsilon \frac{\hat{\alpha}}{\hat{\phi}} \begin{pmatrix} v_0 + Dk_b^2 \\ 1 \end{pmatrix} y_b(x) \\
 &+ 2\varepsilon \left\{ \left[ \frac{\beta}{\kappa} \left( -\frac{\gamma}{\beta} + \frac{\hat{\alpha}}{\hat{\phi}} \left( \frac{\alpha}{\beta} - \frac{\hat{\alpha}}{\hat{\phi}} \right) \right) \right]^{\frac{1}{2}} \begin{pmatrix} v_0 + Dk_1^2 + i \sqrt{2v_0 - (v_0 + Dk_1^2)^2} \\ 1 \end{pmatrix} \right. \\
 &\left. e^{-i[\sigma_1^+ + \varepsilon(\omega - \frac{\hat{\alpha}}{\hat{\phi}} + \phi_0)]t} + \text{C.C.} \right\} y_1(x) + O(\varepsilon^2)
 \end{aligned} \tag{4.35}$$

$\phi_0$  is some constant phase shift which would have to be obtained by integrating (4.20) over the trajectory.

The forms and behavior of the bifurcating solutions are now clear. All that remains is to see which, if any, steady state is approached, how it is approached, and how the amplitudes,  $C_b^+$  and  $F$ , depend on the bifurcation parameter,  $v_1$ , as the unstable region is entered.

We begin the analysis of  $T$  by restricting to

$$\beta < 0 \tag{4.36}$$

This loses very little generality, since each case with  $\beta > 0$  has an analogous case with  $\beta < 0$ , but with  $C_b^+$  replaced by  $(-C_b^+)$ . The bifurcation diagrams look somewhat different, but possess no new phenomena.

Now linearize  $T$  about each steady state. For  $SS^+$ , let



$$\begin{pmatrix} C_b^+ \\ F \end{pmatrix} = \begin{pmatrix} -\frac{\alpha}{2\beta} + \sqrt{\left(\frac{\alpha}{2\beta}\right)^2 - \frac{\eta}{\beta}} \\ 0 \end{pmatrix} + \begin{pmatrix} c \\ f \end{pmatrix} . \quad (4.37)$$

Then to first order

$$SS^+ : \frac{d}{d\tau} \begin{pmatrix} c \\ f \end{pmatrix} = \begin{bmatrix} -\sqrt{\alpha^2 - 4\eta\beta} & K \\ 0 & \hat{\phi} \left( \frac{\hat{\alpha}}{\hat{\phi}} - \frac{\alpha}{2\beta} + \sqrt{\left(\frac{\alpha}{2\beta}\right)^2 - \frac{\eta}{\beta}} \right) \end{bmatrix} \begin{pmatrix} c \\ f \end{pmatrix} . \quad (4.38)$$

For  $SS^-$ , let

$$\begin{pmatrix} C_b^+ \\ F \end{pmatrix} = \begin{pmatrix} -\frac{\alpha}{2\beta} - \sqrt{\left(\frac{\alpha}{2\beta}\right)^2 - \frac{\eta}{\beta}} \\ 0 \end{pmatrix} + \begin{pmatrix} c \\ f \end{pmatrix} . \quad (4.39)$$

Then to first order

$$SS^- : \frac{d}{d\tau} \begin{pmatrix} c \\ f \end{pmatrix} = \begin{bmatrix} +\sqrt{\alpha^2 - 4\eta\beta} & K \\ 0 & \hat{\phi} \left( \frac{\hat{\alpha}}{\hat{\phi}} - \frac{\alpha}{2\beta} - \sqrt{\left(\frac{\alpha}{2\beta}\right)^2 - \frac{\eta}{\beta}} \right) \end{bmatrix} \begin{pmatrix} c \\ f \end{pmatrix} . \quad (4.40)$$

Finally, for MS, let

$$\begin{pmatrix} C_b^+ \\ F \end{pmatrix} = \begin{pmatrix} -\frac{\hat{\alpha}}{\hat{\phi}} \\ \frac{\beta}{\kappa} \left[ -\frac{\eta}{\beta} + \frac{\hat{\alpha}}{\hat{\phi}} \left( \frac{\alpha}{\beta} - \frac{\hat{\alpha}}{\hat{\phi}} \right) \right] \end{pmatrix} + \begin{pmatrix} c \\ f \end{pmatrix} . \quad (4.41)$$

Then to first order

-68-

$$MS: \frac{d}{d\tau} \begin{pmatrix} c \\ f \end{pmatrix} = \begin{bmatrix} 2\beta \left( \frac{\alpha}{2\beta} - \frac{\hat{\alpha}}{\hat{\phi}} \right) & K \\ \frac{\hat{\phi}\beta}{\kappa} \left[ -\frac{\gamma}{\beta} + \frac{\hat{\alpha}}{\hat{\phi}} \left( \frac{\alpha}{\beta} - \frac{\hat{\alpha}}{\hat{\phi}} \right) \right] & 0 \end{bmatrix} \begin{pmatrix} c \\ f \end{pmatrix} \cdot \quad (4.42)$$

The zeros in the above matrices simplify the analysis considerably. Since the matrices in (4.38) and (4.40) are upper triangular, their eigenvalues can be easily read from the diagonal elements.

When  $SS^-$  is real, its linearized system has one positive eigenvalue, so it is either a saddle point or an unstable node, depending upon the sign of the other eigenvalue. However, in any case we can conclude that  $SS^-$  is unstable.

When  $SS^+$  is real, its linearized system has one negative eigenvalue, so  $SS^+$  is either a stable node or a saddle point. Therefore, to determine the stability of  $SS^+$ , the other eigenvalue must be considered. Straightforward calculations allow this to be determined through the use of the following decision tree, which answers the question of  $SS^+$ 's stability in terms of quantities that will prove convenient.

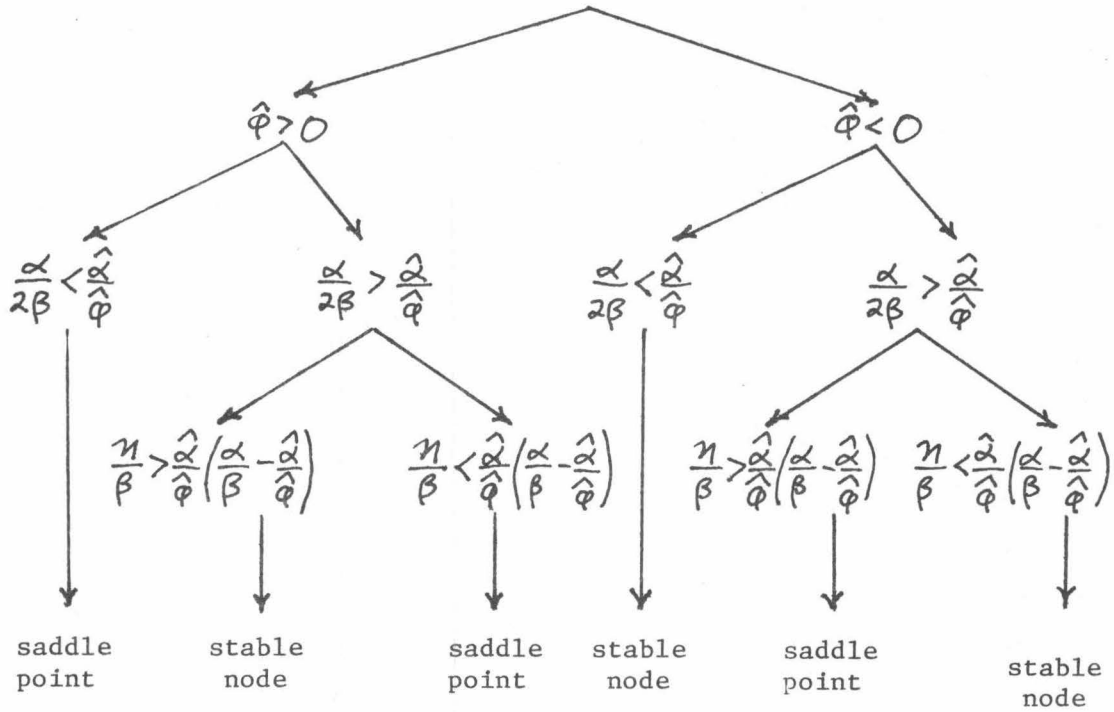


FIGURE 4-15

As for the stability of MS, the zero element of the matrix in (4.42) also allows some easy conclusions. If the product of the off-diagonal terms is positive, then MS will be a saddle point. These are the least interesting cases and will not be pursued. To accomplish this, recall (4.34). Requiring

$$\kappa \hat{\phi} < 0 \tag{4.43}$$

will then insure that the product of the off-diagonal terms in (4.42) will be negative. This implies that MS is either a node or a spiral point. Furthermore, assuming MS is physical ( $F > 0$ ),

$$MS \text{ stable} \longleftrightarrow \frac{\alpha}{2\beta} > \frac{\hat{\alpha}}{\hat{\phi}} \quad , \quad (4.44)$$

and when it changes stability, it can only do so as a spiral changing from winding in to winding out or vice versa.

Finally, if MS disappears out of the physical region, this must happen when its F-component vanishes. From (4.33), this is where

$$-\frac{\eta}{\beta} + \frac{\hat{\alpha}}{\hat{\phi}} \left( \frac{\alpha}{\beta} - \frac{\hat{\alpha}}{\hat{\phi}} \right) = 0 \quad , \quad (4.45)$$

or equivalently,

$$-\frac{\hat{\alpha}}{\hat{\phi}} = -\frac{\alpha}{2\beta} \pm \sqrt{\left(\frac{\alpha}{2\beta}\right)^2 - \frac{\eta}{\beta}} \quad (4.46)$$

So the  $C_b^+$  - component of MS is  $-\frac{\alpha}{2\beta} \pm \sqrt{\left(\frac{\alpha}{2\beta}\right)^2 - \frac{\eta}{\beta}}$  when it disappears.

Comparing these components with (4.28) and (4.29), it can be seen that, when MS disappears (or appears), it does so by bifurcating from  $SS^+$ .

To see whether it is  $SS^+$  or  $SS^-$ , compare the  $C_b^+$ -components of MS and  $SS^+$  and see whether "+" or "-" causes the equality to hold.

$$-\frac{\hat{\alpha}}{\hat{\phi}} = -\frac{\alpha}{2\beta} \pm \sqrt{\left(\frac{\alpha}{2\beta}\right)^2 - \frac{\eta}{\beta}} \quad (4.47)$$

or

$$\frac{\alpha}{2\beta} - \frac{\hat{\alpha}}{\hat{\phi}} = \pm \sqrt{\left(\frac{\alpha}{2\beta}\right)^2 - \frac{\eta}{\beta}} \quad (4.48)$$

Therefore if  $\frac{\alpha}{2\beta} > \frac{\hat{\alpha}}{\hat{\phi}}$ , then MS bifurcates from  $SS^+$ . If  $\frac{\alpha}{2\beta} < \frac{\hat{\alpha}}{\hat{\phi}}$ , MS bifurcates from  $SS^-$ .

The thread running through the above analysis is that all the

important features of T — the existence of singular points, their stability, their intersections — can be determined by three comparisons:

$$\begin{aligned} \frac{\eta}{\beta} &\gtrless \left(\frac{\alpha}{2\beta}\right)^2 \\ \frac{\eta}{\beta} &\gtrless \frac{\hat{\alpha}}{\hat{\varphi}} \left(\frac{\alpha}{\beta} - \frac{\hat{\alpha}}{\hat{\varphi}}\right) \\ \frac{\alpha}{2\beta} &\gtrless \frac{\hat{\alpha}}{\hat{\varphi}} \end{aligned} \tag{4.49}$$

Therefore, one reasonable way to proceed is to plot the five quantities in (4.49) as functions of  $v_1$  and then read off the relevant information using the results just derived. Actually  $\frac{\eta}{\beta}$  is independent of  $v_1$ , and its effect will be studied by, in each case, choosing a representative set of values,

$$\dots < \eta_{-2} < \eta_{-1} < \eta_0 = 0 < \eta_1 < \eta_2 < \dots, \tag{4.50}$$

and seeing what bifurcation diagram results from each member of the set.

Also note that

$$\left(\frac{\alpha}{2\beta}\right)^2 = \frac{\hat{\alpha}}{\hat{\varphi}} \left(\frac{\alpha}{\beta} - \frac{\hat{\alpha}}{\hat{\varphi}}\right) \leftrightarrow \left(\frac{\alpha}{2\beta} - \frac{\hat{\alpha}}{\hat{\varphi}}\right)^2 = 0. \tag{4.51}$$

Therefore, the curves  $\left(\frac{\alpha}{2\beta}\right)^2$  and  $\frac{\hat{\alpha}}{\hat{\varphi}} \left(\frac{\alpha}{\beta} - \frac{\hat{\alpha}}{\hat{\varphi}}\right)$ , as functions of  $v_1$ , are tangent at  $\frac{\alpha}{2\beta} = \frac{\hat{\alpha}}{\hat{\varphi}}$ .

#### 4.6 Phase Portraits for the Various Cases

Based on the results of the previous Section, the graphs and bifurcation diagrams found at the end of this Section are easily obtained. The graphs are of the five quantities in (4.49), which will be referred to as the critical functions of  $v_1$ . In the bifurcation diagrams, solid lines indicate stable states and dashed lines indicate unstable states. To separate genuine intersections from apparent intersections, which arise from the three dimensional to two dimensional projection and from superposing more than one diagram on the same set of axes, genuine intersections will be reinforced with heavy dots. Heavy dots will also mark changes in stability in the middle of a branch. The branches corresponding to  $SS^+$  and MS can be distinguished by recalling (4.31) and noting that, while a MS branch generally has at least one definite endpoint,  $SS^+$ , if taken together, do not terminate, but rather behave as follows.

$$\lim_{|v_1| \rightarrow \infty} SS^\pm \in \left\{ (c_b^+, F) \mid c_b^+ = 0 \text{ or } -\frac{\alpha}{\beta}, F = 0 \right\} \quad (4.52)$$

For each bifurcation diagram the reference case of  $\eta = \eta_0 = 0$  is included to help compare various values of  $\eta$ .

Recall that we have already restricted to  $\beta < 0, \hat{\varphi} \kappa < 0$ . Let  $\alpha$  have its zero at  $v_1 = v_\alpha$  and  $\hat{\alpha}$  have its zero at  $v_{\hat{\alpha}}$ . Then the following table explains the figures.

Major Case	Subcase	Graph of Critical Functions	Bifurcation Diagrams
$\hat{\varphi} > 0$	$v_{\alpha} > v_{\alpha}^{\wedge}$	4-17	4-18 through 4-22
	$v_{\alpha} = v_{\alpha}^{\wedge}$	4-23	4-24
	$v_{\alpha} < v_{\alpha}^{\wedge}$	4-25	4-26 through 4-30
$\hat{\varphi} < 0$ (Slope of $\frac{\alpha}{\hat{\varphi}}$ is between slopes of $\frac{\alpha}{2\beta}$ )	$v_{\alpha} > v_{\alpha}^{\wedge}$	4-31	4-32 through 4-36
	$v_{\alpha} = v_{\alpha}^{\wedge}$	4-37	4-38
	$v_{\alpha} < v_{\alpha}^{\wedge}$	4-39	4-40 through 4-44
$\hat{\varphi} < 0$ (Slope of $\frac{\alpha}{\hat{\varphi}}$ > slope of $\frac{\alpha}{\beta}$ )	$v_{\alpha} > v_{\alpha}^{\wedge}$	4-45	4-46 through 4-50
	$v_{\alpha} = v_{\alpha}^{\wedge}$	4-51	4-52
	$v_{\alpha} < v_{\alpha}^{\wedge}$	4-53	4-54 through 4-58

FIGURE 4-16

The case of  $\hat{\varphi} < 0$  (slope of  $\frac{\alpha}{\hat{\varphi}} < \text{slope of } \frac{\alpha}{2\beta}$ ) is so similar to the case of  $\hat{\varphi} < 0$  (slope of  $\frac{\alpha}{\hat{\varphi}}$  is between the slopes of  $\frac{\alpha}{2\beta}$  and  $\frac{\alpha}{\beta}$ ) that it is not displayed.

As the figures are scanned, many interesting bifurcation phenomena may be observed. There is secondary bifurcation, linkage of two nonintersecting branches by a third, loss of stability at a bifurcation point (exchange of stability), loss of stability where a smooth branch has a vertical tangent, and loss of stability in the middle of a branch for neither of the preceding reasons (Section 4.4). Of special interest is the effect of varying the imperfection parameter,  $\eta$ . As  $\eta$  increases

or decreases from zero, there are cases where  $SS^+$  split apart leaving an empty region between them similar to the behavior in Chapter 2. There are cases where the branch for MS either appears or disappears or even detaches itself entirely from the other two branches. Also note how the bifurcation point of MS from  $SS^+$  creeps around the curve near the vertical tangent between  $SS^+$  and  $SS^-$  and how this affects the stability properties as  $\eta$  becomes increasingly more negative. In short, bifurcation in a reaction-diffusion system that loses stability through one real eigenvalue and a complex pair of eigenvalues and that includes an imperfection parameter possesses a quite rich and varied range of behaviors.



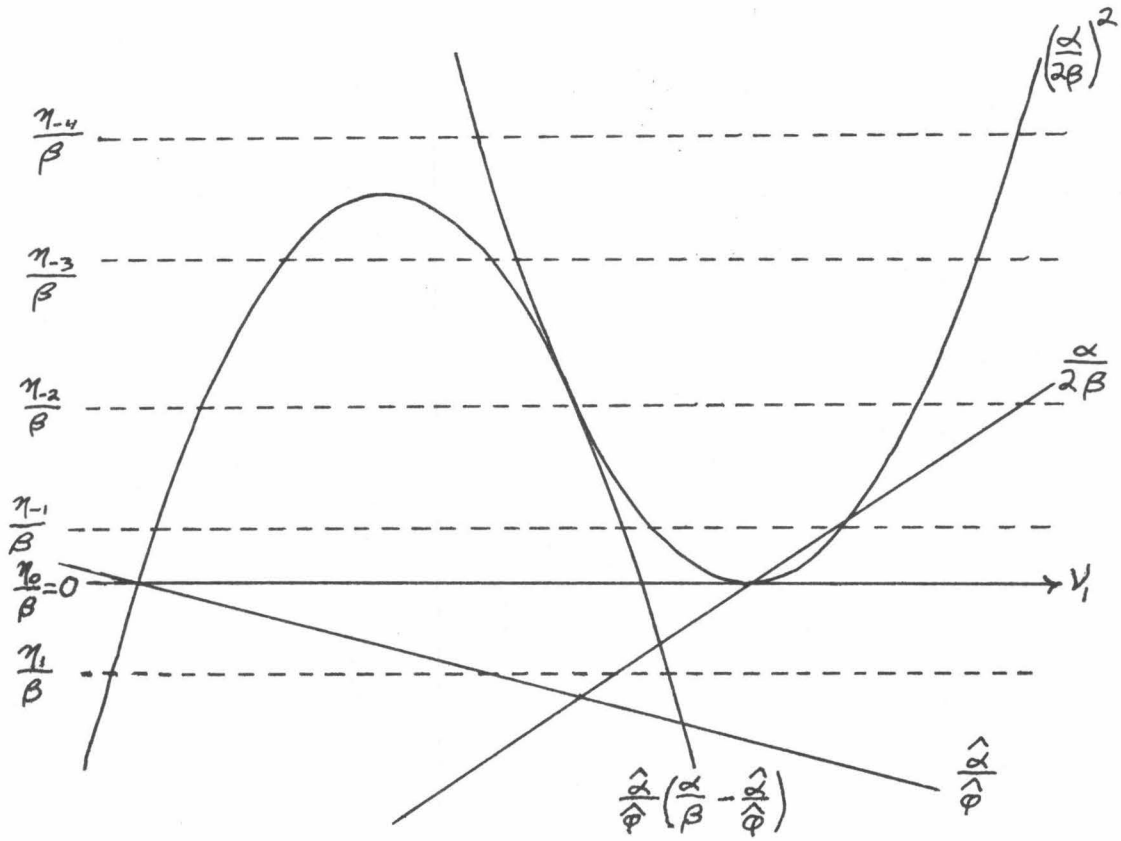


FIGURE 4-17

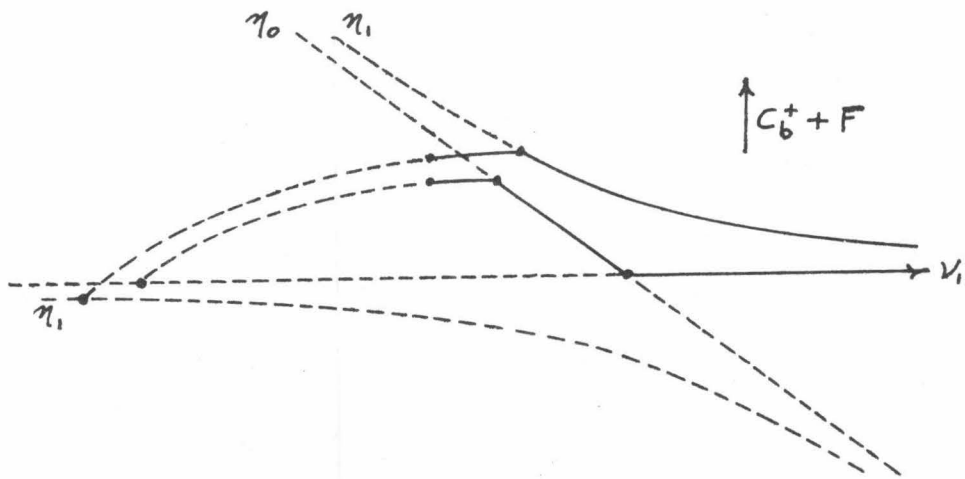


FIGURE 4-18

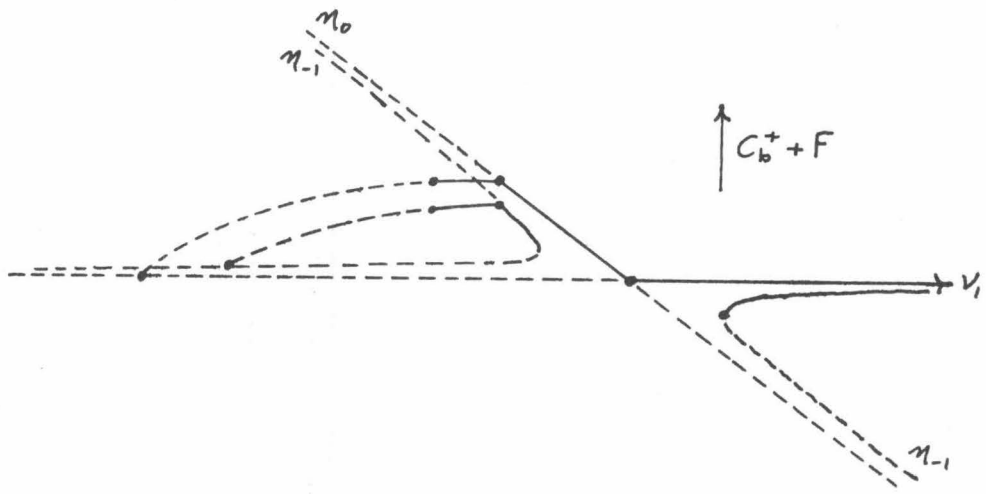


FIGURE 4-19

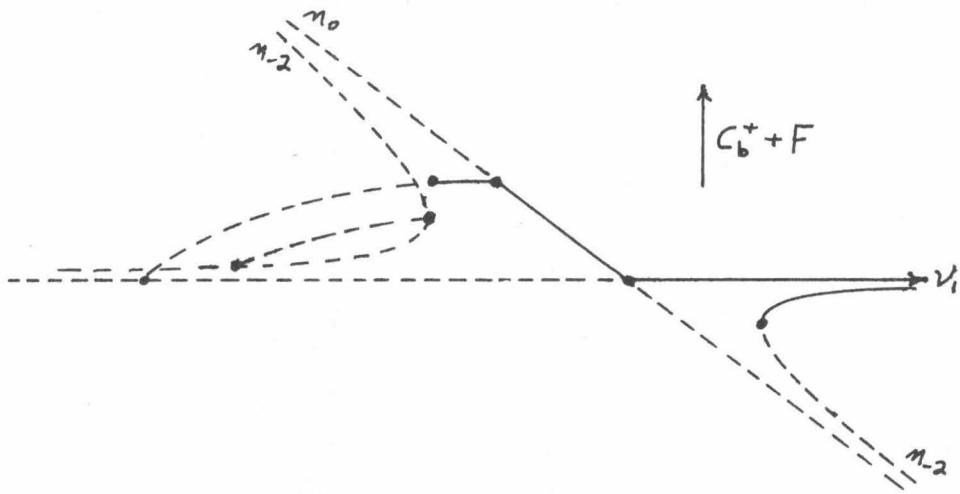


FIGURE 4-20

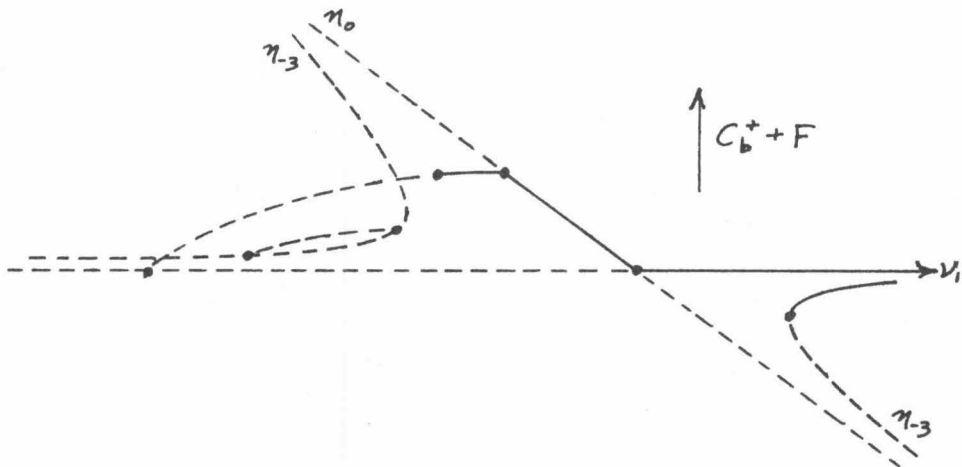


FIGURE 4-21

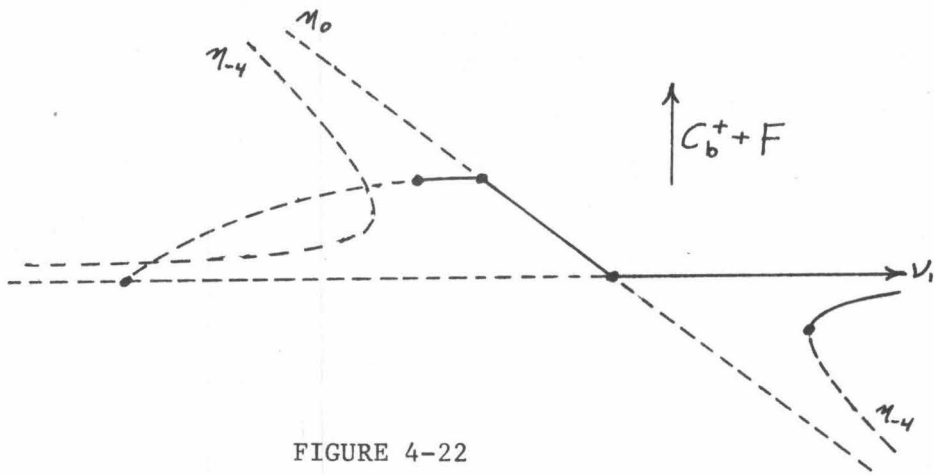


FIGURE 4-22

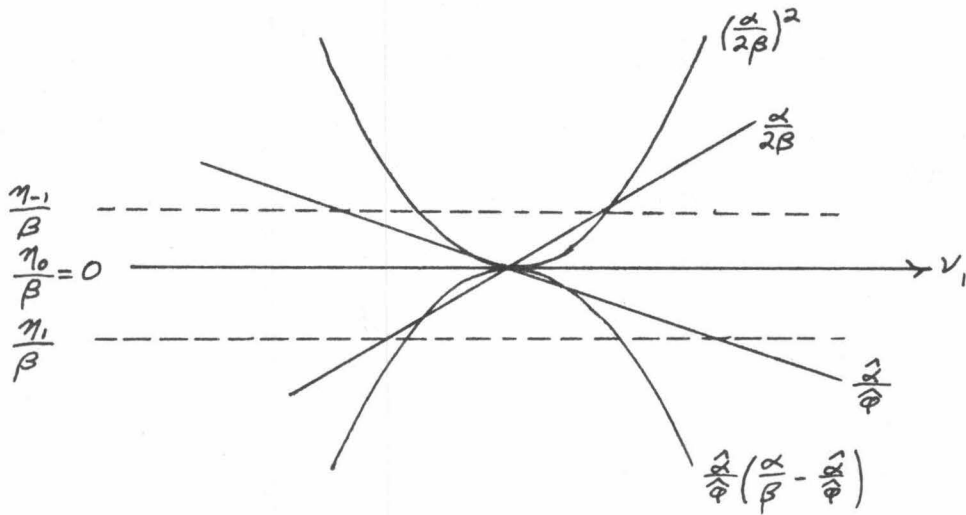


FIGURE 4-23

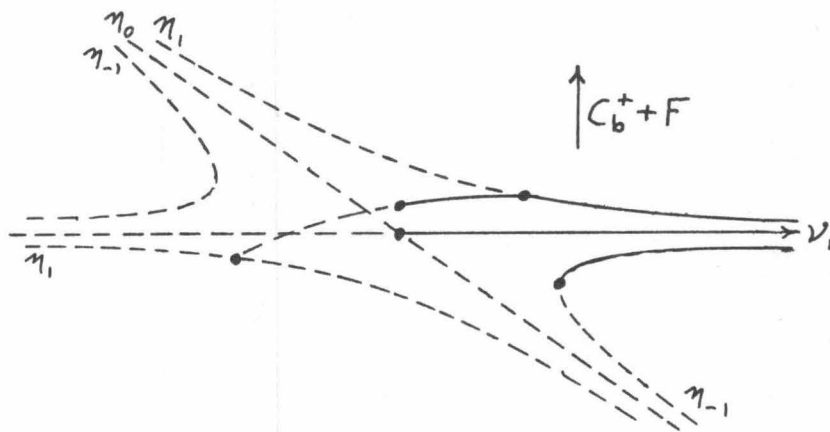


FIGURE 4-24

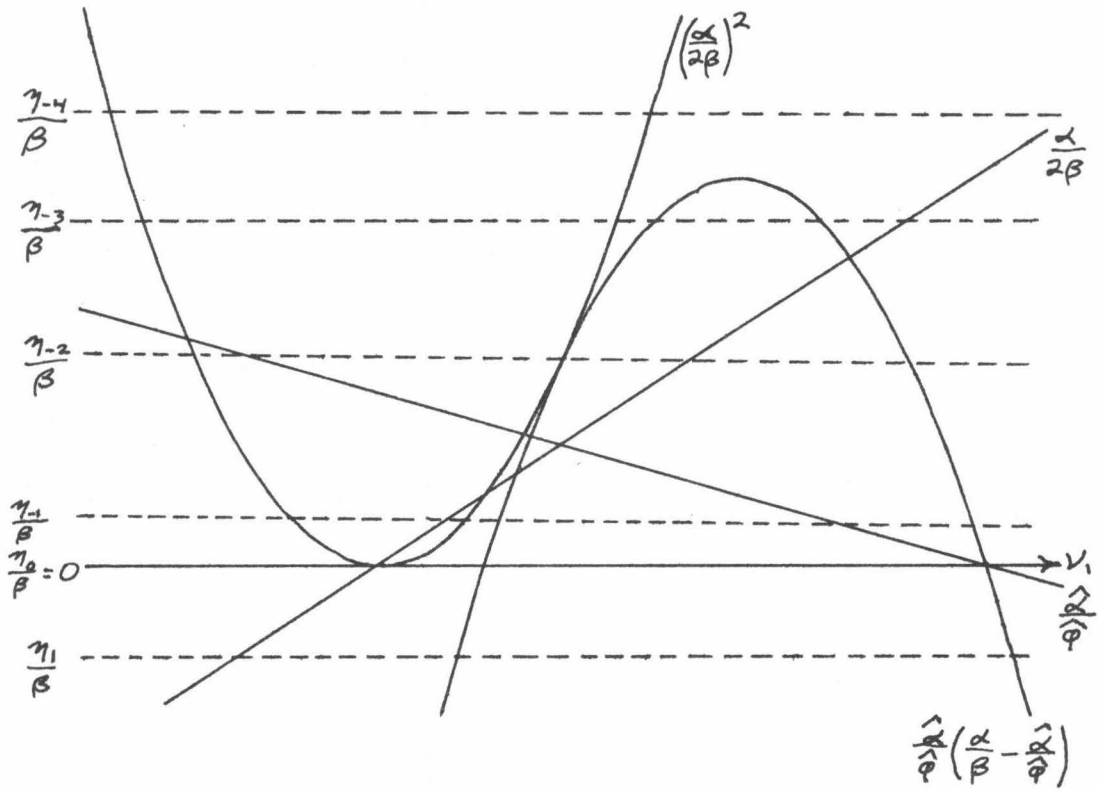


FIGURE 4-25

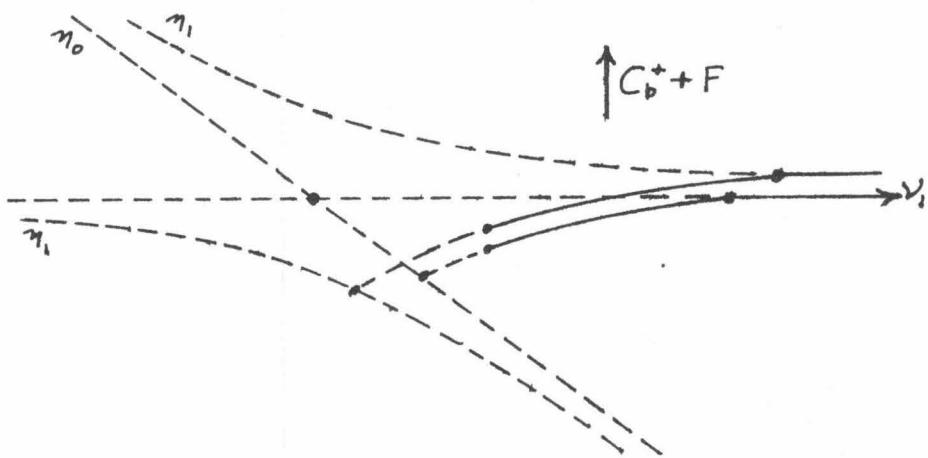


FIGURE 4-26

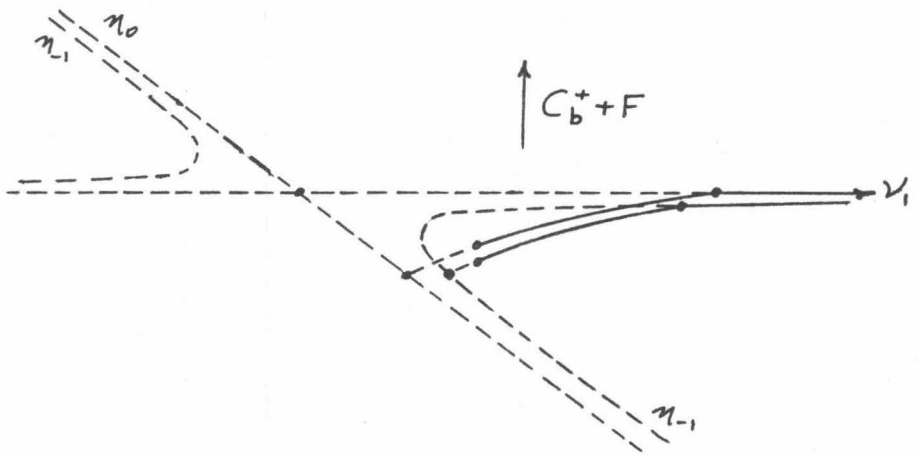


FIGURE 4-27

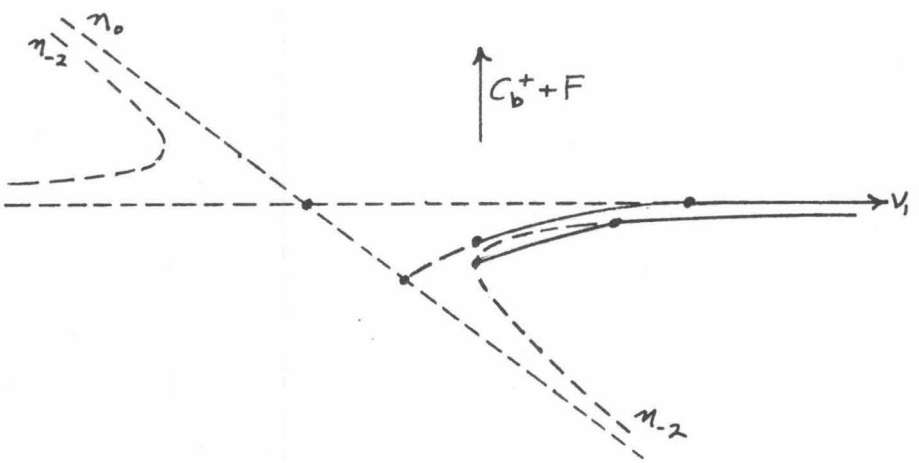


FIGURE 4-28

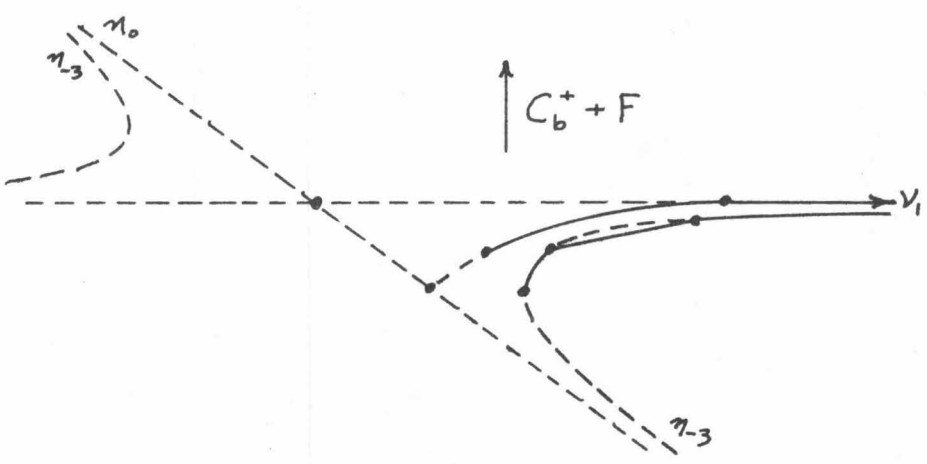


FIGURE 4-29

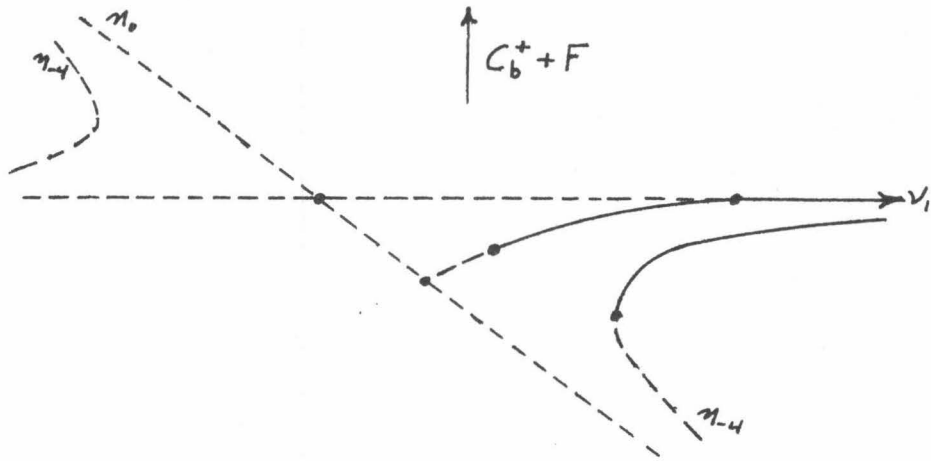


FIGURE 4-30

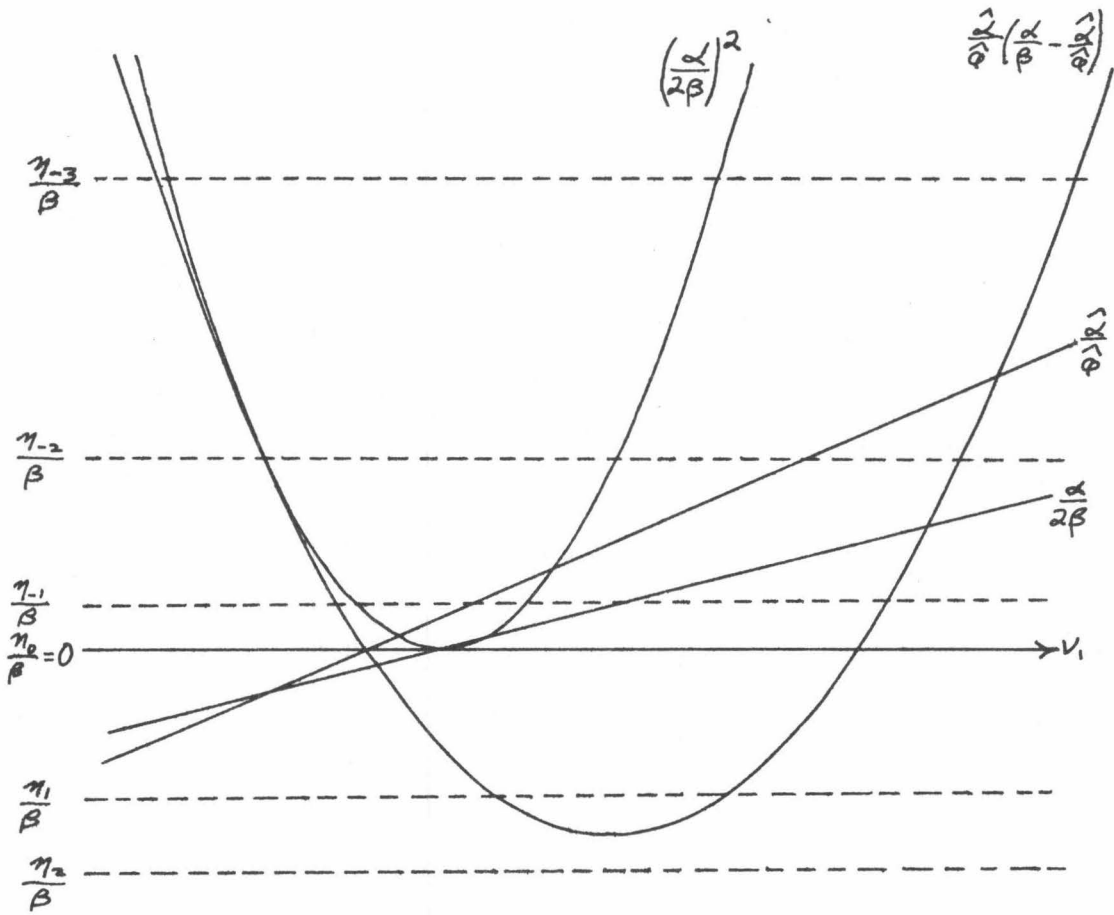


FIGURE 4-31

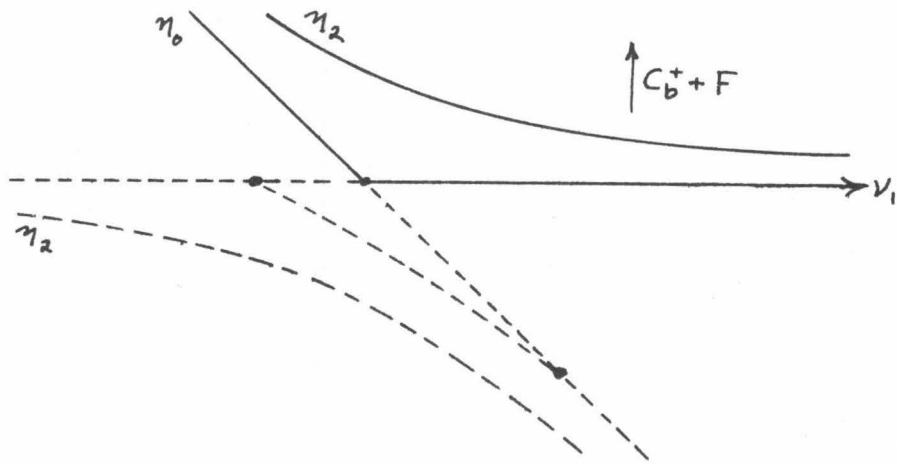


FIGURE 4-32

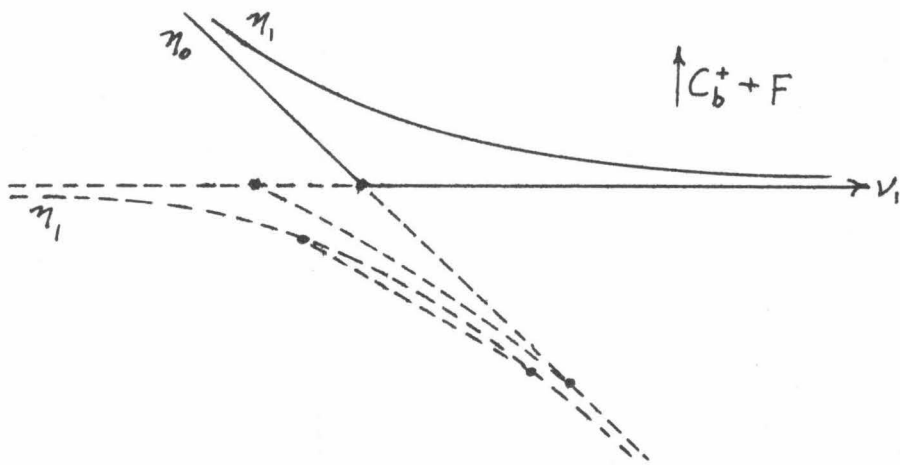


FIGURE 4-33

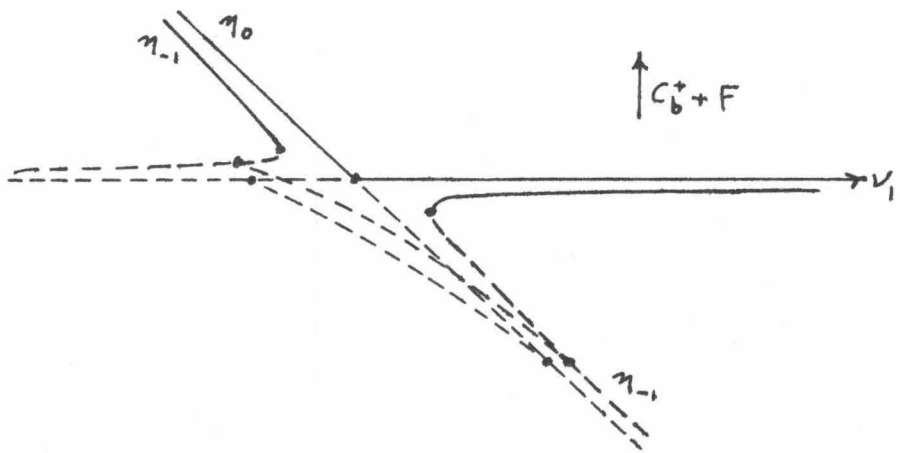


FIGURE 4-34

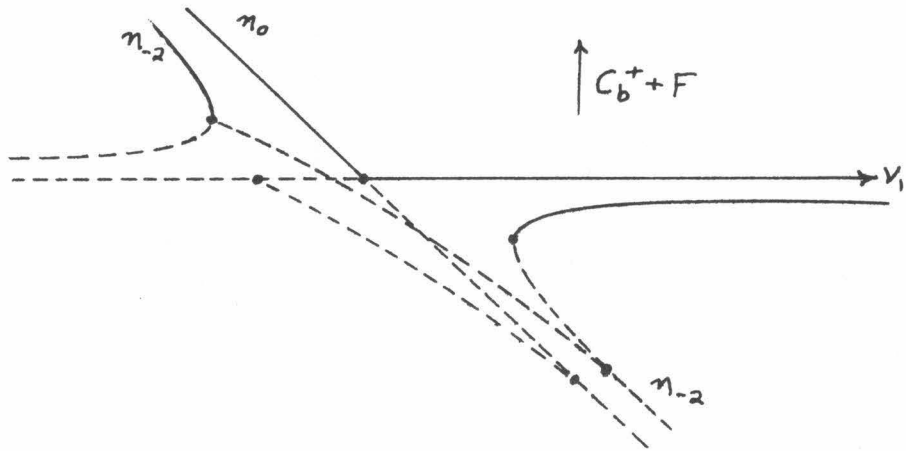


FIGURE 4-35

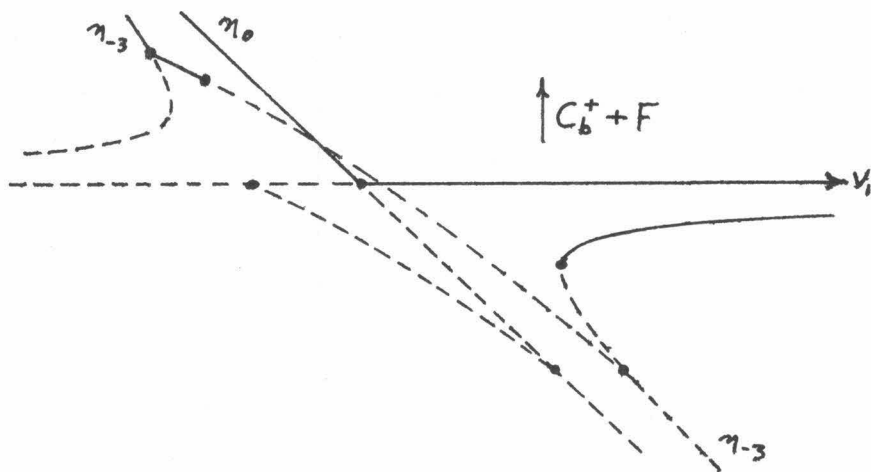


FIGURE 4-36

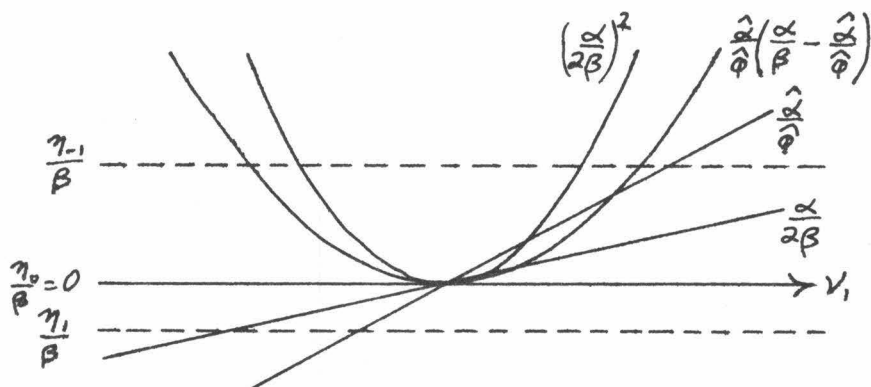


FIGURE 4-37



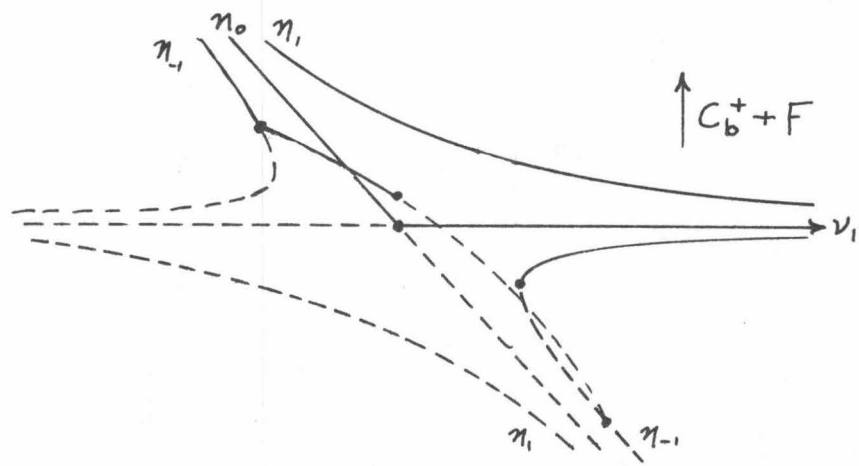


FIGURE 4-38

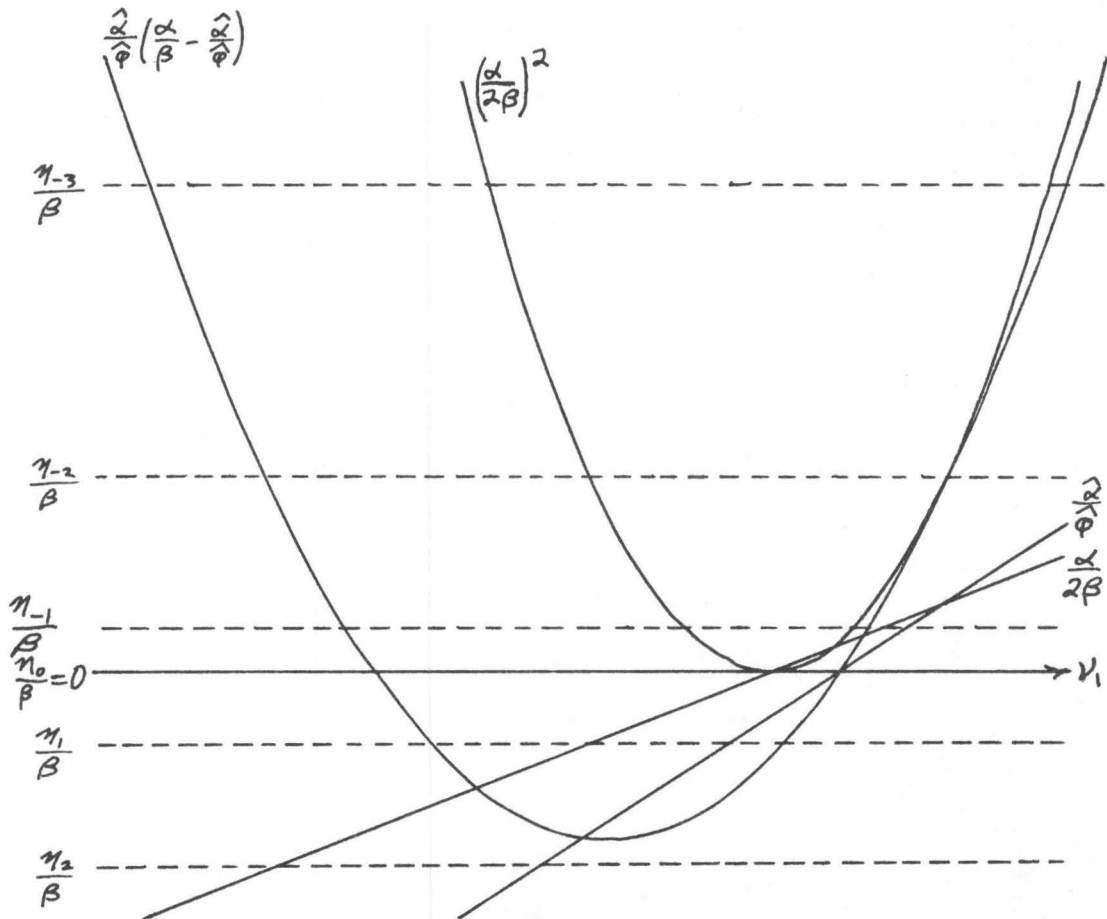


FIGURE 4-39

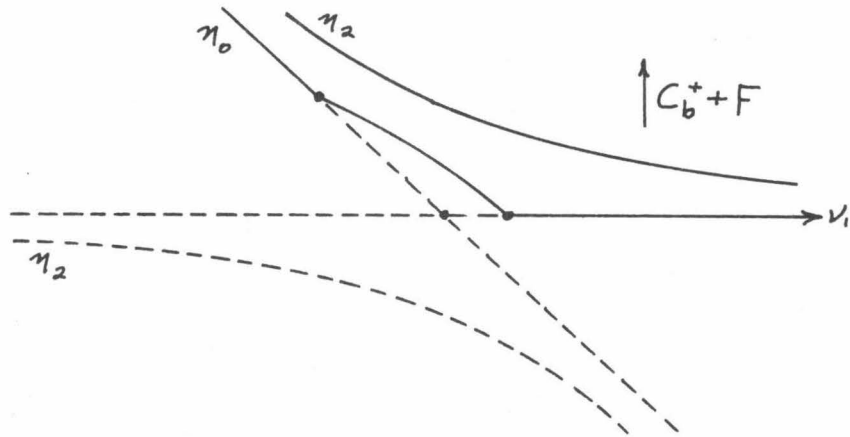


FIGURE 4-40

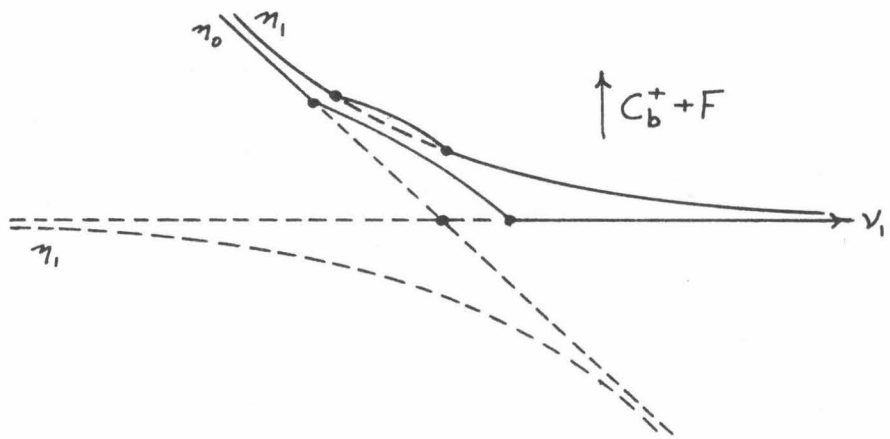


FIGURE 4-41

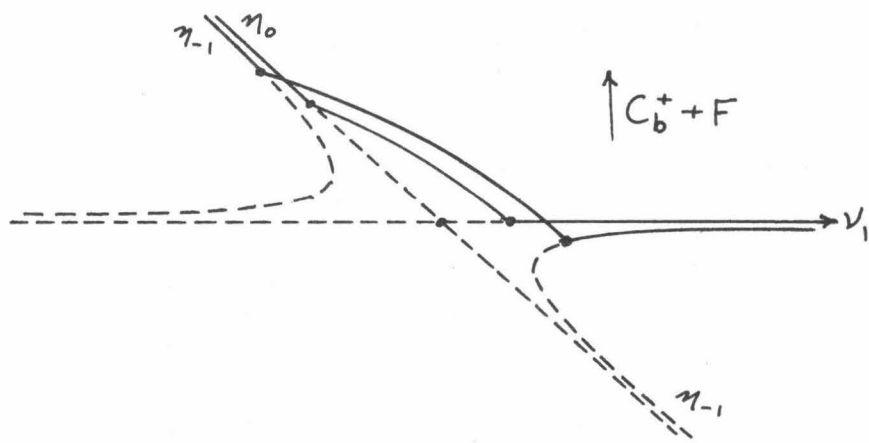


FIGURE 4-42

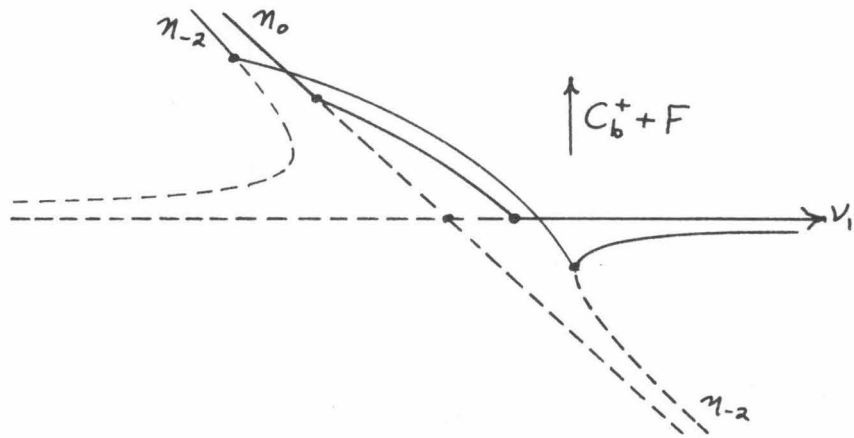


FIGURE 4-43

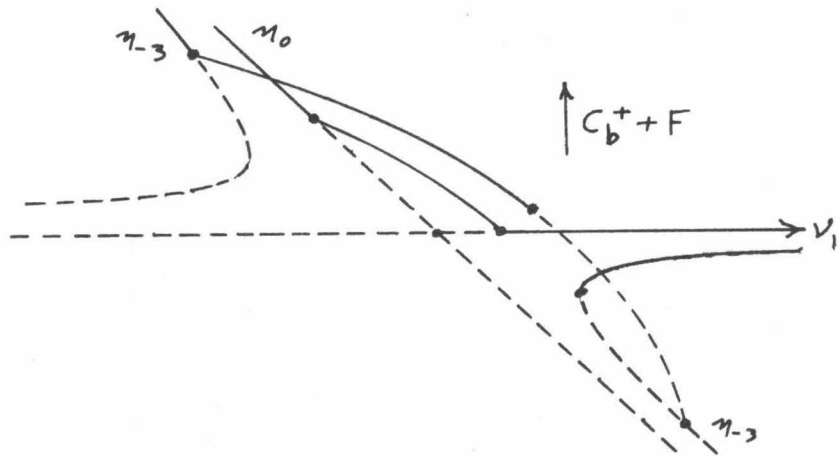


FIGURE 4-44

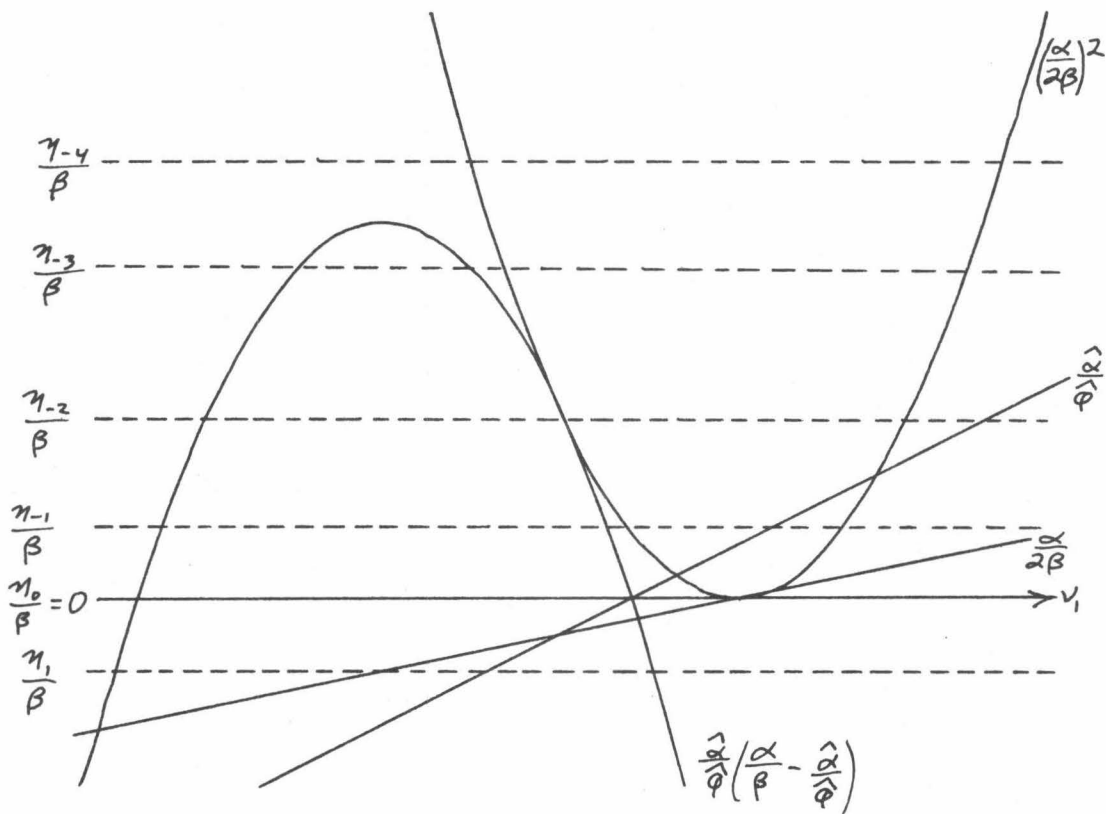


FIGURE 4-45

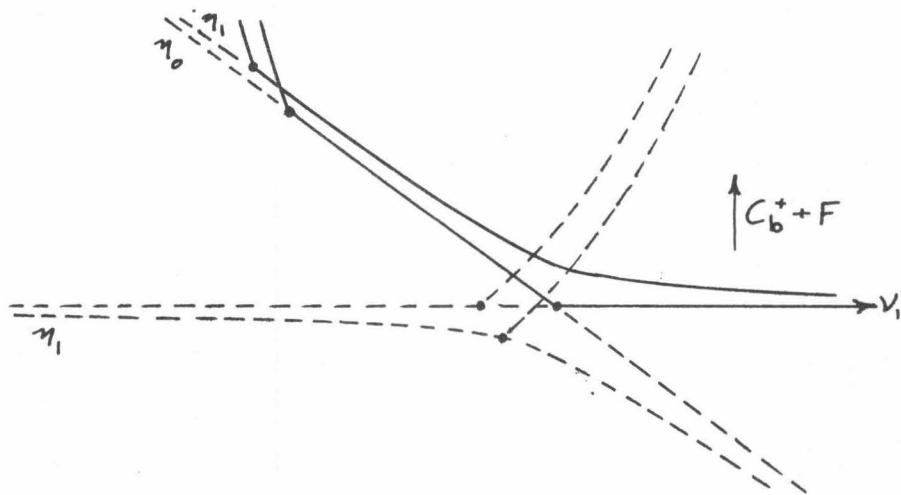


FIGURE 4-46

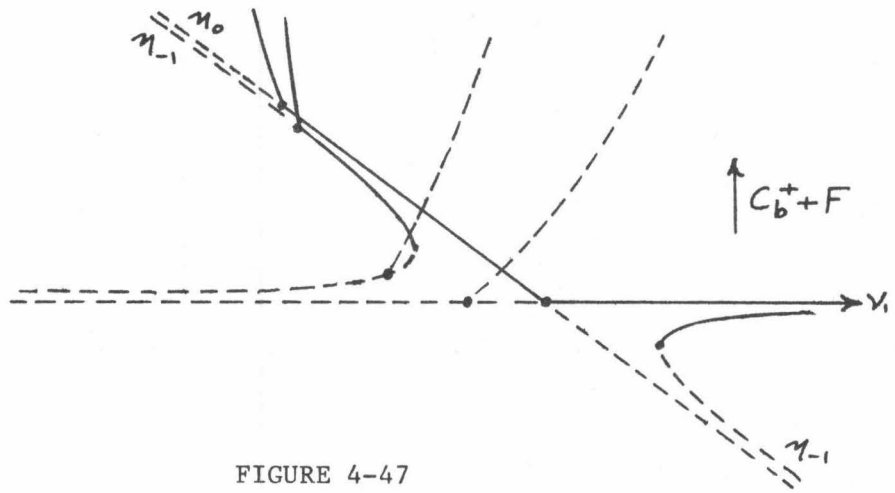


FIGURE 4-47

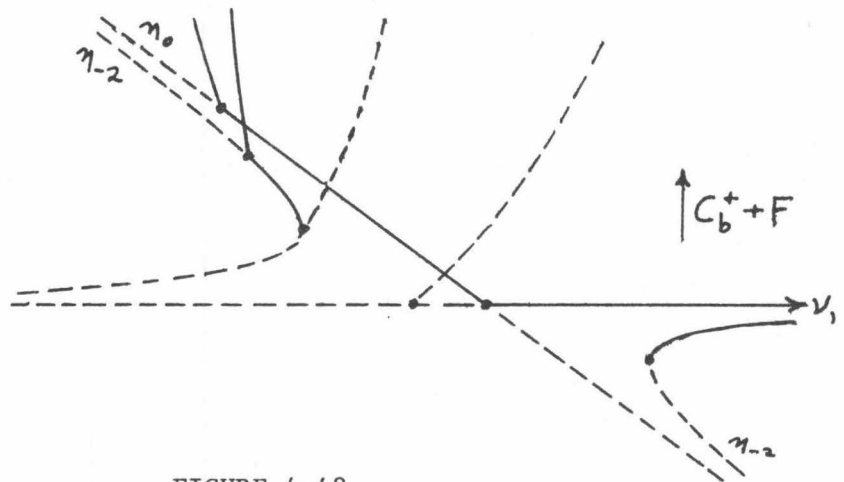


FIGURE 4-48

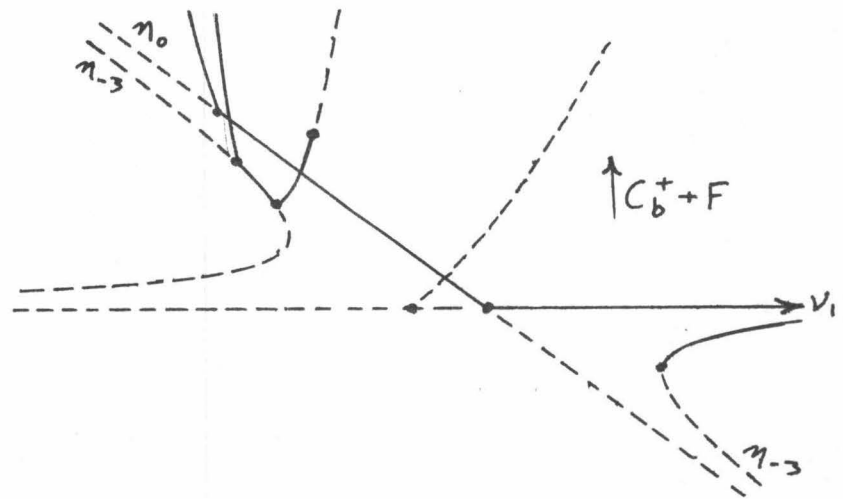


FIGURE 4-49

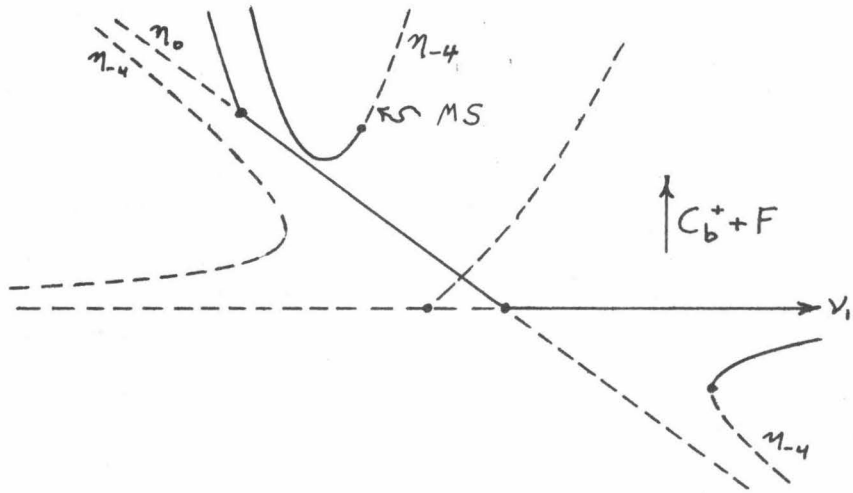


FIGURE 4-50

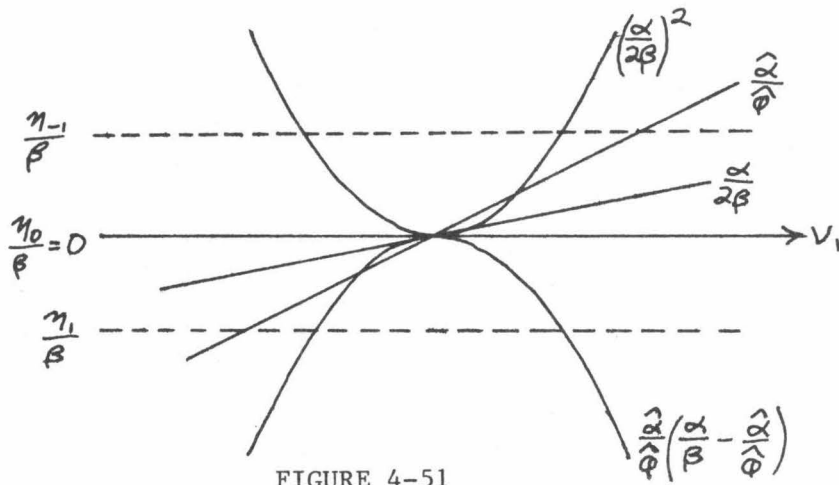


FIGURE 4-51

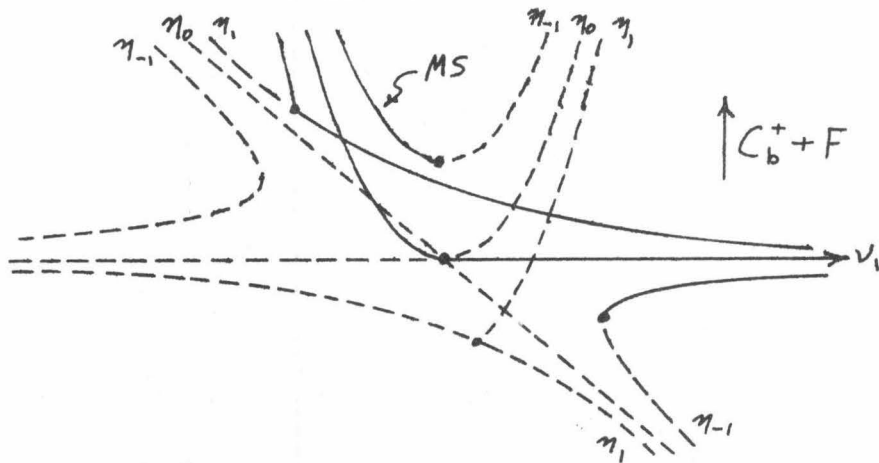


FIGURE 4-52

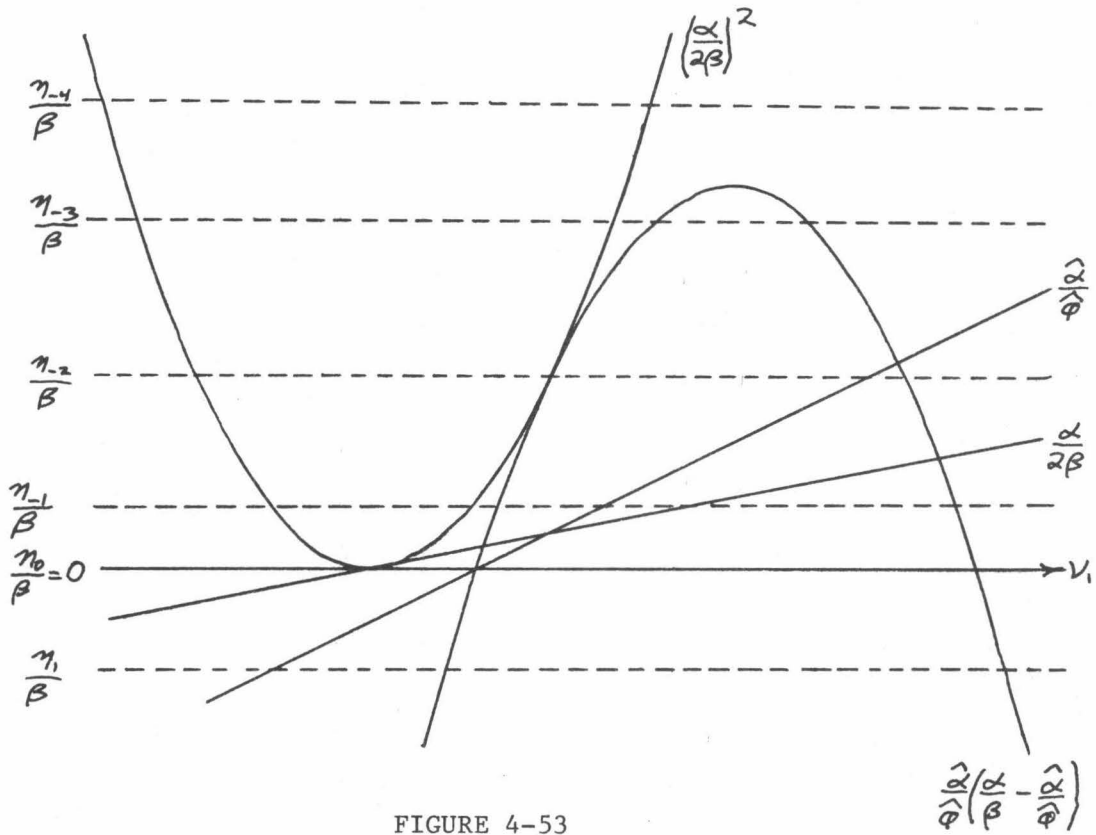


FIGURE 4-53

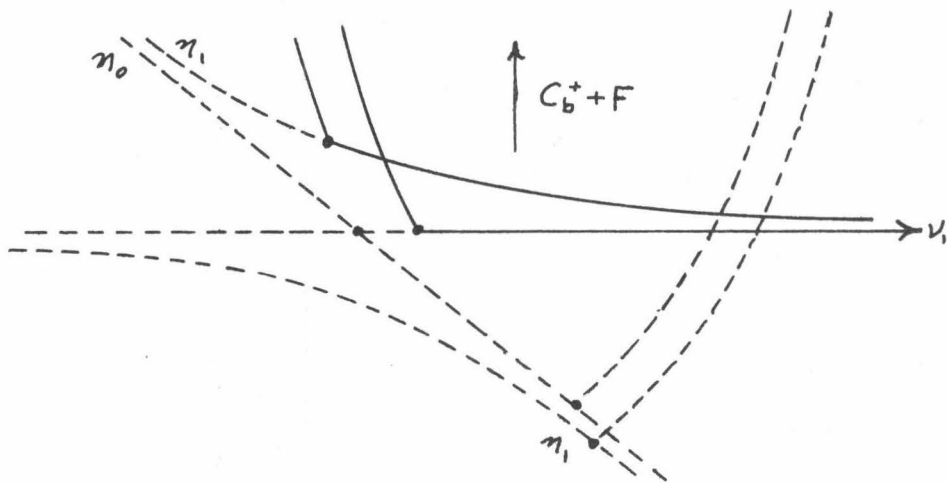


FIGURE 4-54

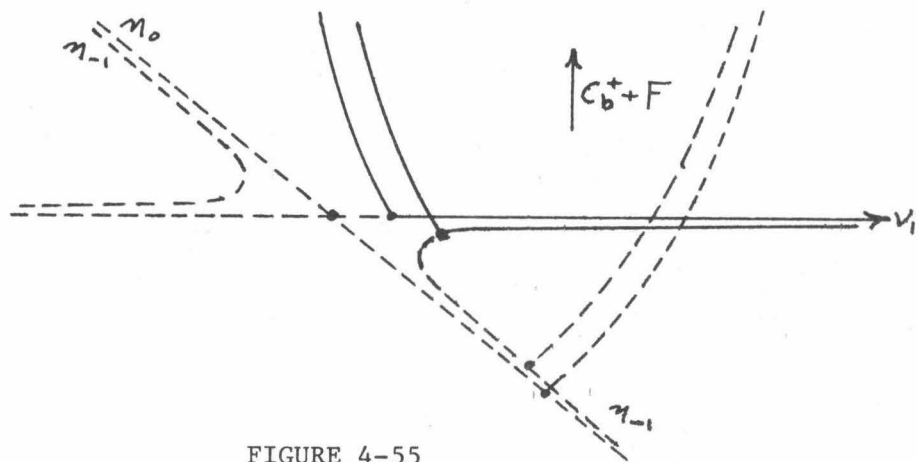


FIGURE 4-55

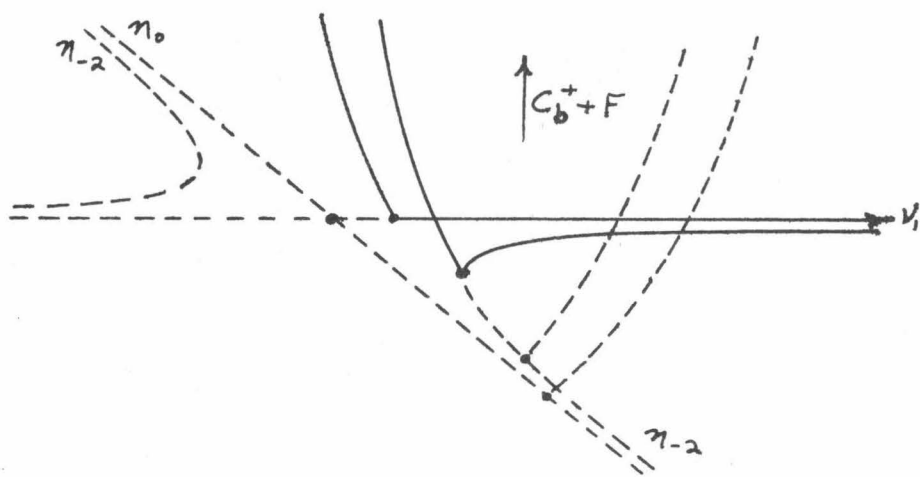


FIGURE 4-56

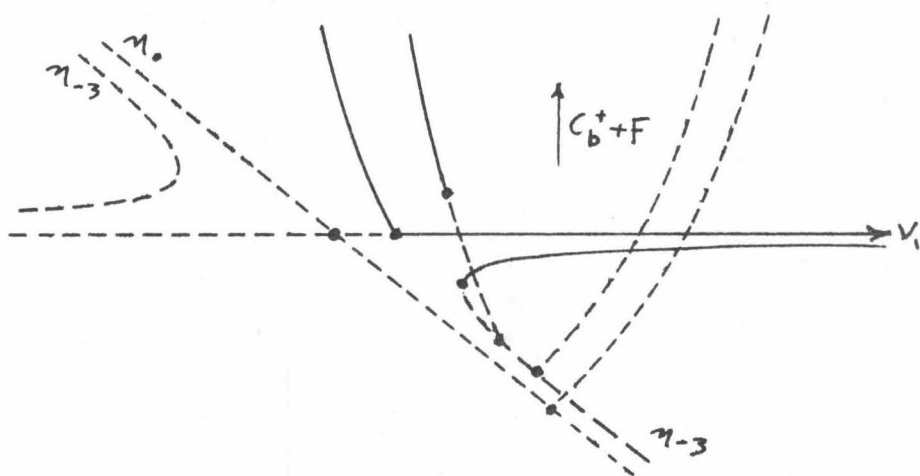


FIGURE 4-57



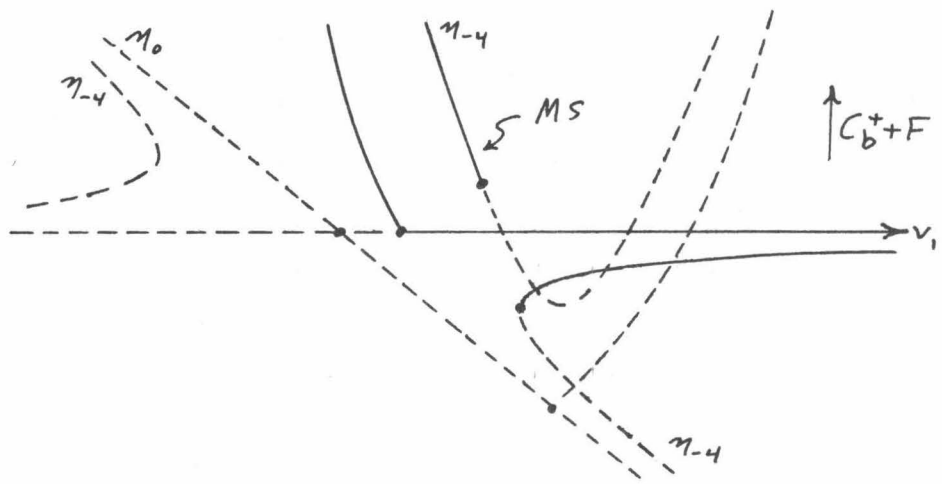


FIGURE 4-58

REFERENCES

- Boa, James A., Multiple Steady States in a Model Biochemical Reaction, Studies in Applied Mathematics, 54(1975), 9-15.
- Boa, James A., and Cohen, Donald S., Bifurcation of Localized Disturbances in a Model Biochemical Reaction, SIAM Journal on Applied Mathematics, 30(1976), 123-135.
- Gierer, A., and Meinhardt, H., A Theory of Biological Pattern Formation, Kybernetik, 12(1972), 30-39.
- Keener, James P., Activators and Inhibitors in Pattern Formation, To appear.
- Keener, J. P., Secondary Bifurcation in Nonlinear Diffusion Reaction Equations, To appear.
- Kogelman, Stanley, and Keller, Joseph B., Transient Behavior of Unstable Nonlinear Systems with Applications to the Bénard and Taylor Problems, SIAM Journal on Applied Mathematics, 20(1971), 619-637.
- Matkowsky, B.J., A Simple Nonlinear Dynamic Stability Problem, Bulletin of the American Mathematical Society, 76(1970), 620-625.
- Meinhardt, H., and Gierer, A., Application of a Theory of Biological Pattern Formation Based on Lateral Inhibition, Journal of Cell Sciences, 15(1974), 321-346.